# FRICTIONAL OSCILLATIONS IN ELASTOMERIC SLIDING

by

Ronald Alvin Lee Rorrer

Dissertation submitted to the Faculty of the
Virginia Polytechnic Institute and State University in
partial fulfillment of the requirements for the degree

of

Doctorate of Philosophy

in

Mechanical Engineering

APPROVED:

N. S. EISS, JR, CHAIRMAN

A. L. WICKS

C. J. HURST

G. WILKES

T. WARD

October 1991

Blacksburg, Virginia

# FRICTIONAL OSCILLATIONS IN ELASTOMERIC SLIDING

by

Ronald Alvin Lee Rorrer

(ABSTRACT)

The impetus for this study was the noise generated by an automotive stabilizer bar, rotating in an elastomeric bushing. The focus of the research is to determine the conditions under which noise or stick-slip occurs. Elastomers tested include natural rubber with 0,5,10 20 and 50 phr (parts per hundred rubber) carbon black, butyl, polydimethyl siloxane, and fluorocarbon. The hard counterfaces include chromium oxide, aluminum, epoxy paint, and glass. Various combinations of these materials were tested in an elastomeric hemisphere-on-flat configuration.

Three regimes of sliding have thus far been identified: 1. Steady state sliding where the sliding friction is constant; 2. A high frequency self-excited oscillation of the test structure superimposed on the mean value of friction; 3. Stick-slip, where the elastomeric specimen goes through alternating periods of no relative and relative motion to the counterface. Friction maps which showed the regimes of stick-slip and steady state sliding as a function of load and velocity were experimentally determined. Stick-slip, the dominant mode of unsteady sliding did not occur below a critical velocity. The effects of surface energy, surface roughness and temperature on the critical velocity for stick-slip were also investigated.

**Abstract**

Stick-slip motion of materials has been attributed to a difference in static and kinetic coefficients of friction (typically for metallic systems) or a negative slope of the friction velocity curve. It has also been related to a maximum of tan delta or the loss modulus. Test results show that it is possible to have stick-slip occur in regions of positive or zero slope of the friction velocity curve. While the mechanism of stick-slip is not known for all of the elastomeric specimens, stick-slip of the butyl specimens appear to be related to Schallamach waves traversing the interface. For the natural rubber elastomers the critical velocity for stick-slip is dependent on the amount of carbon black. Decreasing amounts of carbon black decreases the critical velocity. The carbon black greatly increases the stiffness of the specimen while not appreciably shifting the frequency of the viscoelastic maxima. In addition, it was shown that a reduction in stiffness of the elastomeric speciment in the direction of sliding, by hollowing it out caused the critical velocity to decrease. Thus the critical velocity for stick-slip could be changed without changing the viscoelastic properties.

**Abstract**

ACKNOWLEDGEMENTS

I would like to thank the following people for the assistance they have given me in pursuit of this holy grail:

Dr. Eiss for his infinite patience and guidance; the tribology lab group, Rob De Togni, Brian Weick, Chiun-Chia Kang, Bhawani Tripathy, Hamid Ghasemi, Jong Yoo, and Brian McCann, for keeping me from graduating earlier by their distractions; Francis Webster for help with ellipsometry and FTIR; Dr. Wicks for his time and insight; Drs. Hurst, Wilkes, and Ward for serving on my committee; Dr. Mitchell for his advice and the force transducer obtained from his contacts at PCB Inc.; the Machine Shop (especially Jerry Lucas who machined the majority of the test apparatus) and Electronics shop for their help with equipment; and Ford Motor Company for their financial support.

I also would like to thank all of the friends that I made here and whom made this experience more enlightening; John Herr, Arun Veraraghaven, Mark Archibald, John Schultze and also the aforementioned tribology gang.

I especially have to thank my wife, Velvet, for the support, encouragement and endurance of this prolonged endeavor and for our wonderful son Nicholas.

The average Ph.D. thesis is nothing but a transference of bones from one graveyard to another.

*J. Frank Dobie*

Let us hope I have at least transferred some bones.

*Ronald A. L. Rorrer*

## TABLE OF CONTENTS

## LIST OF FIGURES

Figure No.Page

## LIST OF TABLES

# INTRODUCTION

Noise generation during sliding by either metallic or elastomeric systems occurs by a deviation from smooth steady sliding. Historically, two modes have been identified. The first mode is stick-slip, where the counterface and slider go through periods of alternating relative motion and no relative motion to each other. The second mode is harmonic or quasi-harmonic oscillations where there is always relative motion between the counterface and the slider which vibrates at or near (due to nonlinearity of the friction-velocity relationship) its tangential natural frequency.

The current study was prompted by noise problems encountered by Ford Motor Company with the front stabilizer bar rotating in an elastomeric bushing. The bar is epoxy coated steel, while the current bushing is 50 phr carbon black filled natural rubber. The configuration is shown in Fig. 1. When the brakes are applied very suddenly the front end of the car nose-dives and the stabilizer bar rotates in the bushing. It also goes through small rotations due to road bounce.

Ford has made the following observations concerning the occurrence of noise:

1. Approximately 8,000-10,000 miles of running before the initiation of noise.

2. Noise starts when the epoxy paint wears through and the elastomer is sliding on bare metal.

3. Noise occurs at cold temperatures ($T < -7$ °C), but never at high temperatures ($T > 38$ °C).

4. Water at the interface produces noise. Additionally, a contaminant slurry of water, salt and air cleaner dust has also produced noise.

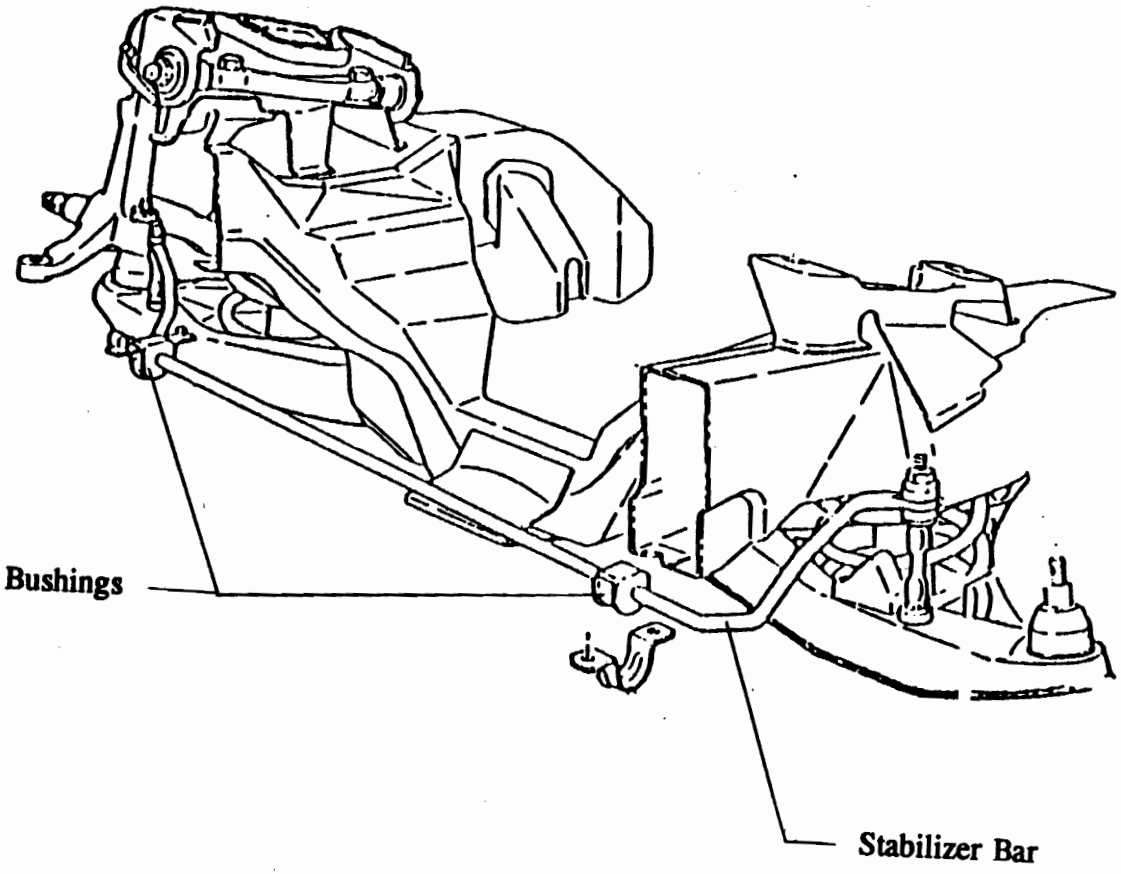


Figure 1. Stabilizer Bar and Bushing.

Ford has attempted to mitigate the problem with Teflon/silicone paste in the interface and also by molding in a teflon/polyester fabric liner into the rubber. However, the paste eventually migrates away from the interface. The elastomer squeezes through the weave of the fabric during the molding process and the noise problem still exists. Ford desires a modification to the rubber compound that will eliminate the cost of the paste and/or the liner.

The study undertaken here was to determine, if possible, the mechanism by which noise generation occurs in the dry sliding of elastomers against a smooth hard counterface. If the mechanism of noise generation is understood, then potential solutions to the problem can be proposed. In the past the sliding of elastomers against smooth counterfaces was thought to occur with little or no transfer. The shape of the friction-velocity curve generated by a series of independent time histories has been considered to be related to the actual friction-velocity relationship that occurs during a single test. Investigation of these two ideas form the backbone of the following study.

## LITERATURE REVIEW

Noise generation of sliding elastomeric systems can be described as a frictional oscillaHxon or discontinuity which leads to acoustic output. In regular steady-state sliding the friction is of uniform character and no noise is generated. Audible noise occurs when the sliding system goes into one of three modes. The most dominant mode is known as stick-slip. In this mode the slider initially sticks to the counterface with no relative velocity. As the static friction force is reach the slider breaks free "slipping" backwards until it reattaches to the sliding counterface. This phenomenon was originally observed in metal-on-metal sliding systems [1,2,3,4,5,6,7].

Historically, it has been assumed there is a fundamental difference between elastomeric stick-slip and metallic stick-slip. Elastomeric stick-slip occurs above a critical velocity [8,9,10,11,12,13,14,15,16], while metallic stick-slip occurs below a critical velocity [1,17,2,3,4,5,6,7]. In the literature this difference is attributed to differing mechanisms of sliding between the two material systems. The stick-slip of metallic systems has been attributed to a greater static coefficient of friction than kinetic [1]. In elastomeric sliding the stick-slip phenomenon is attributed to a negative slope of the friction velocity curve [8,18,10,16].

### VISCOELASTIC PROPERTIES OF ELASTOMERS

At this point it is helpful to introduce the principles of viscoelasticity and how

these principles apply to the sliding of elastomers. Many, if not, all of the friction theories that follow, incorporate viscoelasticity as the primary basis for the general shape of the friction-velocity curve and also where this curve peaks.

The majority of consideration will be given to the modulus of the elastomer. The modulus of an elastomer is complex as shown below.

$$E^* = E' + jE'' \tag{1}$$

where:

$E^*$ = *complex modulus*

$E'$ = *elastic or storage modulus*

$E''$ = *viscous or loss modulus*

The storage modulus relates to the strain component that is in phase with the applied stress, whereas the loss modulus relates to the component that is 90° out of phase with the applied stress. All polymers have components of their modulus that are 90° out of phase. Metals at temperatures below their melting temperature, have moduli that can be considered purely elastic. The next important concept to introduce is tan $\delta$= E''/E'. Many of the adhesion theories of friction will attempt to link the coefficient of friction to tan $\delta$. Both of the moduli, and therefore tan $\delta$, are a function of both frequency (or rate) and temperature.

Unlike metals or even glassy polymers (PMMA, polycarbonate, etc.) the sliding of elastomers is very sensitive to small changes in temperature. This occurs for a simple reason. For example, a 10 °C change in environmental temperature can give the same change in friction as a decade change in frequency or velocity. If the thermomechanical

spectrum of a polymer is examined it is seen that one requirement of an elastomer is a polymer with a glass transition temperature below room or operating temperature. Figure 2 shows a generalized thermomechanical spectra for polycarbonate and natural rubber. For now, a working definition of the glass transition temperature will be the inflection point where the storage modulus drops dramatically. As can be seen from Fig. 2, for an elastomer (i.e. natural rubber) the glass transition temperature is well below room temperature (typically -73 - (-123) °C) and for a glassy polymer it is usually well above room temperature (200-250 °C). In addition, the modulus of the glassy polymer is virtually constant within the glassy range. The change of modulus is a good macroscopic indicator of molecular motions that become important in tribological processes of an elastomer. Since the modulus is relatively insensitive to changes in operating temperature around room temperature the tribological properties are not affected dramatically by changes in temperature or velocity. It should also be noted that increasing temperature has the same effect on modulus and tan $\delta$ as decreasing velocity. In fact, this leads to the well-known WLF (Williams-Landel-Ferry) equation [19] which allows transformation between rate and temperature. This relationship was first verified experimentally for shifting of modulus data. It is very useful since most test apparatus can usually only provide 2-3 decades of rate changes and utilization of the time-temperature superposition can extend this range by 4-10 decades. The WLF equation was originally used to transform between angular frequency, $\omega$ and temperature. However, since it is based on the molecular relaxations of the elastomer chain it has been shown to apply to the relationship between experimental friction data and sliding velocity and

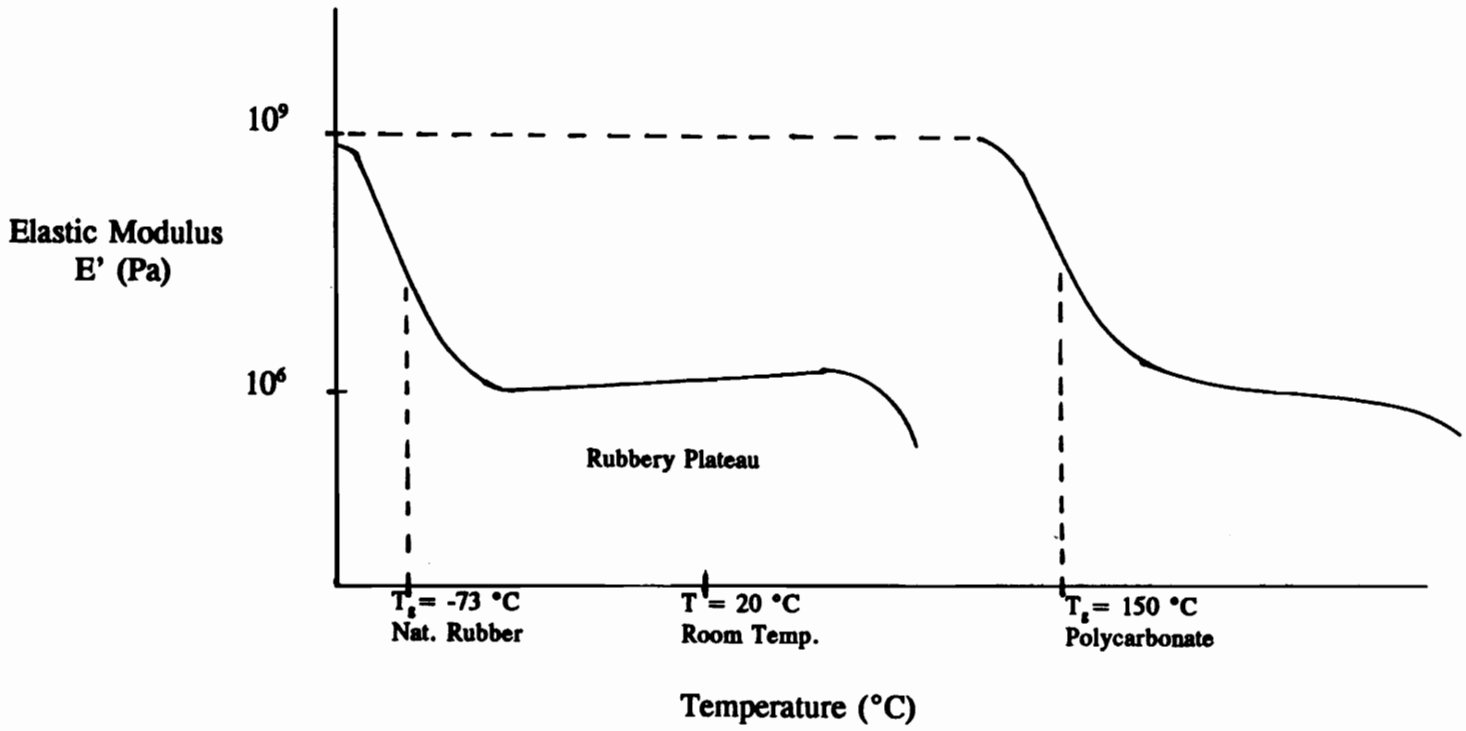


Figure 2. Thermomechanical Spectra for PMMA and Natural Rubber.

temperature [8,18]. Essentially, the WLF equation provides a shift factor to transform data obtained at the available rate range with differing temperatures to data at desired rates for a given temperature.

## SLIDING FRICTION OF ELASTOMERS

In general the dry sliding friction of elastomers is composed of the following components:

$$F = F_{adhesion} + F_{deformation} \tag{2}$$

where:

$F_{adhesion}$ = Friction force due to breaking interfacial bonds. Limiting value is shear strength of weaker material.

$F_{deformation}$ = Friction force from bulk deformation or deformation due to passing asperities.

When sliding occurs against smooth, dry surfaces the dominant contributor to the observed friction force is typically considered to be the adhesive component of friction. The cohesive friction component is the upper limit on the adhesive friction. Cohesive friction occurs when the adhesive bond is stronger than the bulk material and the bulk material shears a small distance away from the interface. The adhesive component of friction is due solely to the making and breaking of the interfacial bonds. Various theories of adhesive rubber friction have been proposed. These theories can be separated into molecular and macroscopic phenomenon, with both classes of theories containing

viscoelastic properties. There are many useful reviews of elastomeric friction which summarize various aspects of the following review [20,21,23].

### Molecular-Kinetic Theories

The molecular-kinetic theories of friction all incorporate the idea that the elastomer chains are in a state of constant motion. The elastomeric chains are continuously making and breaking interfacial bonds with the opposing counterface [22,23,22,24]. All of the theories assume that the chains are oriented in the direction of sliding due to the tangential friction force. This process is considered to be thermally activated [22,23,24]. These chains break loose from the surface under the combined effects of tangential loading and temperature jumping forward a distance, $\lambda$, which is on the order of molecular dimensions of the spacing between bonded chains. This process has been described by some [9] as a molecular stick-slip process.

Without going into all of the details, examination of the fundamentals of these theories is enlightening. The chains detach from the surface for a time, $\tau$, that is dependent on the temperature in an Erying rate process as shown.

$$\tau = \tau_o e^{\left(\frac{E_a}{kT}\right)} \tag{3}$$

where:

$\tau_o$ = $10^{-12}$ s, characteristic relaxation time for detachment

$E_a$ = activation energy or energy barrier

T = absolute temperature in °K

k = universal gas constant, 1.97 kcal/mole °K

Upon application of a tangential force the detachment time is decreased in the direction of sliding. The friction force is proportional to the number of bonds existing between the two surfaces at any given time. Therefore the total friction force in the tangential direction can be written as a summation of the tangential force in all the individually bonded chains.

$$F = \sum F_i \tag{4}$$

The force in the tangential direction of a given chain is assumed to increase linearly with displacement, acting in effect as a linear spring.

$$F_i = E^* V t_i \tag{5}$$

where:

$E^*$ = complex modulus

By substitution the total friction force becomes:

$$F = NE^* \bar{Vt} \tag{6}$$

where:

t = average life of the bonds

N = number of bonded sites

and N, $E^*$, and t vary with velocity and/or temperature. The mean bond force increases with increasing velocity. However, the number of bonds decrease with increasing speed leading to the peak in the friction-velocity curve. A peak in the friction-velocity curve results from these two competing effects.

Another molecular theory [9] considers the stick-slip event on the molecular basis while modeling the dissipation and storage of energy with the classic Voigt element. The resulting expression for the friction force is proportional to bulk tan delta.

$$F = K\sigma_o\left(\frac{W}{H}\right)\tan\delta \tag{7}$$

where:

K = proportionality constant

W = normal load

H = hardness

$\sigma_o$ = stress required for chain detachment

Many other theories [25,24] can be manipulated to show the same proportionality to tan delta, thus attempting to link friction to the viscoelastic properties.

## SIMPLE THEORY

Ludema and Tabor [15] present the simplest explanation of the viscoelastic peak in the friction-velocity curve. The friction force can be expressed as a function of the area and shear strength.

$$F = As \tag{8}$$

where:

$A$ = real area of contact

$s$ = shear strength

The area of contact from Hertzian theory is proportional to $E^{-2/3}$, where E is the storage modulus of the elastomer. It is assumed the variation of E with sliding velocity is analogous to its variation with frequency. This is no doubt true for the case of a hard slider on viscoelastic material, but, to date there has not been sufficient evidence to extend the concept to a viscoelastic slider on a hard, smooth surface. The difference in the two systems is shown in Fig. 3. As can be seen from this figure, a hard indenter deforms the elastomer giving rise to bulk viscoelastic effects. The bulk deformations change the area of contact with sliding velocity as expected from viscoelastic theory. However, there is no mechanism for the sliding velocity to change the area of contact for an elastomeric slider on a hard counterface.

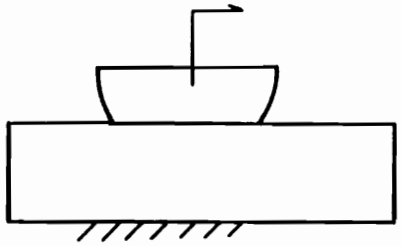

Soft Slider (Elastomer)/Hard Counterface

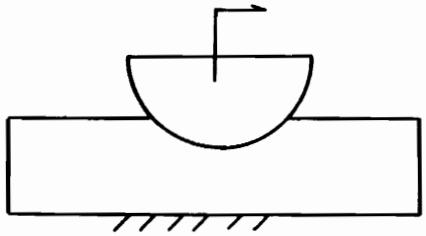

Hard Slider/Soft Counterface (Elastomer)

Figure 3. Comparison Between Rubber and Hard Sliders.

The shear stress is assumed to possess the same speed dependence as the tensile strength, which increases with increasing strain rate. Since the area of contact is decreasing with sliding velocity and the shear stress is increasing with velocity, the potential for a maximum in the friction-velocity curve exists as shown in Fig. 4. The area of contact depends on the frequency dependence of the storage modulus. As an initial approximation the elastomer experiences a frequency on the order of the linear velocity of the slider divided by the contact diameter. This forcing frequency is usually low due to the low sliding velocity and moderate contact areas. The shear strength requires high strain rates before reaching a plateau in magnitude. It is generally assumed that the strain or strain-rate is effective at a depth of approximately 100 angstroms into the elastomer.

## SCHALLAMACH WAVES

Prior to 1971, the sliding of elastomers was universally thought to occur by pure shearing of the interface of the materials. However, in a set of novel observations, Schallamach [26] observed "waves of detachment" lifting the elastomer off the counterface and traversing the contact area. The wave lifts off from the leading edge of contact and propagates to the rear against the direction of bulk sliding. The propagating waves form a line perpendicular to the direction of sliding. In many cases, the size and velocity of the waves account for the bulk forward motion. Figure 5 shows a representative series of photographs for a sliding test. In some cases, waves were

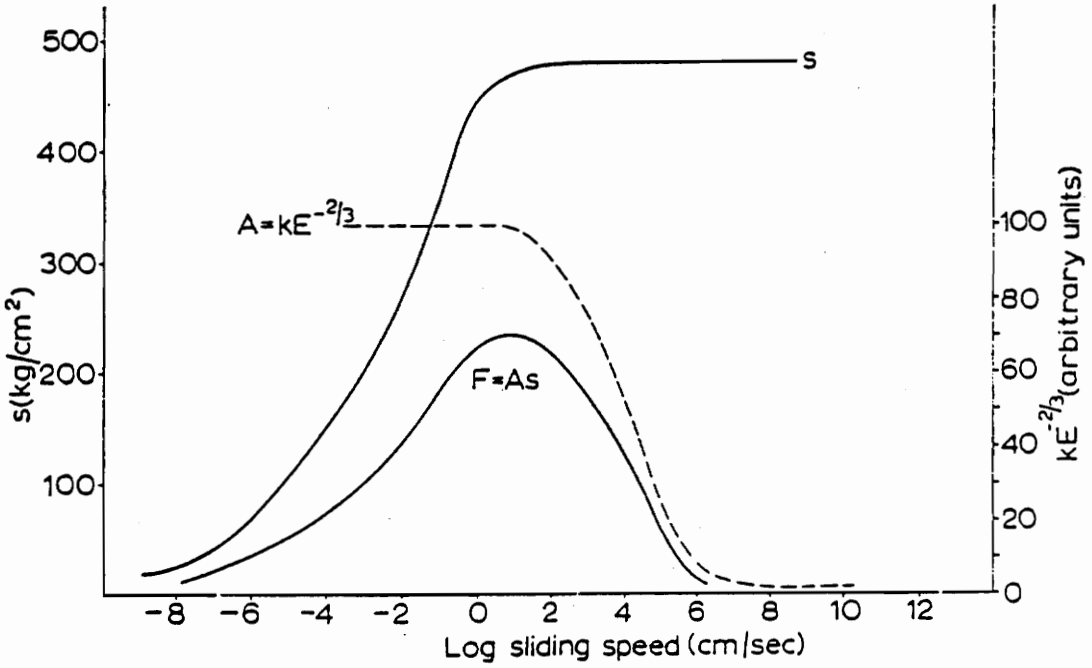


Figure 4. Simple Model of Elastomer Friction [15].

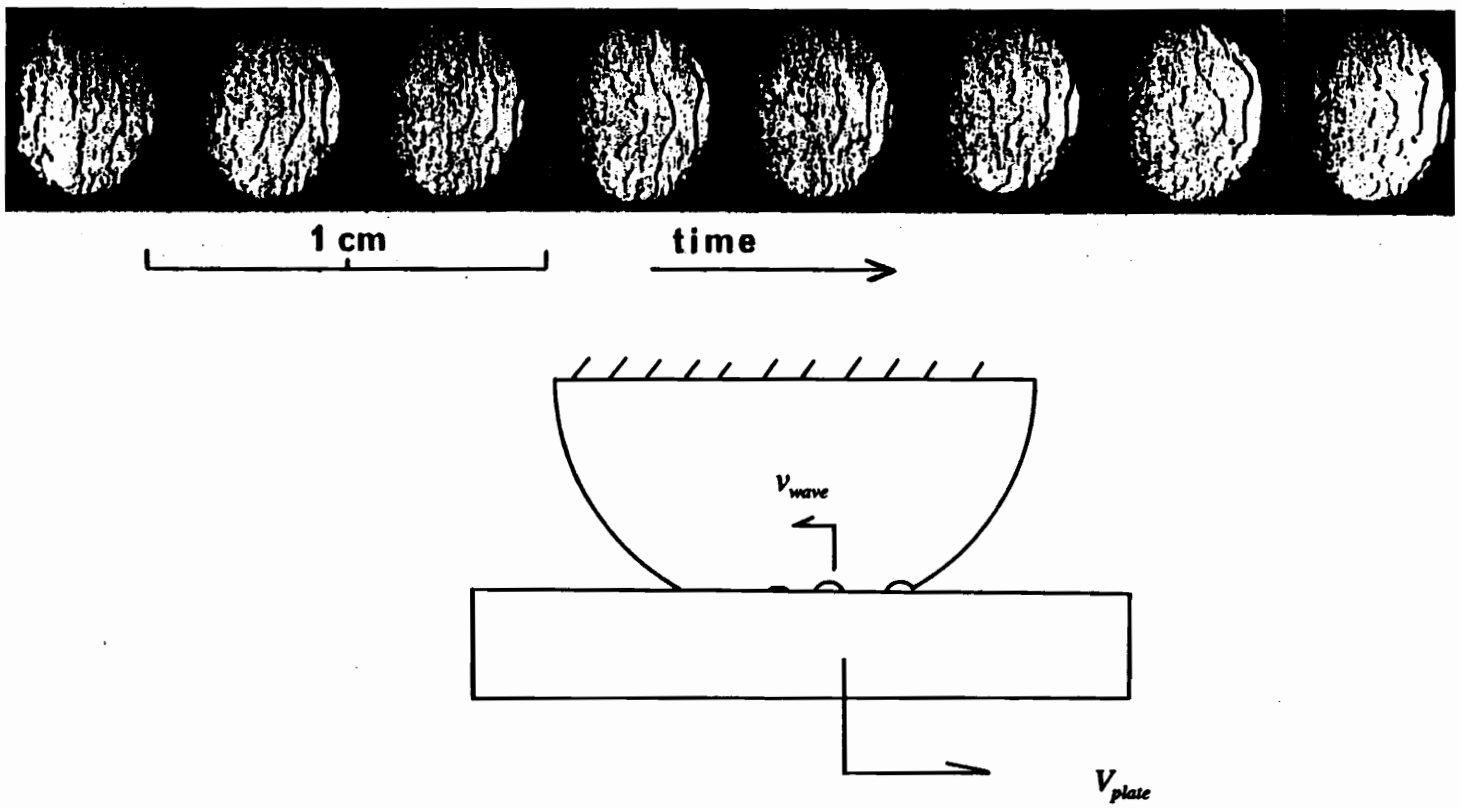


Figure 5. Typical Series of Schallamach Waves [26]. Natural Rubber Sphere Sliding against Perspex Plate at .43 mm/s. Eight Frames at 1/32 frames/s.

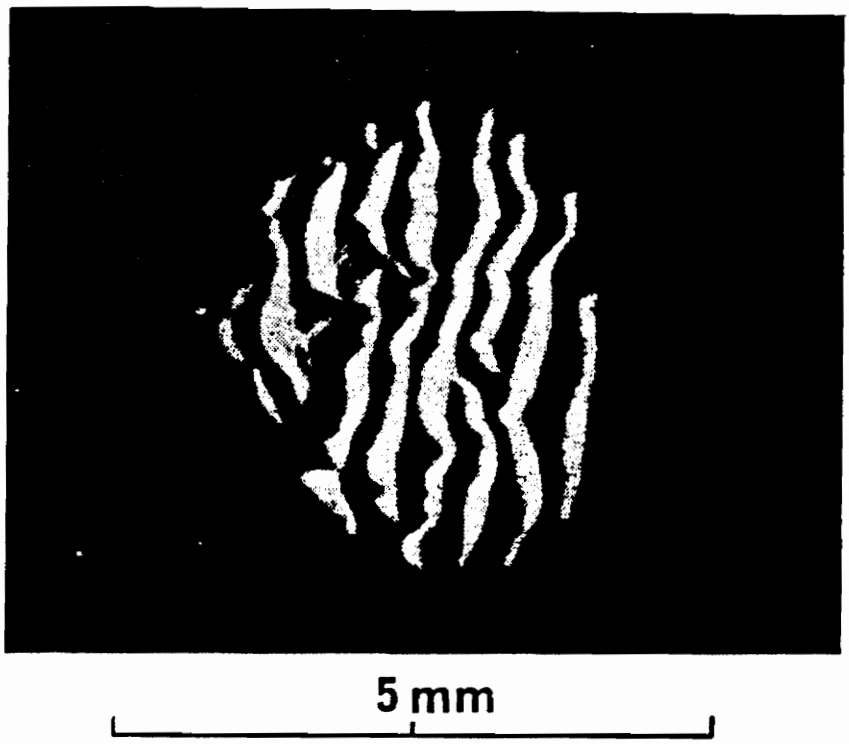


Figure 6. Stationary Buckles without Propagation [26].
Butyl Sphere Sliding on Perspex at .43 mm/s.

produced that did not propagate. Figure 6 show a photograph where the detachment waves were formed but did not propagate. "True" sliding occurred at the material interfaces that were in contact. It is also possible that true sliding occurs at the areas in contact when the waves are propagating. However, calculations have shown that the correct order of magnitude of the friction force can be accounted for by the peeling of the waves as they traverse the interface. The origin of these waves is the large compressive stresses and strains that occur in the rubber due to the friction force and normal load.

Surface instability (i.e. buckling) has been predicted for incompressible materials when the compressive stress or strain reaches a critical value [27]. Biot [27] has shown through rubber elasticity that the critical extension ratio, $\lambda$ ($\lambda = 1/l_o$), for incipient buckling of the surface in uniaxial compression is:

$$\lambda > 0.444 \tag{9}$$

This results in the following critical stress:

$$\sigma > 2.05\ E \tag{10}$$

where:

$E$ = Elastic Modulus

The results are independent of wavelength of the buckle with all wavelengths having equal probability of occurring. The only exception is that the wavelengths are limited by the thickness of the rubber if one side is fixed. In this case wavelengths are limited to 1/3 the thickness.

## EXPERIMENTAL VISCOELASTIC RESULTS OF ADHESIVE FRICTION

As stated earlier the adhesion component of friction is generally considered as possessing viscoelastic properties [8,9,28,20]. Adhesion is considered to be solely a property of the surface of materials, typically only concerned with material depths on the order of 100 angstroms. In what is perhaps the classic experimental work in the sliding friction of elastomers, Grosch [8], has demonstrated that the WLF (Williams-Landel-Ferry transformation holds for shifting velocity and temperature with respect to friction. While his work is elegant, it will be shown that some of his conclusions are controversial. An example of the velocity-temperature shift is shown for acrylonitrile-butadiene on wavy glass. The friction results were obtained over a velocity range of $10^{-2}$-$10^{0}$ cm/s. The unreduced friction data is shown in Fig. 7. This data is shifted by the WLF transformation with the shift factor shown below:

$$\log a_t = \frac{-8.86(T-T_s)}{101.5+(T-T_s)} \tag{11}$$

where:

$T$ = Test temperature

$T_s$ = Reference Temperature (20 °C)

$a_t$ = Shift factor.

This shifting results in the master curve shown in Fig. 8. However, there is a

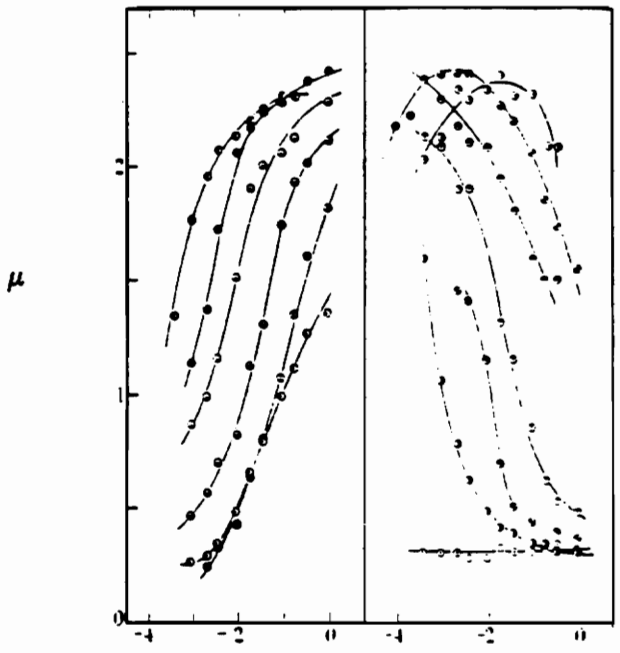


Figure 7. Unreduced Friction Data for Acrylonitrile-Butadiene on Wavy Glass [8].
⊖, 85 °C; ⊕, 70 °C; ⊜, 55 °C; ⊙, 40 °C; ⊖, 30 °C; ◐, 20 °C; ◑, 10 °C; ⊘, 5 °C; ⊜, 0 °C; ⊃, −5 °C; ⊘, −10 °C; ◑, −12·5 °C; ⊙, −15 °C.

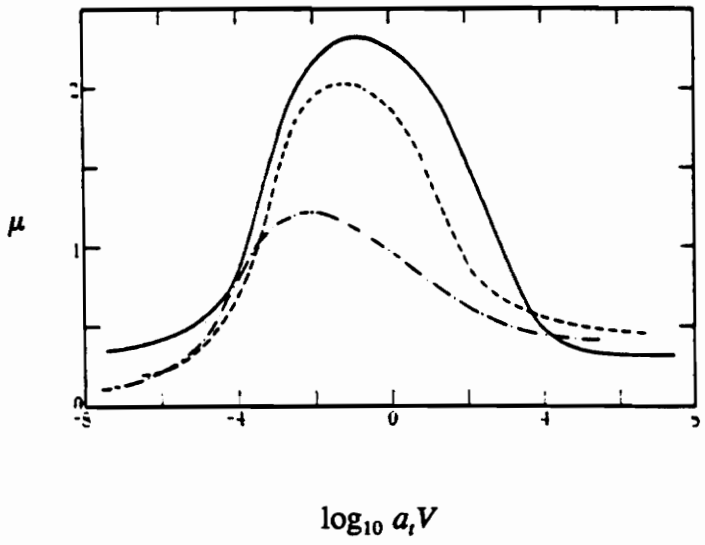


Figure 8. Master curve for Acrylonitrile-Butadiene on Wavy Glass. Reference temperature is 20 °C. ———— Gum Rubber, - - - 20 phr carbon black, — • — • — 50 phr carbon black. [8]

problem with interpretation this shifting of the coefficient of friction. Obviously, the peak at which the maximum occurs is valid, since in this particular example the peak is shown in the raw data for a series of velocities at constant temperature. There is some doubt, however, about the validity of the velocity temperature correspondence implied by the experimental results. In the experiments, the tests were performed in an enclosed chamber that essentially acted as an oven. This meant the entire elastomer saw the test temperature. This results in changes of the area of contact (due to changes in modulus) in addition to changes of the interfacial properties.

For the four different rubbers tested the ratio of maximum velocity, $V_c$ (cm/s), to the frequency of the loss modulus peak, $f_{E''}$ (rad/s),

$$\lambda = \frac{V_c}{f_{E''}} \tag{12}$$

was relatively constant, on the order of $6.0(10^{-7})$ cm. This value corresponds to a molecular jump distance on the order predicted by the molecular-kinetic theories of friction for a stick-slip process on the molecular level. The friction curves can be shifted by $\lambda$ to overlap the loss modulus curves as shown in Fig. 9. This result is in contrast to the majority of theoretical predictions which relate the peak to tan delta [25,23]. Grosch considers this agreement of $\lambda$ to be validation of his results to the molecular-kinetic theories of friction.

The other most pertinent observation that Grosch made was that the occurrence of stick-slip was related to the negative slope of the friction-velocity curve. However,

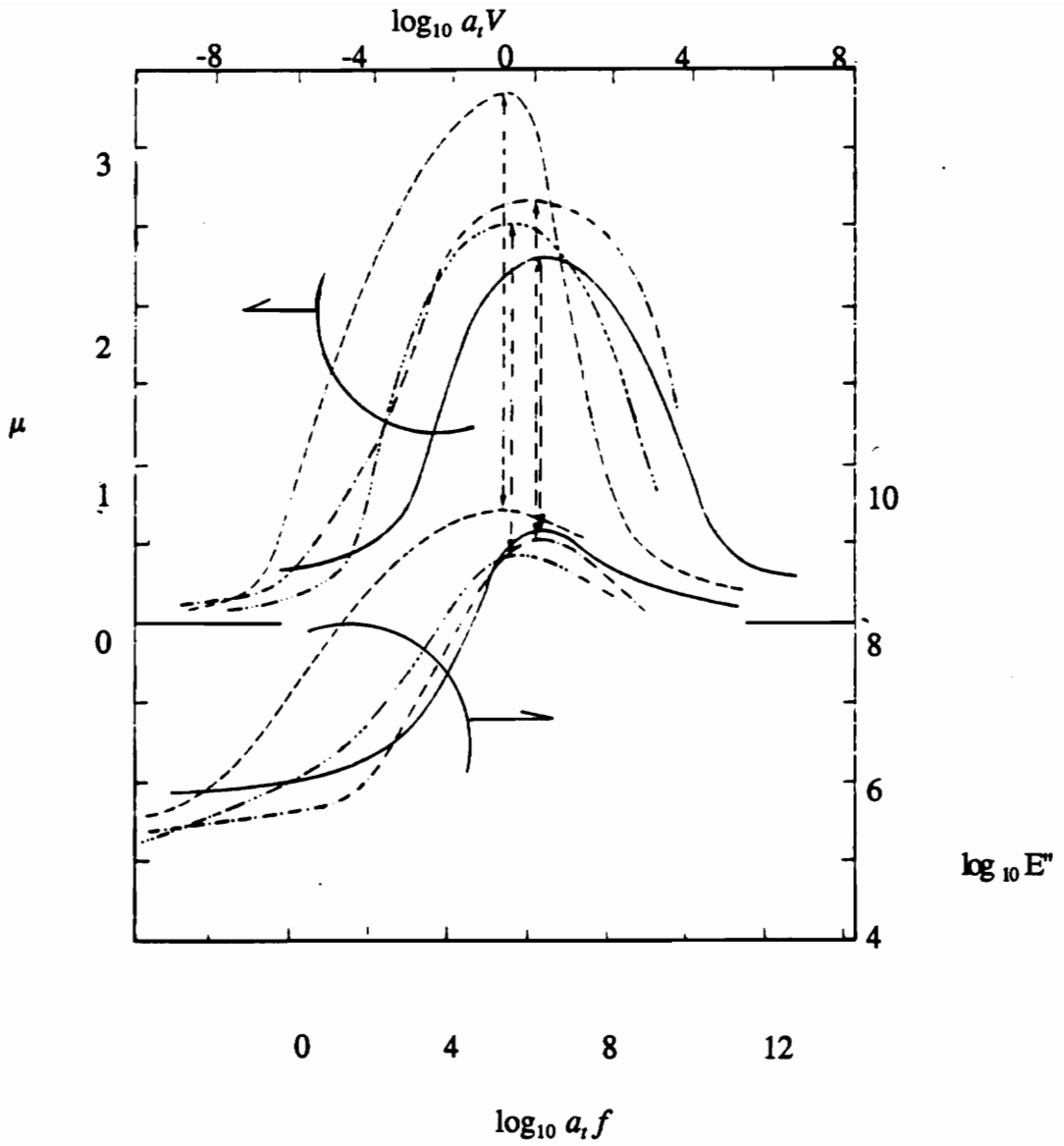


Figure 9. Overlap of Loss Modulus on Friction-Velocity Curve [8].
— • • — Styrene Butadiene: ———— Acrylonitrile Butadiene
- - - Butyl Rubber: — • — • — Natural Rubber

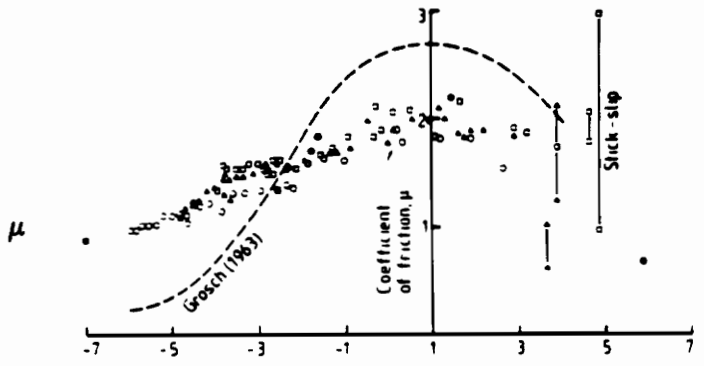


Figure 10. Overlap of Barquins and Grosch Curves [29]. Natural Rubber on Wavy Glass. $T_{ref} = T_g + 60$ °C.

he had data in his paper for 50 phr carbon black natural rubber which contradicted this conclusion, showing that stick-slip could occur in regions of zero slope of the friction-velocity curve.

Barquins and Roberts [29] have performed similar tests with the same rubber compounds and wavy glass as those performed by Grosch. The curve of friction versus velocity is much flatter without exhibiting the same viscoelastic peak as shown by Grosch. There was no apparent explanation for the discrepancy. Barquins and Roberts [29] claim that the onset of stick-slip occurred in a relatively flat portion of the friction-velocity curve. Upon examination of the curve it appears that there is a slight negative slope to the friction-velocity curve. Their experimental results are compared to Grosch's in Fig. 10.

## SURFACE ROUGHNESS AND SURFACE ENERGY

As the surface energy of either member of a sliding pair increases the friction force required to slide one past another should also increase. Surface energy can be viewed as the attraction a surface possess to other surfaces or liquids. This is usually determined by placing a drop of liquid (usually water, or in some cases mercury) on the surface. A high energy surface tends to spread the water making the contact angle low, usually less than 90°, whereas a low energy surface tends to repel the water and the droplet will bead with a contact angle greater than 90°. A good example of this is the beading of rainwater on a freshly waxed car which has a low surface energy.

The work of adhesion or the work required to separate two mating surfaces is as follows.

$$W_{adh} = \gamma_1+\gamma_2-\gamma_{12} \tag{13}$$

where:

$\gamma_1$ = surface energy of body 1

$\gamma_2$ = surface energy of body 2

$\gamma_{12}$ = interfacial surface energy

The work of adhesion, after manipulation can be written for elastomer and mating solid in the following form

$$(W_{adh})_{es} = \phi_1(\gamma_e\gamma_s)^{1/2} \tag{14}$$

where $\phi_1$ is a constant. The contact angle, $\Theta$, of a liquid drop gives an indication of the solid's surface energy from Young's equation, where *s* and *l* refer to solid and liquid respectively.

$$\gamma_s = \gamma_l\cos\theta+\gamma_{sl} \tag{15}$$

After various substitutions the work of adhesion between the elastomer and the solid surface can be written in the following form [30], which shows the dependence on the static contact angle. Specifically there should be a linear dependence of work of adhesion and $(1 + \cos \Theta)$.

$$(W_{adh})_{es} = \left(\frac{\phi_1}{\phi_2}\right) \gamma_s^{1/2} \gamma_l^{1/2} (1 + \cos\theta) \qquad (16)$$

Johnson et al. [31] has shown that when pressing together identical spherical surfaces of high compliance, there is an increase in real contact area over that predicted by classical Hertzian analysis. This deviation occurs due to the mutual attraction between the two surfaces. In addition, after a load has been applied a negative load is required to separate the two surfaces. Fig. 11 shows the increase in contact area for a high and low (Hertzian) surface energy pairs. Figure 12 shows the effect of high surface energy on the load-contact area relationship. The dotted line is the Hertzian prediction of contact area which does not take into account the effect of surface attraction. In essence, the effect of increasing surface energy is analogous to an increase in normal load in terms of the effect on the area of contact.

Savakoor [32] has looked at the effect of increasing surface energy on the measured coefficient of friction. His results show an increase in the coefficient of friction with increasing surface energy, in particular there is the linear relationship predicted from the work of adhesion. This is shown in Fig. 13.

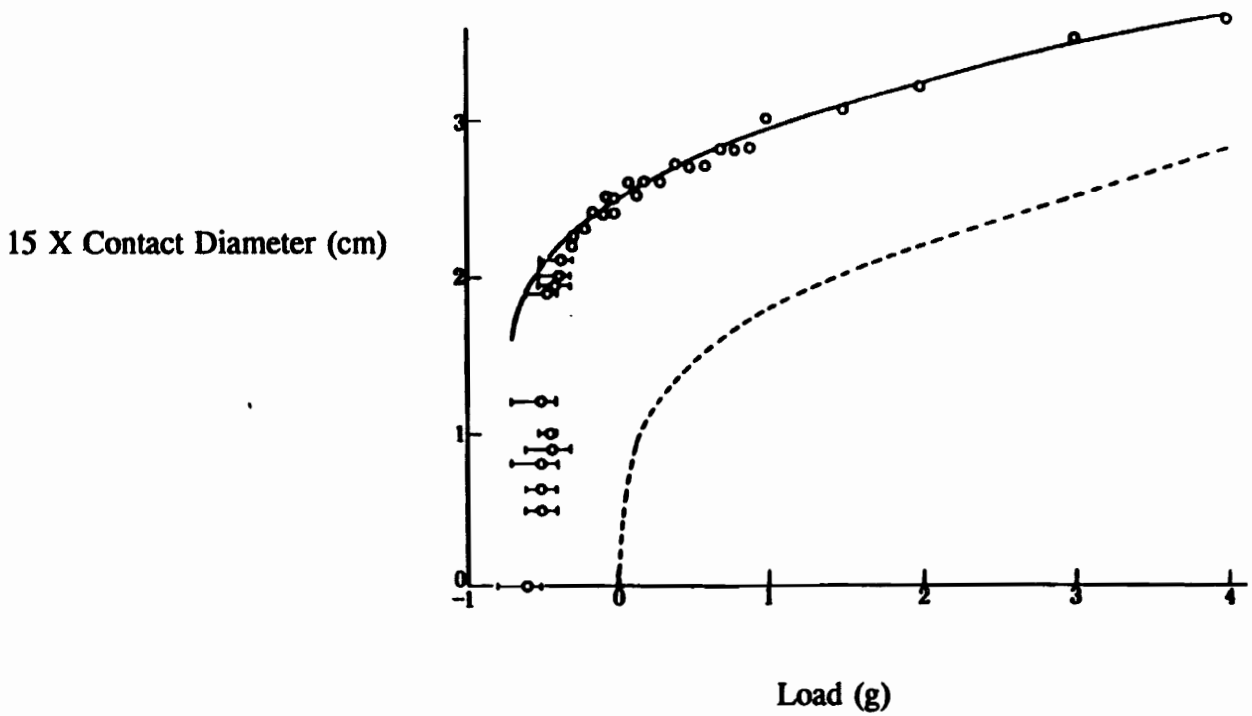


Figure 11. Increase in Contact Area for Positive and Negative Loads [31].
o Experimental Result, - - - - Hertzian Prediction.

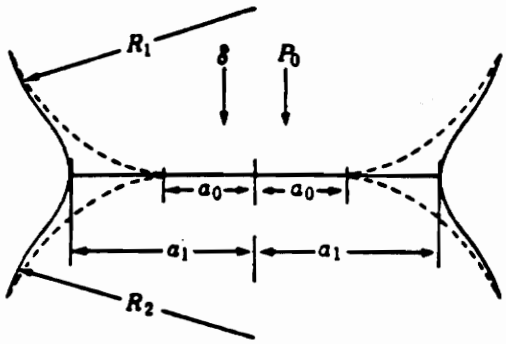


Figure 12. Contact Area in Presence and Absence of Surface Forces [31]. ($a_o$ contact radius in absence of surface attraction, $a_1$ contact radius in presence of surface attraction).

## TRANSFER FILMS

Even though the sliding of elastomers against smooth surfaces is considered to be mainly adhesive in nature, there is evidence that transfer does occur. It has been noted experimentally, in some cases, that transfer does not occur at low speeds but does occur as the speed increases [20].

## THEORY OF OSCILLATIONS

Excluding Schallamach waves, there are essentially two mechanisms for friction oscillations, stick-slip and harmonic oscillations. Both of these oscillations fall under the topic of self-excited oscillations. The reason for this classifications is that both phenomena can occur with periodic or nearly periodic response of the system without a periodic forcing function. The theoretical requirements for these phenomena to occur will be discussed in the following two sections. It will be shown that there are circumstances where harmonic oscillations can occur for a given friction-velocity relationship that will not lead to conditions for stick-slip. However, in general when the friction-velocity relationship will lead to stick-slip the conditions are present that will also lead to harmonic oscillations.

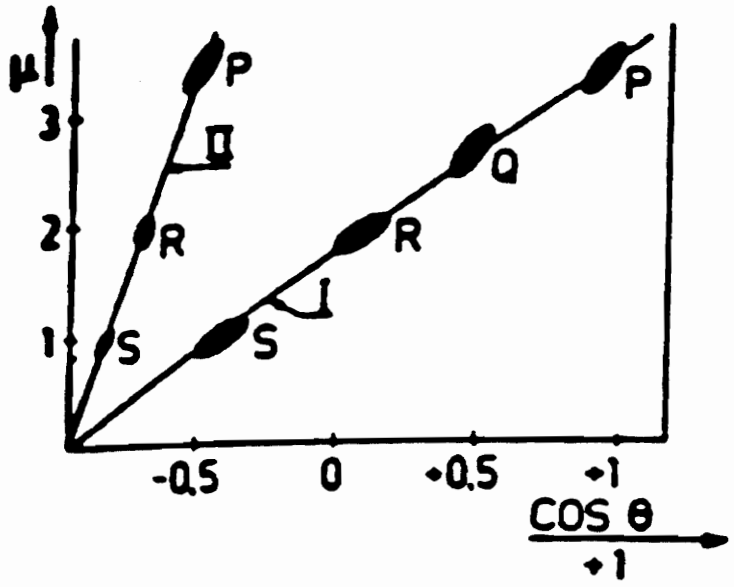


Figure 13. Relationship of Friction to Surface Energy [32]. (P-glass, PMMA, granite, clean stainless steel, Q- polystyrene, unclean steel, unclean glass, R- polyethylene, S- PTFE), (I- water drop, II- mercury).

### Harmonic Oscillations

Theoretically, harmonic oscillations only require a negative slope to the friction-velocity curve to occur [33,34,35,36]. If a simple one degree of freedom system is considered as shown in Fig. 14a with the friction-velocity relationship as shown in Fig. 14b, harmonic or quasi-harmonic oscillations can occur. Examining the governing differential equation of motion of the system results in the following:

$$mx''+cx'+kx=f(x') \tag{17}$$

Rearranging and bringing the forcing function to the left hand side, it is noted that whenever the value of f(x') is greater than cx' the system can become unstable. When the magnitude of f(x') is greater than cx' this is referred to as "negative damping". This is an unfortunate choice of words because the system does possess positive damping. However, the forcing function, which is a function of velocity, can result in situations which are analogous mathematically to negative damping. In these systems more energy can be pumped into the system than is lost due to system damping resulting in potential instability.

Instability can occur for both the linear and the general case of a non-linear function of velocity. It is instructive to first examine the linear case. If the system shown in Fig. 14a has a negative linear slope to the friction-velocity curve as shown in Fig. 14b. the following differential equation applies.

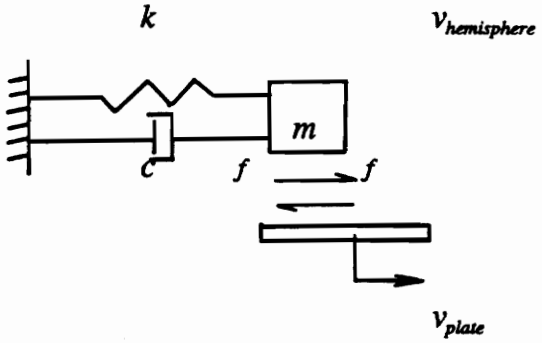


14a. Idealized Model.

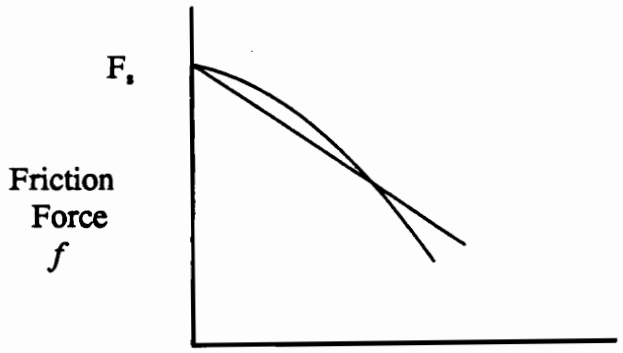


$$v_{rel} = v_{plate} - v_{hemisphere}$$

14b. Friction-Velocity Relationship.

Figure 14. Single Degree of Freedom Friction Oscillator.

$$mx''+cx'+kx=F_s-\lambda v_{rel} \tag{18}$$

where:

$$v_{rel}=v_{plate}-x' \tag{19}$$

Rearranging yields the following:

$$mx''+(c-\lambda)x'+kx=F_s+\lambda v_{plate} \tag{20}$$

The constant term $F_s + \lambda v_{plate}$ results in a dc offset to the displacement, but does not yield any information about the potential of oscillations. There are three possibilities that can occur. First $\lambda < c$ results in an oscillatory system that decays with time. The second possibility is $\lambda = c$ in which case the system oscillates at its undamped natural frequency. The final possibility is $\lambda > c$ in which case the system is unstable and the displacement grows without bound. In frictional sliding, oscillations do not grow without limit because real components are nonlinear. However, it is improbable that this implies $\lambda \leq c$ for a real world situation. Since this is a extremely simplified view of the sliding process there are physical limits on the motion that have not been taken into consideration which no doubt effect the phenomenon.

Harmonic or quasi-harmonic oscillations can also occur if the friction-velocity relationship is non-linear. Additionally, Fig. 14b shows a nonlinear shape to the friction-velocity relationship that will lead to the oscillations.

### Relaxation Oscillations

Of the three aforementioned modes of non-steady sliding, stick-slip is the mode most commonly observed. Stick-slip belongs to a class of phenomenon called relaxation oscillations. Relaxation oscillations are more prominent in the study of electrical circuits. Their occurrence in mechanical phenomena is very limited. Frictional systems are one of the few mechanical examples [33,34]. Harmonic oscillations are the second most encountered non-steady sliding phenomenon. From the mathematical viewpoint, harmonic oscillations can occur as a stage leading to relaxation oscillations. The requirements for relaxation oscillations is illustrated by Fig. 15 which shows a non-linear friction-velocity curve that is double valued. A necessary requirement for relaxation oscillations is the doubled valuedness of the driving function [33,34,35,36].

It is instructive to examine, in detail, various aspects about Fig. 15 of relevance to the current investigation. The friction-velocity curve has been simplified to aid in interpretation, but will later be expanded to apply to the sliding of elastomers. The first thing to consider is stability of points $S$ and $U$. Once again a single d.o.f. (degree of freedom) system model is assumed. The differential equation is the same as before with the exception of the non-linear driving function f(x'). The form of the governing differential equation is the same as before, however the forcing function is now non-linear in velocity as shown on page 37.

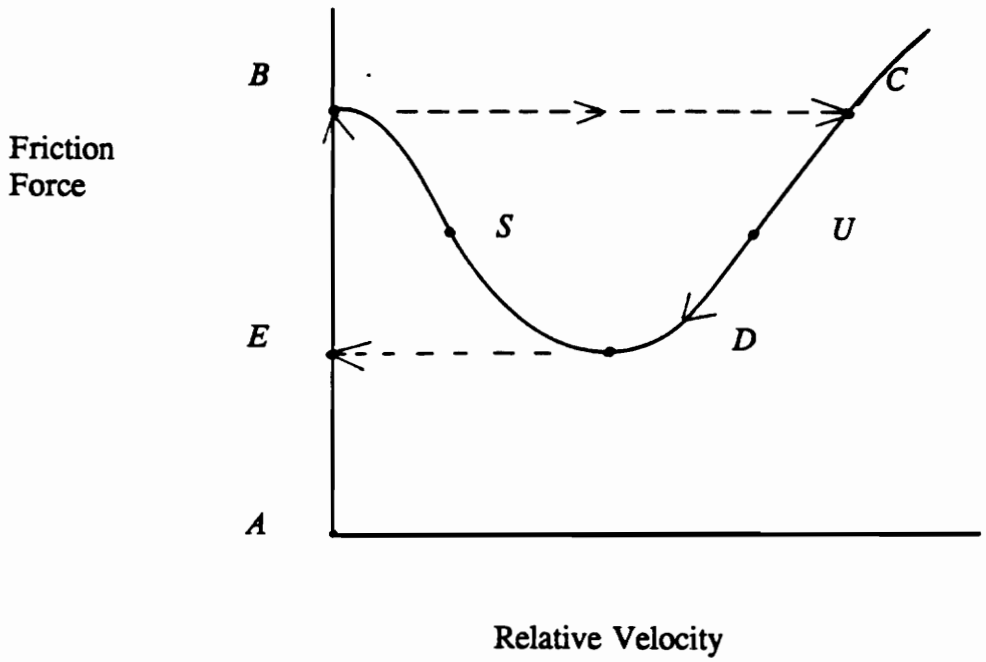


Figure 15. Friction-Velocity Relationship Required for Relaxation Oscillations.

$$mx'' + cx' + kx = \epsilon f(v_p - x') \tag{21}$$

Where $f(v_p-x')$ is nonlinear.

When $\epsilon$ is small the differential equation is quasi-linear and can be solved with approximately periodic solutions [33]. However when $\epsilon$ is large ($\epsilon > 1$) then there exist no analytical solutions and the differential equation must be solved numerically or qualitative information can be obtained by the graphical analysis of Lienard [37]. It is necessary to consider the mass negligible for the following theoretical development. In addition the system damping (i.e. non-friction damping) will be considered contained in the forcing function term.

When the mass, $m \approx 0$ and damping is neglected, $c \approx 0$ the preceding differential equation degenerates into the following equation.

$$\begin{aligned} f(v_{rel}) &= kx \\ f(v_p - x') &= kx \end{aligned} \tag{22}$$

This equation is differentiated with respect to relative velocity to yield:

$$-\frac{df(v_{rel})}{dx'} \cdot x'' = kx \tag{23}$$

If $df'_v < 0$ then x' and x'' have the same sign and the motion is unstable. If $df'_v > 0$ then x' and x'' have opposite sign and the motion is stable. The stability criterion arises from the fact that acceleration in the direction of the velocity tends to increase the velocity without bound, whereas acceleration opposed to the direction of the velocity tends to drive the velocity towards an equilibrium value. At points where $df'_v = 0$ it is

obvious that a discontinuity occurs. In the idealized case of $m \approx 0$ the kinetic energy is zero and the system makes a jump that conserves energy (Mandelstam condition). In this case the jump occurs in velocity and not displacement. Additionally, it can be seen when $df'_v$ goes to zero the acceleration, x'', goes to $\infty$. A discontinuous jump in velocity at point $B$ ($df'_v = 0$ ) occurs from point B to point C with infinite acceleration. Then the velocity is reduced from point $C$ to point $D$ in a finite time where once again $df'_v = 0$ and another discontinuous jump occurs to point $E$. Here the cycle is continually repeated with $F_{max}$ and $F_{min}$ determined by the bounds of the friction-velocity curve. A few comments on this cycle are in order. All the discussion thus far has centered on the velocity domain. Now the observations are converted to the time domain. The majority of time in the cycle is spent on the $E$-$B$ section of the curve and this time is a reasonable approximation of the fundamental stick-slip time period. Obviously, no time is spent on the sections $B$-$C$ and $D$-$E$ since they are traversed with infinite acceleration and velocity. The next significant portion of time is spent on the $C$-$D$ section, which for this highly idealized case can be considered the slip phase. Obviously when $m$ is non-zero the velocity jumps of infinite acceleration can not be attained.

### Displacement Controlled Stick-slip

Rabinowicz [38], describes another type of stick-slip that can occur that is not due to a double-valued friction-velocity curve. The relaxation oscillations described earlier can be considered to be velocity controlled. The case that will be considered now is the

condition of displacement controlled. Rabinowicz describes this type of stick-slip as irregular due to the initiating mechanism. In the Discussion Section, the displacement controlled stick-slip will be reexamined in light of the results presented later and it will be shown that there are situations where the stick-slip can become regular.

Displacement controlled stick-slip occurs when the slider traverses an area on the counterface that possessess a low coefficient of friction. The slider can only move as fast as its inertia and stiffness will allow. The stiffness of the slider forces the slider to follow as a maximum displacement $\Delta x = \Delta F/k$. If the slider encounters an area on the counterface which has a lower coefficient of friction the slider attempts to follow the drop in friction with a corresponding change in deflection. However, the slider can only move to the new equlibrium position with a velocity governed by the stiffness. When the friction drop is larger than the slider can follow it overshoots the equilibrium position due to excess kinetic energy. In general, this type of behavior has usually been observed in the sliding of clean metals.

# EXPERIMENTAL APPARATUS AND PROCEDURES

## EXPERIMENTAL TEST APPARATUS

The basic philosophy of the test apparatus design was to provide linear motion to a glass plate which would have an elastomeric specimen loaded normal to the plate direction of travel. The apparatus was designed such that the glass plate could be replaced at a later date with other plate materials of suitable interest. Glass was initially chosen as the counterface to observe if any interfacial phenomenon occurred. An overall schematic of the test apparatus is shown in Fig. 16. The test apparatus provides a plate velocity range from 0.919 to 50.8 mm/s. The normal load is limited only by the stall torque of the drive motor at the desired velocity setting, but was typically kept below 55 N.

## SLIDING MOTION

The fixture that holds the glass plate is driven by a lead screw coupled to a DC motor as shown in Fig. 16. As can be seen from Fig. 16, the lead screw serves as one guide rail while the other guide rail is simply a ground shaft over which the linear bearings travel. Vibration from the motor is damped by a flexible coupling that connects to the lead screw. The lead screw transmits the rotational motion to linear motion via a acetal lead screw nut that is filled with teflon and silicone. The linear velocity is

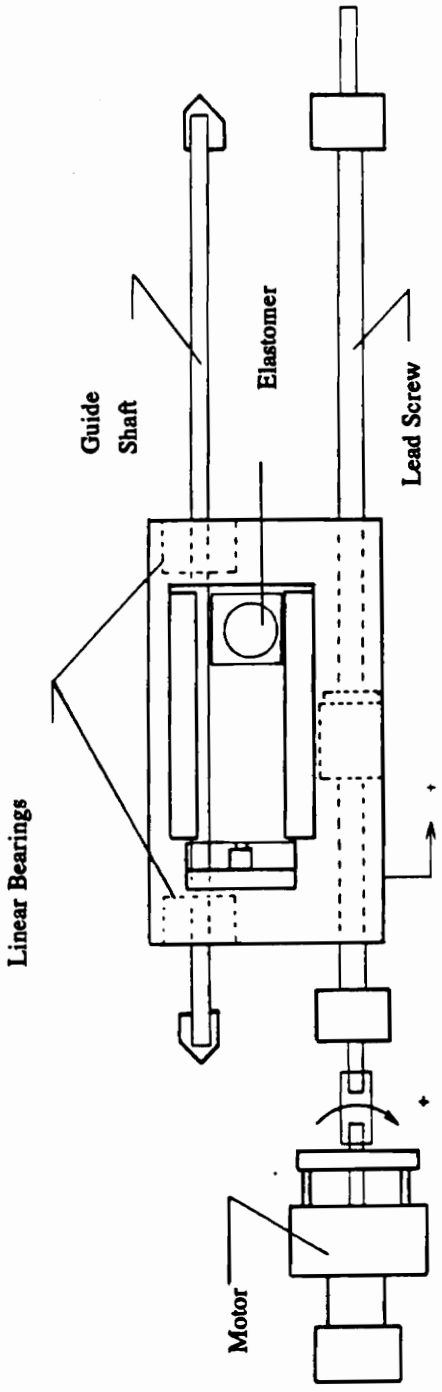


Figure 16. Top View of Test Apparatus.

controlled by the rotational velocity of the lead screw. The velocity controller is rapid enough to cause the initial velocity to be considered a step input to the system. Figure 17 shows a typical force and velocity time history to illustrate the initial transient response of the controller. The motor controller can control transients up to 25.4 khz. The plate had a useful travel length of 175 mm.

## FRICTION TRANSDUCER

The friction force was measured with a PCB Piezotronics Inc., piezoelectric force transducer. The transducer has a range of 100 lb with a resolution of 0.002 lb and a stiffness of 1 ($10^{6}$) lb/in.. The sensitivity of the transducer is 51.5 mv/lb. The force transducer was mounted on the end of the glass plate as shown in Fig. 18. As can be seen from Fig. 18, the glass plate is held in place by teflon coated guides which allow the plate to slide relative to the mounting fixture, thus compressing the force transducer during motion. The teflon guides resulted in a slight uncertainty of the coefficient of friction ($\mu_{\text{teflon/aluminum}} = 0.02$). Even though the normal mode of operation of the force transducer is ac coupled, the transducer was able to measure dc values of force for reasonably long periods of time (on the order of +20 s). The long time constant was provided by a line power supply and amplifier that drained the voltage output from the piezoelectric transducer very slowly. The voltage dropped only 1% in 20 s. The voltage dissipation is shown in Appendix D.

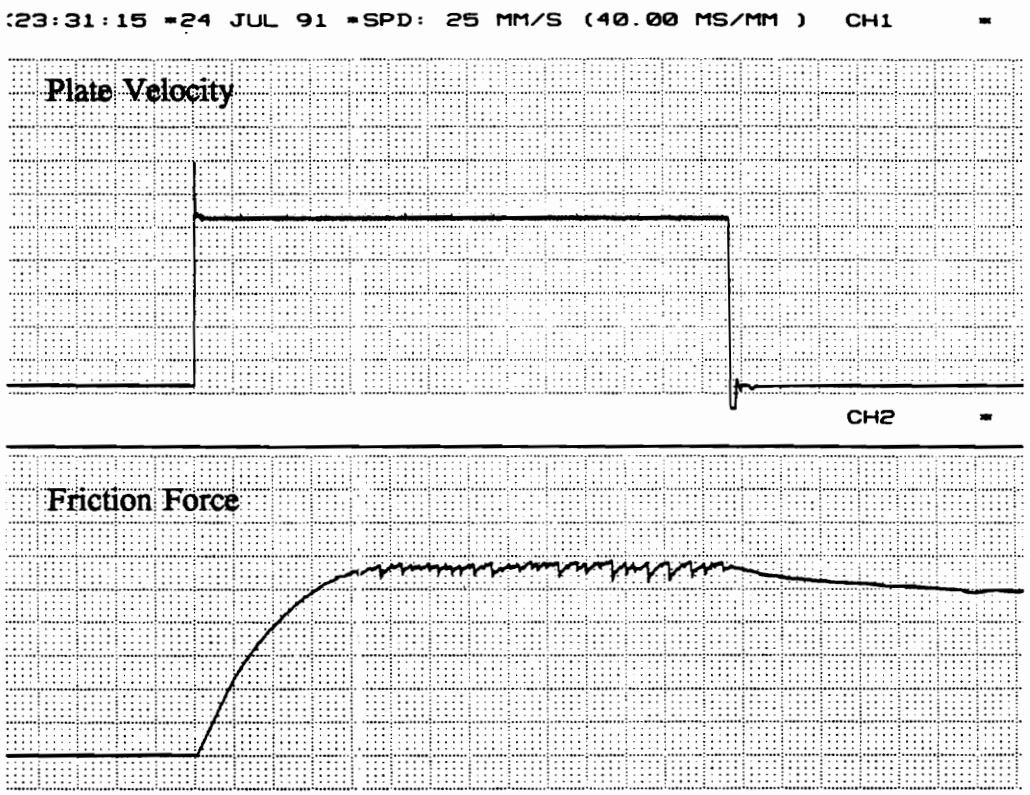


Time (25 mm= 1s)

Figure 17. Transient Velocity Control (Test Velocity= 2.819 mm/s)

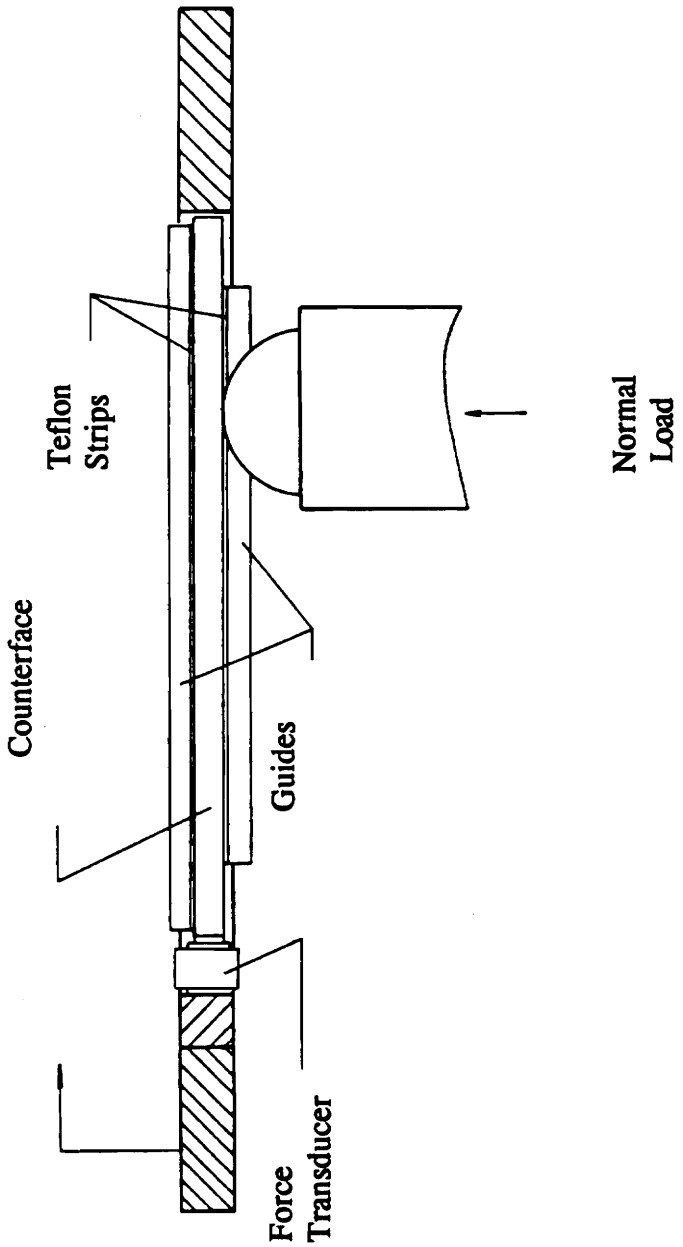


Figure 18. Location of Force Transducer.

## DATA ACQUISITION

Data was acquired by use of either a stripchart recorder or a personal computer (PC) based data acquisition board. The majority of the data was acquired with use of the PC system. The data acquisition board was a Data Translation DT-2821 with 16 channels and an maximum aggregate sample rate of 100 kHz. The highest frequency oscillation observed in the tests was on the order of 1400-1500 Hz. Therefore, for tests that produced noise the signal was typically sampled at a frequency greater than 3125 Hz ( 6250 was a typical sample rate). Tests that did not produce noise due to the slow test velocities were sampled at appropriate frequencies (as low as 100 Hz) to reach steady-state levels of friction within 8000 data points.

### Materials

#### Elastomers

Various elastomers were molded into 38.1 mm diameter hemispheres by Ford Motor Company. The following were provided: 0,5,10, 20 and 50 phr c.b. (carbon black) natural rubber (NR), butyl rubber (isobutene-isoprene, IIR), polydimethylsiloxane (PDMS), and Fluorel® Fluorocarbon (FPM). The elastomer that is currently used as the stabilizer bushing is the 50 phr c.b. natural rubber. The elastomers have the repeating monomer structure prior to crosslinking and glass transition temperatures, $T_g$, as shown

Table 1. Repeat Structure of Elastomeric Materials

| Elastomer | $T_g$ (°C) | Repeat Structure |
|---|---|---|
| PDMS | -123 | 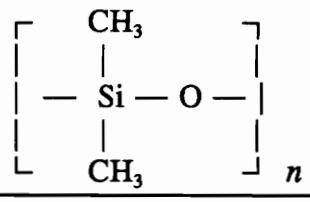 |
| Butyl Rubber | -72 | 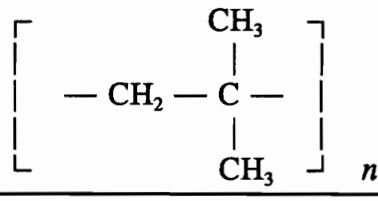 |
| Natural Rubber | -73 | 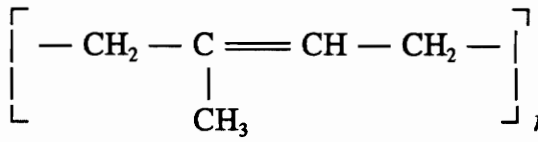 |
| Fluorocarbon Copolymer | -55 | 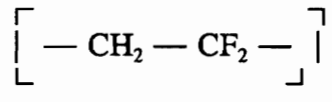 and 1:4 Ratio 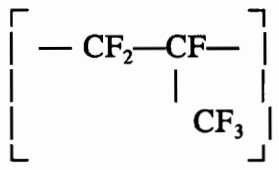 |

in Table 1. The material formulations of the elastomers are listed in Appendix C. The water contact angles are listed in Table 2.

### Counterfaces

As stated earlier various materials were used as counterfaces for the elastomeric hemisphere. The materials were chosen for various reasons. The materials tested included glass, chromium oxide, powder and cathodic epoxy and aluminum and polycarbonate. Initially glass was chosen because it was transparent and very smooth. Attempts were made at high speed filming of the interface ($\approx$10,000 frames/s) to observe the interfacial phenomena as it occurred. Unfortunately, the spatial resolution and clarity of the film work was not adequate for this purpose. Chromium oxide, commonly called "ferro-type plate", was chosen because it was the smoothest counterface available commercially. Aluminum was used because it was readily available and easily roughened. Finally and obviously, the epoxy counterfaces were chosen to duplicate the actual material interface of the stabilizer bar.

The counterfaces had the following surface roughnesses and water contact angles as listed in Table 3.

Table 2. Water Contact Angles of Elastomers

| Elastomer | Water Contact Angle (degrees) |
|---|---|
| Natural Rubber - 0 phr c.b. | 103.8 ± 2.7 |
| Natural Rubber - 20 phr c.b. | 82.2 ± 4.2 |
| Fluorocarbon | 92.0 ± 6.0 |
| Butyl | 89.5 ± 5.2 |
| PDMS | 103.8 ± 1.5 |

Table 3. Counterface Properties.

| Counterface | Roughness, $R_a$ ($\mu$m) | Water Contact Angle[1,2] (degrees) |
|---|---|---|
| Chromium Oxide Acetone Cleaned | 0.05 | 74.4 ± 4.4 |
| Glass Acetone Cleaned | 0.01 | 36.8 ± 6.36 |
| Isopropanol Cleaned | | 54.4 ± 7.76 |
| Stored in Dessicator for 3 months | | 56.0 ± 2.40 |
| Epoxy, Powder Detergent and Distilled Water Cleaned | 0.20 | 77.5 ± 4.9 |
| Epoxy, Cathodic Detergent and Distilled Water Cleaned | 1.15 | 58.3 ± 6.6 |
| Aluminum Acetone Cleaned | 0.105 | 81.7 ± 3.2 |
| | 0.200 | 94.8 ± 1.0 |
| Polycarbonate Detergent and Distilled Water Cleaned | 0.20 | 62.0 ± 3.4 |

[1] (± standard deviation)

[2] # of measurements 4-10

### Sample Preparation

The hemispheres were bonded on 50.8 mm square aluminum mounts as shown in Fig. 19. The mounts were then bolted to the load arm. Originally the counterface was commercially available plate glass (76 mm wide X 177.8 mm long X 6.35 mm thick). At first other counterfaces were bonded directly to this glass plate. Eventually, an aluminum fixture was constructed (of the same dimensions as the glass plate) to hold thin counterfaces (38.1 mm wide X 127 mm long X (2.54-3.2 mm) thick). This fixture is shown in Fig. 20.

The hemispheres were cleaned with acetone prior to a series of tests to remove any bloom (processing oils, etc. that migrate to the surface) that had occurred. In between tests the hemisphere surface was cleaned with distilled water and dishwashing liquid by wiping with a Kimwipe. This procedure served two purposes. The first was to remove any body oils or dust that may have contaminated the surface. The second was to mechanically remove any loose elastomer wear debris. The loose material was found to reduce the coefficient of friction as it built up and eliminated noise.

Since different plate materials were used as the sliding counterface, various cleaning procedures were used. The glass and chromium oxide plates were cleaned with acetone within 1-3 minutes immediately prior to the test run. The epoxy plates were cleaned with the same procedure as the hemispheres. The polycarbonate plates were not wiped with acetone since that step may have promoted crazing and crystallization. They were only cleaned with detergent and water.

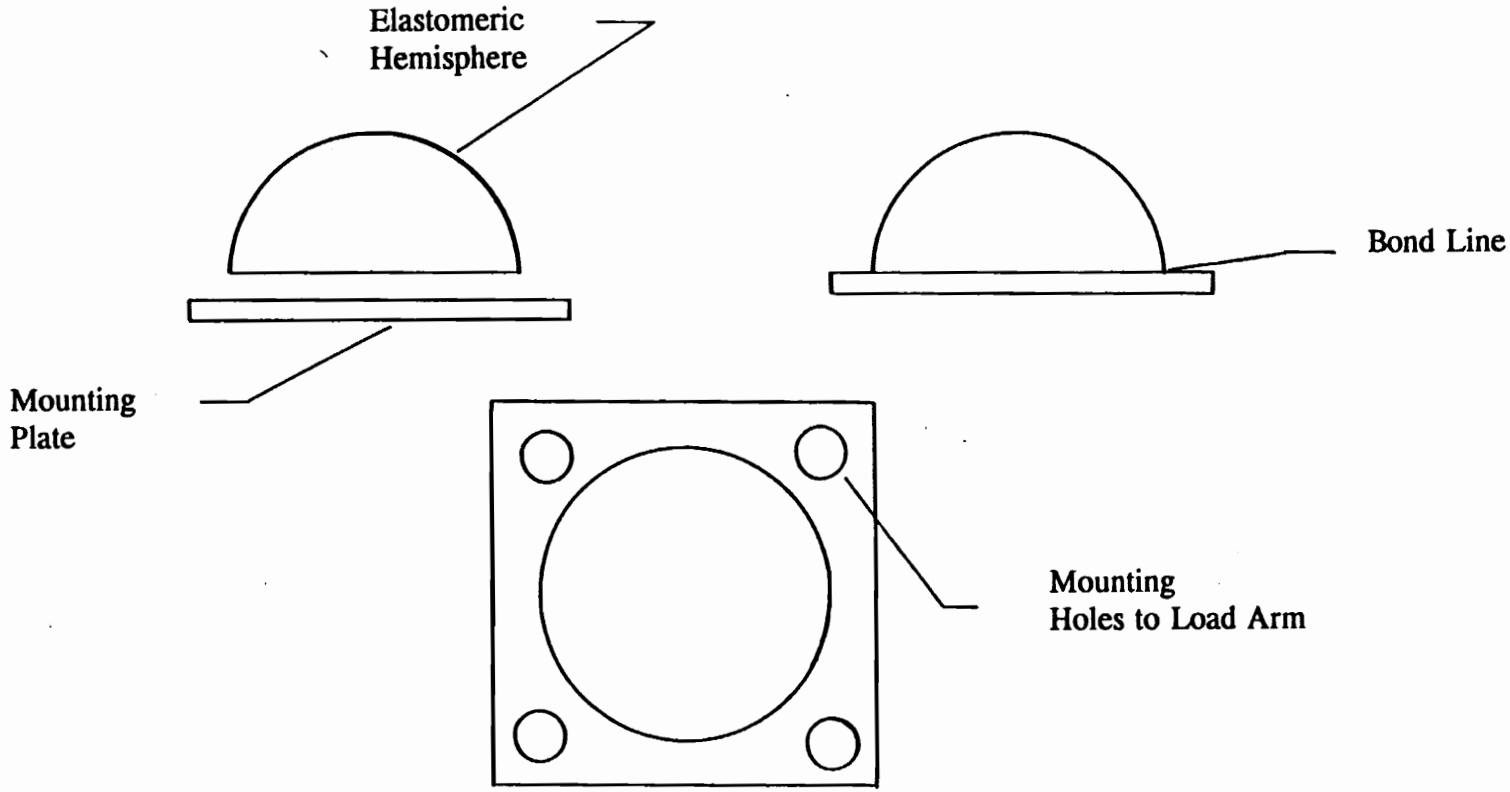


Figure 19. Hemisphere Mounting.

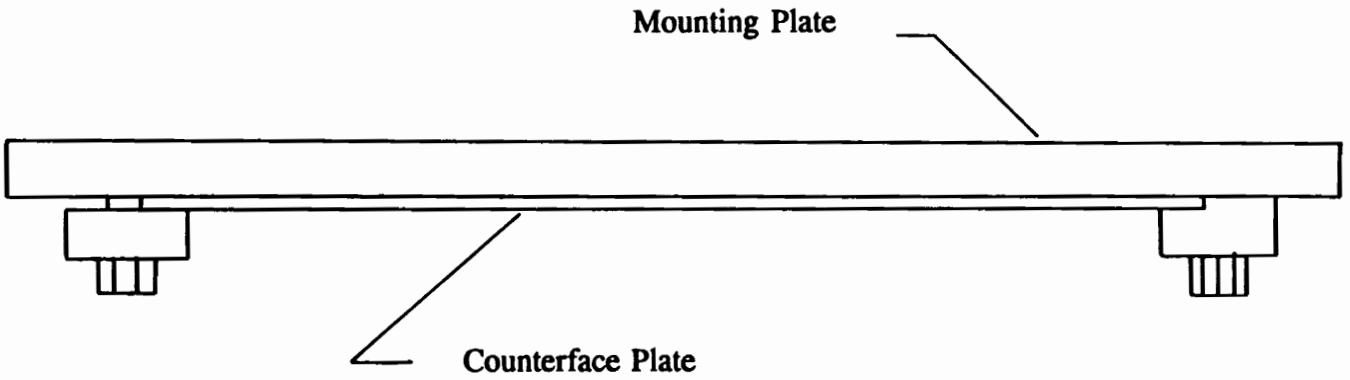


Figure 20. Counterface Mounting Fixture.

### Heated Tests

Since the test apparatus was not enclosed so that ambient temperature could be varied, only the counterface was heated by placing a rectangular strip heater directly on top of the counterface mounting fixture. A thermocouple was placed directly on the sliding surface of the fixture to monitor the surface temperature. The heater control configuration is shown in Fig. 21. A controller monitored the counterface surface temperature and maintained the temperature to $\pm$ 1 °C. The heating was allowed to equilibrate for approximately 10 minutes prior to the test run. This amount of time was necessary to equilibrate the force transducer to induced thermal stresses.

After constant output was attained by the force transducer the hemisphere was placed against the counterface for 2 minutes. Heating for this amount of time affected only a thin layer (on the order of $\mu$m depths) of the material not the bulk properties. Heating for less than 2 minutes resulted in varying friction force readings during a single test run. As sliding commenced, the thin heated layer was transferred to the counterface, and the cooler subsurface material was in contact during the rest of the pass. Figure 22 shows a representation of the friction time histories for a test at 20 and 30 °C which were allowed to rest on the surface for 2 minutes. In addition a test at 30 °C which was tested almost immediately after being placed in contact is shown. The friction force approaches the 20 °C value as time passes.

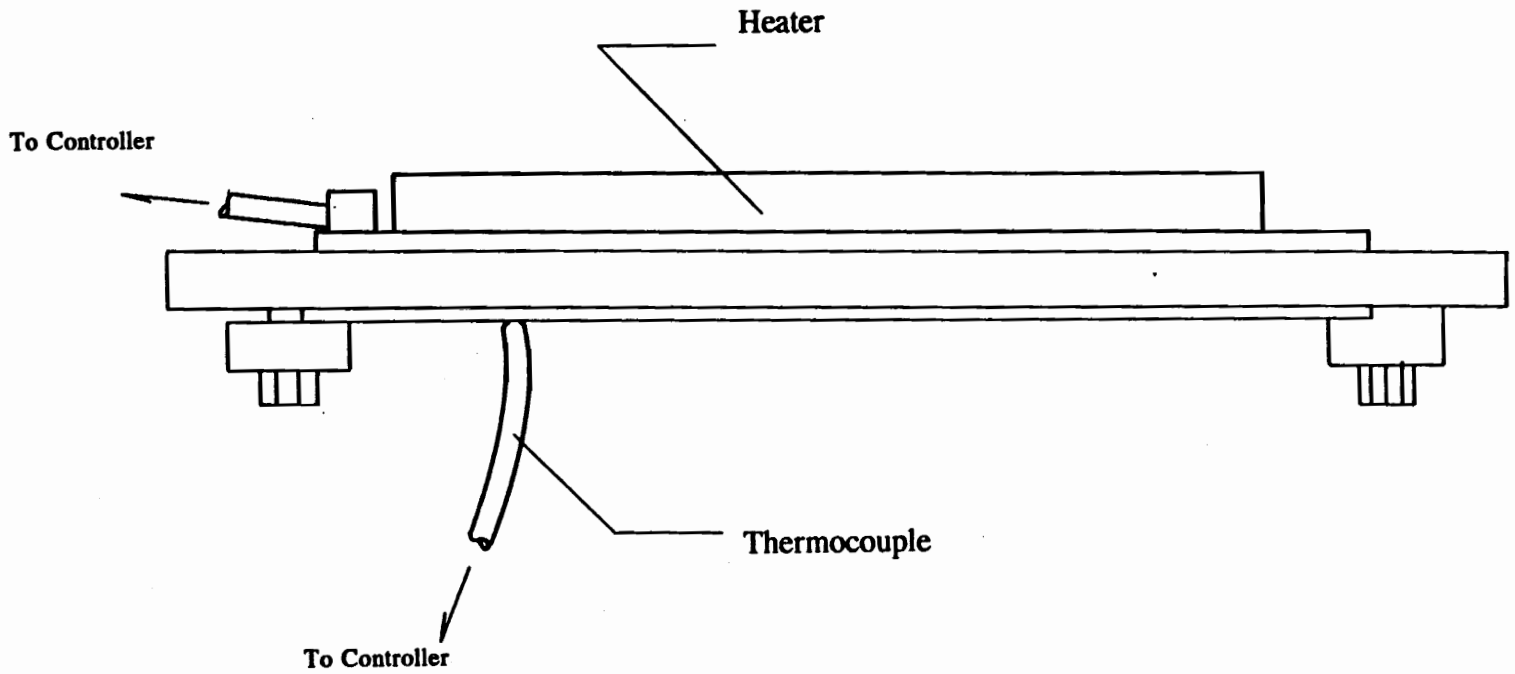


Figure 21. Heating of Counterface.

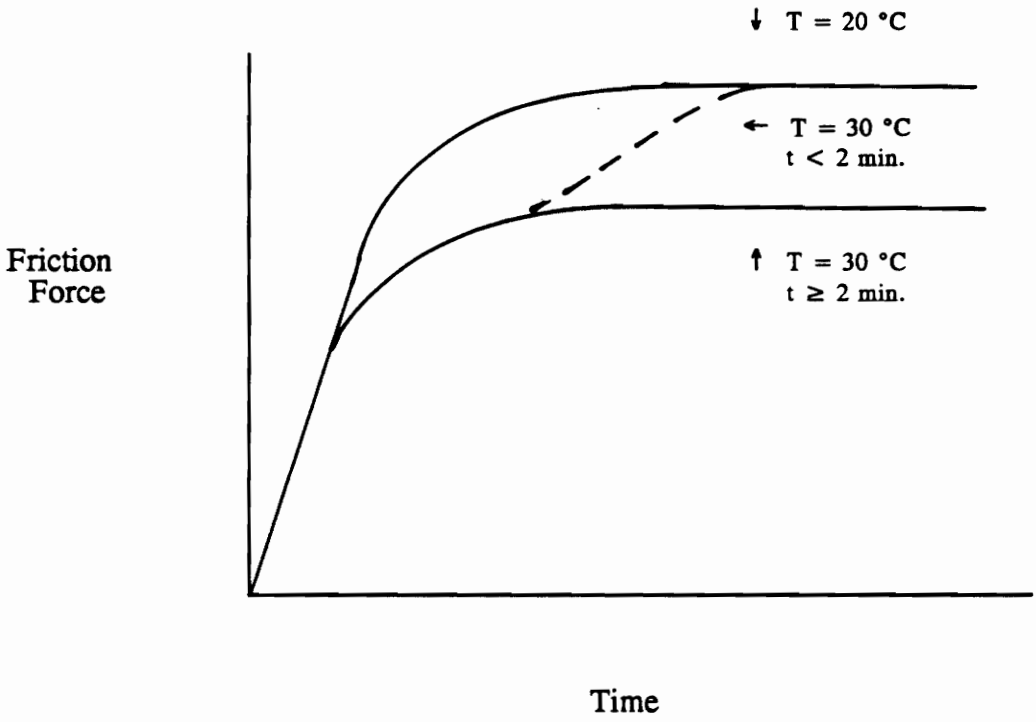


Figure 22. Friction Time Histories for Various Dwell Times and Temperatures.

## WET TESTS

The wet tests were performed in the same manner as all the other tests. The water was applied to the counterface and the hemisphere with a Kimwipe that was saturated with distilled water. The Kimwipe was allowed to sit on the surface of the hemisphere until immediately prior to the test run. This was done to ensure a uniform coating coating of distilled water. Since the tests were not performed in a flooded water environment the possibilty of hydrodynamic effects were very limited.

## THICKNESS MEASUREMENTS OF TRANSFER FILM

The thickness of the elastomer transfer film on the chromium oxide plate was investigated using ellipsometry. Ellipsometry is a technique where polarized light is projected at an angle relative to the surface and captured at the same angle on the other side of the surface. This is shown in Fig. 23. Since there is a thin film of transfer on the surface the rotating polarized light, previously circular, hits the detector as an ellipse. This distortion of the circle is caused by the different path lengths that the polarized light has to travel.

When a test was used to determine the thickness of the transfer film, the chromium oxide plate was plasma cleaned with oxygen. The plasma cleaning was done to reduce the oxide layer from the manufacturing process and provide consistent optical properties. Immediately prior to the test run the plate was cleaned with acetone. In

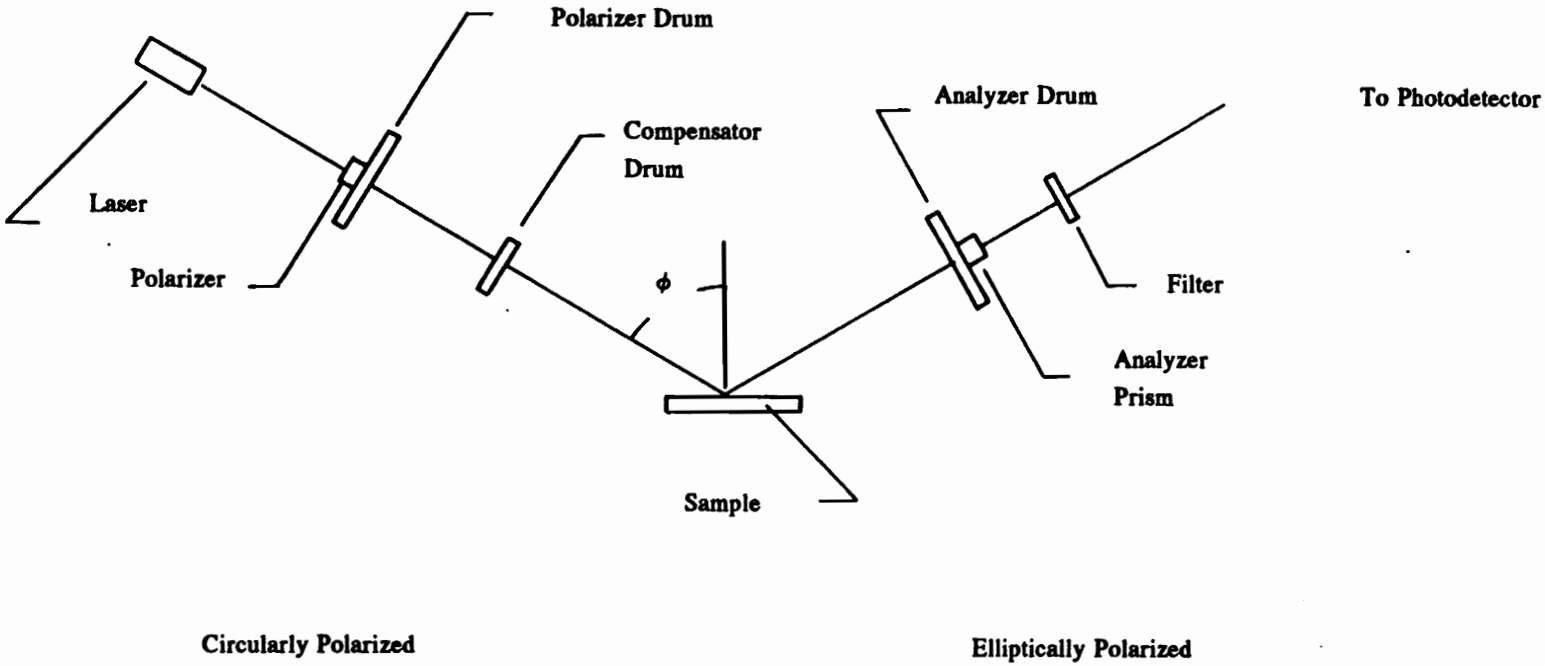


Figure 23. Ellipsometry Measurement.

reality, this contaminated the surface relative to the plasma cleaning. However, this was done to provide consistent surfaces between tests. Immediately following the test run the plate was transported to the ellipsometer to determine the film thickness. The optical constants of the plate were averaged from 6-10 measurements around the transfer film for reference optical properties as shown in Fig. 24. The 10 readings were then averaged and used as the properties of the plate. The averaged optical properties resulted in a minimum resolvable thickness of approximately 4 - 6 angstroms.

## NORMAL LOAD AND TANGENTIAL FORCE COUPLING

In the design of the test apparatus there is coupling between the normal load and tangential (i.e. friction) force. Figure 25 shows that the pivot point for the load is not in-line with the application of the friction force. Elimination of the coupling was not possible within the constraints of the current design. An entirely new test apparatus would have had to been built to eliminate the coupling. The coefficient of friction was no longer the measured friction force divided by the nominal normal load. The calculation of the coefficient of friction was modified to take into account the coupling which reduced the normal load with increased friction force.

By summing moments and forces around the load arm pivot point the normal load can be determined from the nominal initial load and the measured friction force.

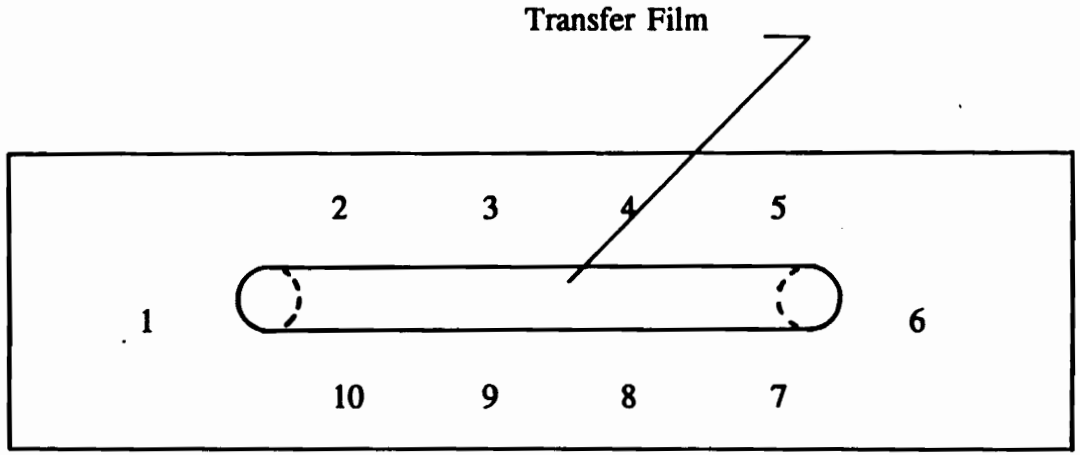


Figure 24. Location of Reference Measurements for Optical Properties of Chromium Oxide Plate.

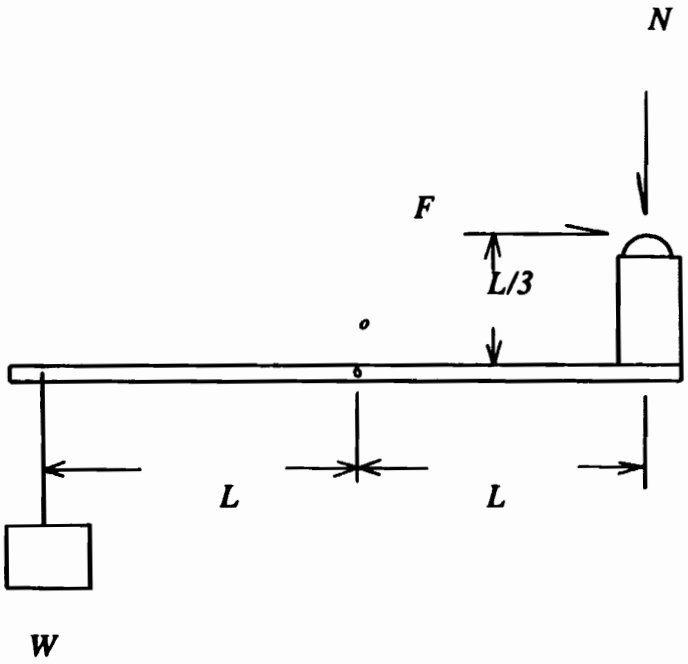


$$\Sigma M_o = F\,(L/3) + N\,L - W\,L = 0$$

Figure 25. Coupling of Tangential and Normal Forces.

$$N = W - \frac{F}{3} \tag{24}$$

where:

$W$ = initial applied normal load

$F$ = measured friction force

The actual coefficient of friction can be determined from the following relation which is the value used in all the results and discussion.

$$\mu_{actual} = \frac{\mu_{apparent}}{(1 - \mu_{apparent} / 3)} \tag{25}$$

where:

$\mu_{apparent}$ = F/W

Due to the above considerations the normal load given in subsequent figures is the nominal initial load not the actual load at the point of slip.

## EXPERIMENTAL RESULTS

In this section the friction results of the various elastomers and counterfaces will be presented. The friction-velocity curves for curves will be presented along with various representative friction time histories of individual points on the curve to illustrate pertinent trends. In addition, the first data presented will be the thickness results of a series of tests for the 5 phr carbon black natural rubber in order to investigate the validity of the dominance of adhesive friction. These results will be presented ahead of the rest of the natural rubber results, but this order will be beneficial to the interpretation of the subsequent results. Even though the original purpose of the research was to investigate dry sliding a series of tests were run under wet conditions. Unsteady oscillations depend upon the system properties (e.g. stiffness, damping and inertia) and the frictional properties of the sliding pair. It so happens that these wet tests yield valuable insight into the requirements for oscillations and provide an additional factor that must be considered in the use of elastomers in sliding applications.

### Transfer Films

In dry sliding it was found that stick-slip occurred only when a transfer film was deposited on the counterface. The hemispheres had to have the molding "skin" broken to in order to transfer material to the counterface. In addition the test velocity had to be above a critical value for noise to occur.

In tests against glass, the transfer of material was sensitive to the cleaning procedure. Glass cleaned with isopropanol (isopropyl alcohol) had a lower coefficient of friction than glass cleaned with acetone and exhibited no transfer. Stick-slip was not evident in the isopropanol/glass tests for the velocity range tested.

Measurements show that the transfer films were very thin, on the order of 20-100 angstroms. The presence of the transfer was visually detectable by the reduced reflection of light from the chromium oxide counterfaces. The high polish of the surface yielded a reflective mirror finish which made it the only material of those included in the test plan suitable for the ellipsometry measurements. The transfer films appeared to be coherent rather than patchy.

A series of tests at constant normal load (17.8 N) were run to determine if the transfer film thickness was a function of velocity or temperature. Fig. 26 shows the transfer film thickness for a series of velocity tests. Tests were run both below and above the minimum velocity ,$v_{crit}$, required for noise generation. A slight upward trend to the data with increasing velocity can be noticed with a linear regression line calculated from all the data points, not just the means. A comparison of means between the data at $v$ = 1.397 mm/s and the data at $v$ = 25.4 mm/s with the smallest standard deviation was performed.

Similarly, the thickness of the transfer film was determined for a series of tests with varying temperature at a constant velocity ( $v$ = 2.819 mm/s). None of these tests produced noise. The result is shown in Fig. 27. Ignoring the outlying data at 40 °C (no explanation for the deviation) there appears to be a slight downward trend with increasing

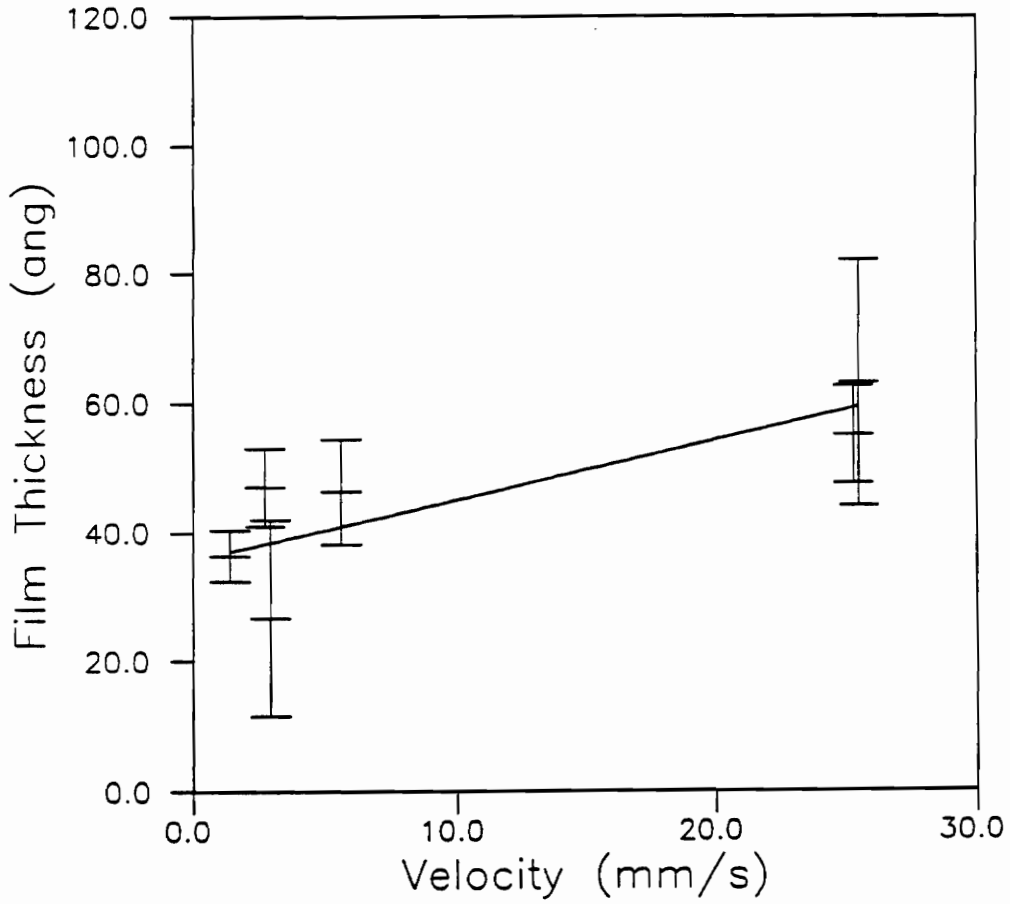


Figure 26. Velocity Effect on Film Thickness of 5 phr c.b. Natural Rubber against Chromium Oxide (Load = 17.8 N, T = 20 °C)
* Bars indicate minimum, mean and maximum values.

temperature. Once again the regression line was fit through all the data points with the exception of the outliers at 40 °C. Qualitatively this is in agreement with the upward trend of increasing velocity. Comparison of means of the data at $T$ = 15 °C and $T$ = 51 °C yields the same result as before. Namely, the means are not significantly different at the 99% confidence level, but are different at the 95% confidence level.

Figures 28a-d shows the film thickness for various conditions. The intent of Fig. 28 is to show that there is no consistent trend to the transfer film thickness as a function of distance slid. Figure 28a has the largest change in transfer film thickness over the distance traveled of all the tests measured.

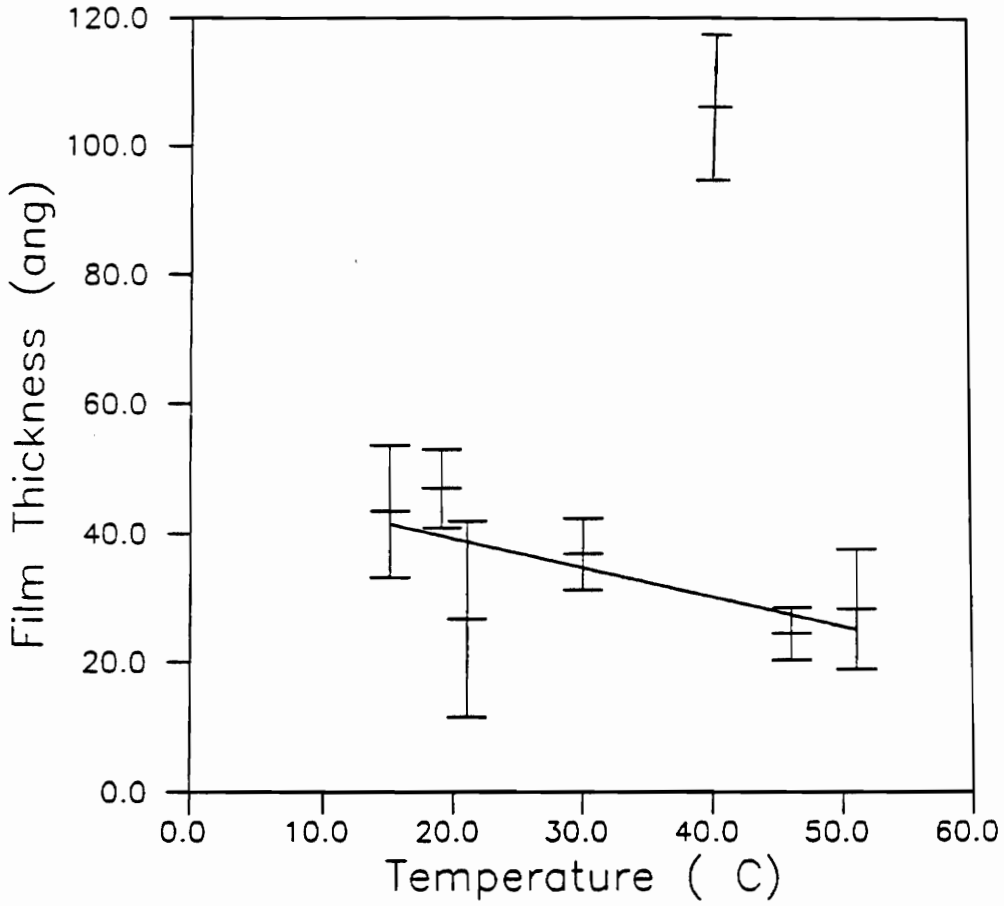


Figure 27. Temperature Effect on Film Thickness of 5 phr c.b. Natural Rubber against Chromium Oxide (Load = 17.8 N, Velocity = 2.819 mm/s)
* Bars indicate minimum, mean and maximum values.

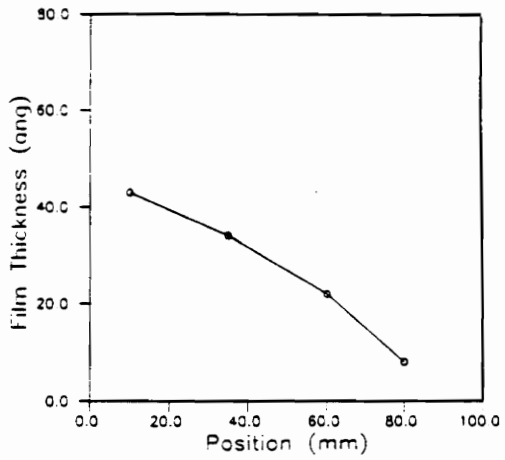


a. v= 2.819 mm/s
T= 20° C

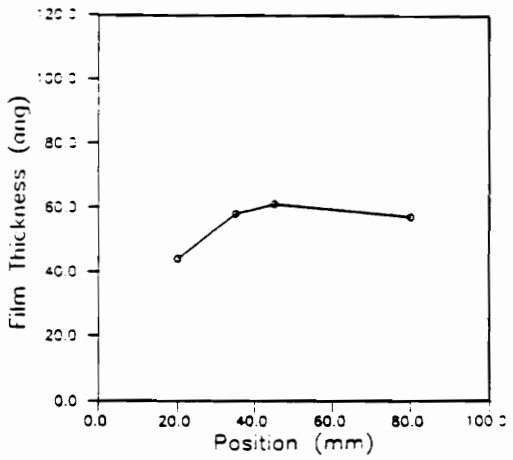


b. v= 25.4 mm/s
T= 20° C

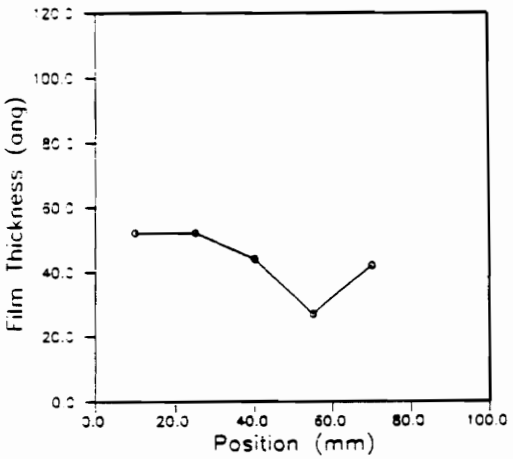


c. v= 2.819 mm/s
T= 15° C

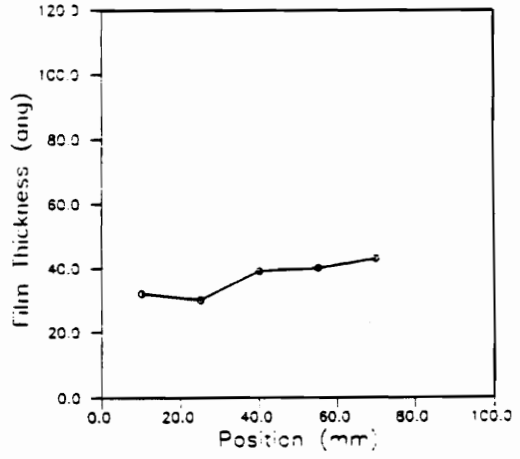


d. v= 2.819 mm/s
T= 30° C

Figure 28a-d. Dependence of Film Thickness on Sliding Distance of 5 phr c.b. Natural Rubber against Chromium Oxide. (Load= 17.8 N)

Figures 29, 30 and 31 show the results of the FTIR (Fourier Transform Infrared Spectroscopy) of the transfer film against chromium oxide and aluminum and the photoacoustic analysis of the bulk material to determine any differences. Comparison of Figs. 29, 30 to Fig. 31 shows that the chemical composition of the transfer and the bulk is the same. Figure 32 shows the spectrum of isoprene for comparison. Table 4 shows the major peaks from Figs. 29,30 & 31, tabulated for comparison. In addition, the spectra for $C_4H_{10}$ is tabulated to show the agreement with the transferred material.

**Friction Results**

Friction results were obtained at various velocities and load to determine the shape of the friction-velocity curve. Stick-slip or harmonic oscillations, in theory, require certain general shapes to the friction-velocity curve to occur. Historically, even the experimental results [8,18] have shown a negative slope to the friction-velocity curve in regions of stick-slip. Therefore, prior to this research it was generally predicted that noise or oscillations are incipient at the velocity where the slope of the friction-velocity curve becomes negative.

The critical velocity at which stick-slip occurs has been theoretically related to the peak in tan $\delta$ and experimentally to the peak in E''. Thus, elastomers should possess a critical velocity that is related to $T_g$. Specifically, increasing $T_g$ should result in an decrease in the critical velocity. Generically, the elastomers can be ranked according to the $T_g$ of the monomer unit. In the case of filled elastomers, the $T_g$ of the the elastomer

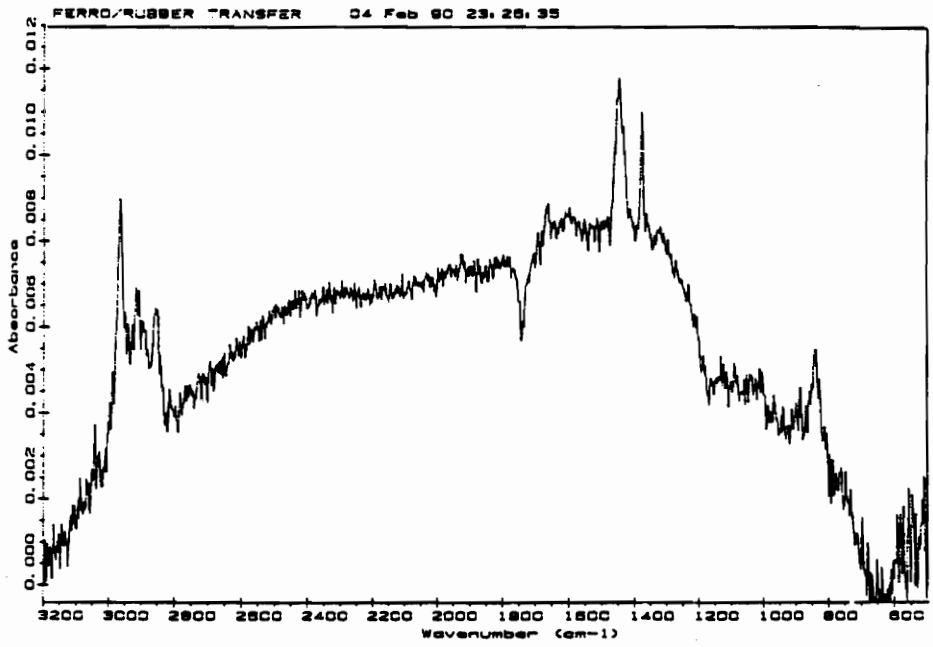


Figure 29. FTIR of Natural Rubber Transfer Film (5 phr c.b. against Chromium Oxide).

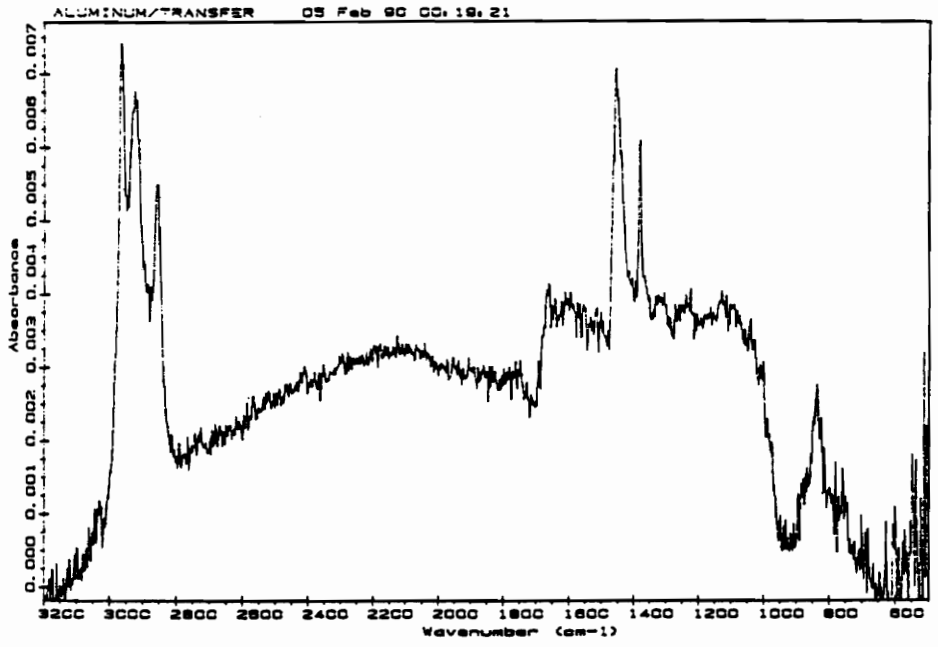


Figure 30. FTIR of Natural Rubber Transfer Film.
( 5 phr c.b. against Aluminum).

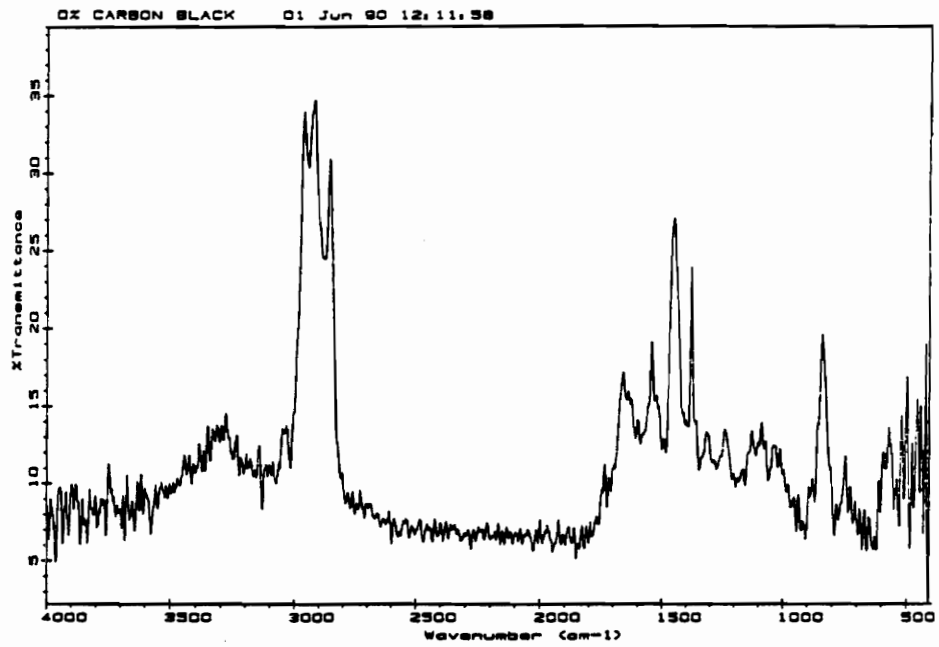


Figure 31. Photoacoustic Analysis of the Bulk Natural Rubber ( 0 phr c.b. ).

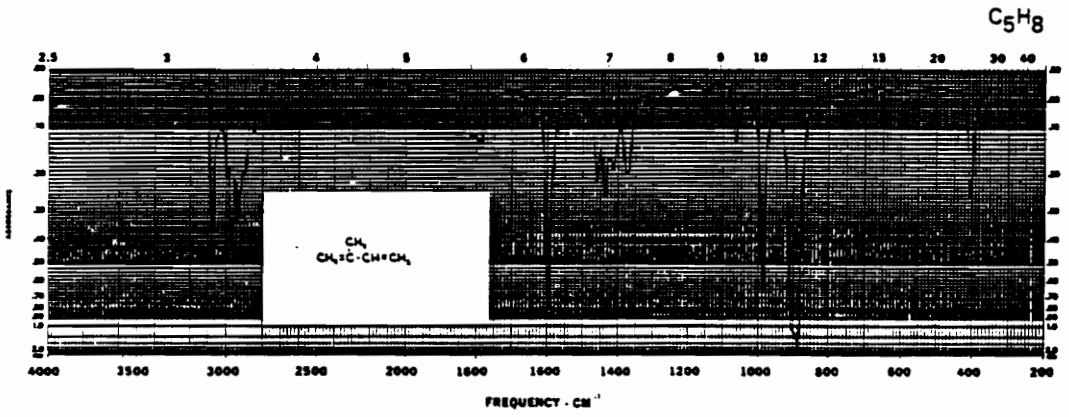


Figure 32. Infrared Spectra of Isoprene [39].

Table 4. Wavenumbers for Bulk and Natural Rubber

| Peak # | Type of Bond | Transfer Film 5 phr c.b. Natural Rubber | | Bulk 0 phr c.b. Natural Rubber |
|---|---|---|---|---|
| | | Chromium Oxide | Aluminum | |
| 1 | $CH_3$ Asymmetric Stretching | 2963 | 2963 | 2961 |
| 2 | $CH_2$ Asymmetric Stretching | 2911 | 2911 | 2922 |
| 3 | $CH_2$ Symmetric Stretching | 2855 | 2855 | 2855 |
| 4 | $CH_2$ Scissoring | 1449 | 1449 | 1449 |
| 5 | $CH_3$ Bending Vibration | 1376 | 1376 | 1376 |
| 6 | C-H Deformation Vibration | 839 | 839 | 839 |

changes slightly with the amount of filler. In the particular case of the carbon black filled natural rubber, increasing the amount of carbon black increases the hysteresis which results in an increase in $T_g$. The following order should be observed in the critical velocities (ranked from highest to lowest).

1. PDMS $T_g$= -123 °C
2. Natural Rubber $T_g$= -73 °C (0 phr c.b.)
    a. 0 phr c.b.
    b. 5 phr c.b.
    c. 10 phr c.b.
    d. 20 phr c.b.
    e. 50 phr c.b.
3. Butyl $T_g$= -72 °C
4. Fluorocarbon $T_g$= -55 °C

There are some general comments about the friction-velocity and friction-time histories that can be made for all the elastomers. For all the elastomers tested the coefficient of friction rises with increasing velocity, reaching what can be described as a breakpoint where the friction starts to level off. In some cases it continues to gradually increase with increasing velocity. The critical velocities for the above elastomers ranged from 5 to 25 mm/s. This disagrees with the friction theories which predict critical velocities that should be related to the $T_g$ of the elastomer. Shifts of up to 3 decades in velocity should be apparent due to the different $T_g$'s of the elastomers tested.

The friction-time histories also evidence common features between the various elastomers and counterfaces. The greatest commonality is the roll off of the friction force from a linear rise rate prior to reaching the maximum kinetic friction level. Figure

33 shows the deviation from the linear rise rate of the friction force. The kinetic coefficient of friction for steady-state and unsteady sliding is defined as the maximum value attained. The static and kinetic coefficients of friction for steady sliding are shown in Fig 33. For unsteady sliding the maximum and minimum kinetic coefficients of friction, $\mu_{kmax}$ and $\mu_{kmin}$, are defined as shown in Fig. 34. In many cases $\mu_{kmin}$ appears to be approximately the same as $\mu_{static}$.There is some ambiguity in interpretation of the minimum value because the natural frequency of the test apparatus in the tangential direction is excited.

Additionally, the critical velocity for noise generation by all the observed phenomena (harmonic oscillations, stick-slip, and Schallamach waves) was a function of load. In general, increasing load or normal pressure reduced the velocity at which unsteady sliding commenced.

### Modal Analysis

Figure 34 shows the high frequency ringing after a slip event. For the time being this can be thought of in the context of classical stick-slip. Later the concept of stick-slip will be rexamined in light of results that will be presented. Modal analysis of the the test apparatus showed that the high frequency ringing was the natural frequency of the test apparatus in the tangential direction. The modal

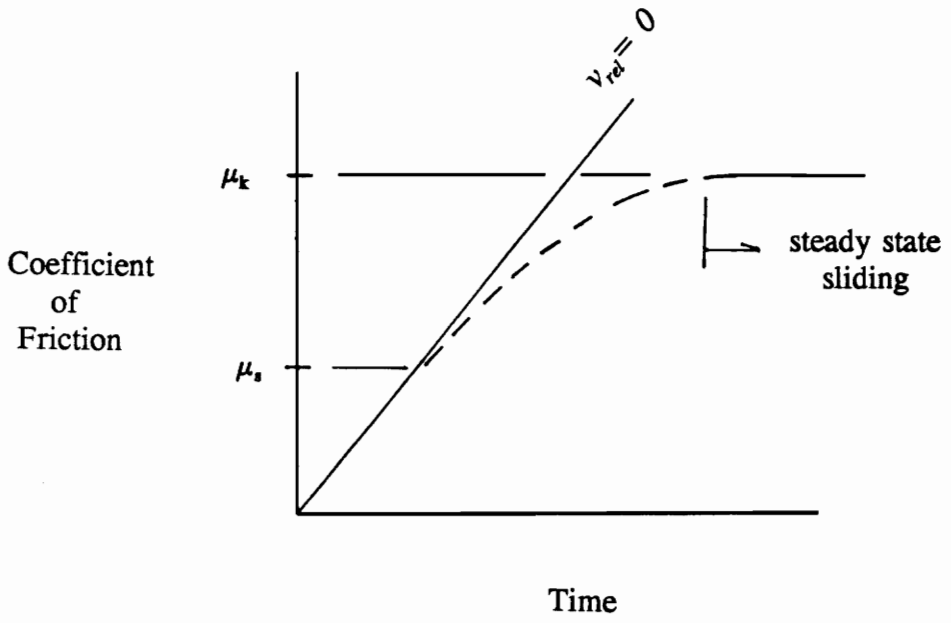


Figure 33. Deviation from Linear Rise Rate for Friction Time History.

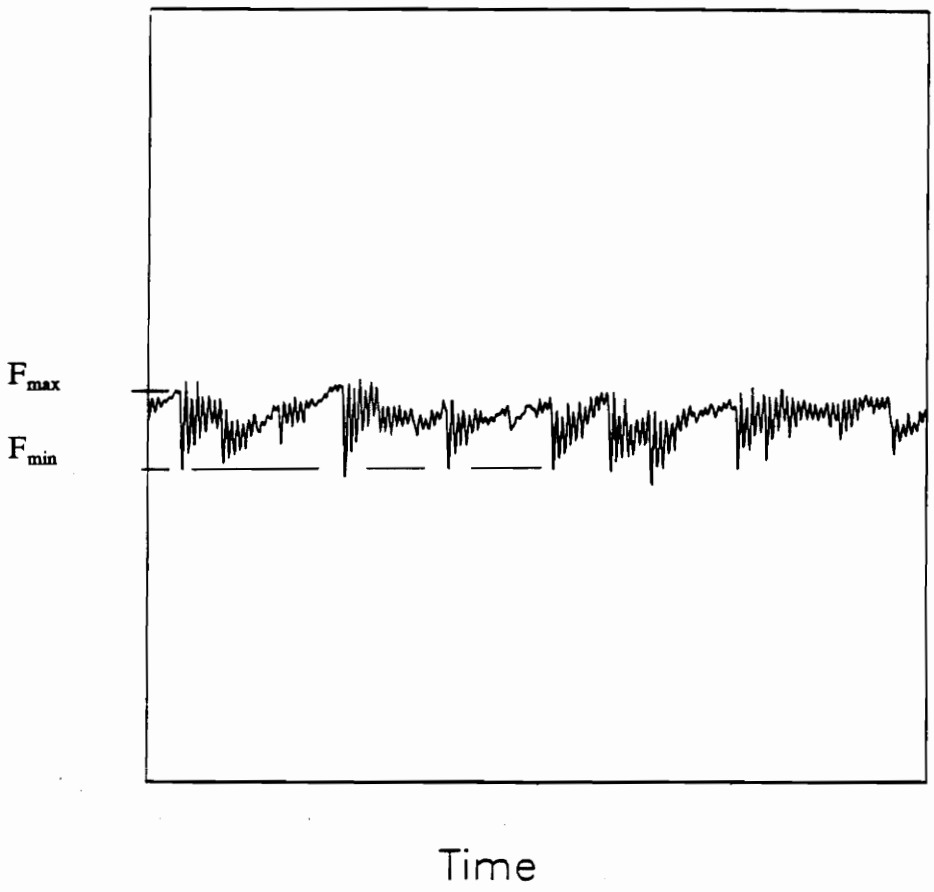


Figure 34. Definition of Minimum and Maximum Friction Forces.

analysis was performed by striking one end of the plate assembly and performing a transfer function analysis with the hammer force transducer and the force transducer mounted in the test apparatus. The friction force transducer was measuring the vibration present in the plate in the tangential direction. The natural frequency was 1450 Hz with or without the elastomer loaded against the counterface. The lack of noticeable shift in the natural frequency was not suprising considering the low mass and stiffness of the elastomer. As future results will illustrate, the stick-slip frequency and therefore the high frequency of oscillation appears periodic but lacks stationarity. Therefore the typical data analysis techniques in the frequency domain were not as effective as just measuring the frequency of stick-slip in the time domain to determine whether or not the stick-slip frequency changed with veloctiy.

## Dry Friction Results

### Natural Rubber

As previously stated, natural rubber hemispheres were provided by Ford Motor Co. with 0, 5, 10, 20 ,50 phr carbon black. The 0 phr specimens could not be tested because the lack of carbon black filler yielded very poor rupture properties and the specimens failed with a large crack ($\approx$ 5 mm long) running perpendicular to the hemisphere surface and perpendicular to the direction of sliding. This failure occurred in the rear of the contact area in the region of the largest tensile stresses.

For the rest of the natural rubber specimens, the frictional instabilities stick-slip or harmonic oscillations were encountered. There was no evidence when sliding against glass that Schallamach waves were present. However, due to the poor reflectance of the black specimens the existence of Schallamach waves can not be discounted entirely.

**Natural Rubber-5 phr c.b.**

A wide range of tests were run with the 5 phr c.b natural rubber specimens. The majority of work with the various counterfaces was performed with this elastomer since it would yield noise more easily than the elastomers containing higher amounts of carbon black.

The first set of data to examine is a test matrix of varying load and velocity. Figure 35 shows the effects of varying load and velocity on the maximum kinetic coefficient of friction and the initiation of noise. It is obvious from Fig. 35 that as the load is increased the coefficient of friction decreases. The lowest load or pressure level does not create noise over the velocity range tested. For the load values tested, the critical velocity for the initiation of noise decreases with increasing load.

Examination of the median load value of 17.8 N with more detail shows the friction-velocity relationship as shown in Fig. 36. There is the large increase in coefficient of friction with a small increase of velocity until the critical velocity is reached and the increase becomes more gradual. Time histories of the 5 phr c.b. natural

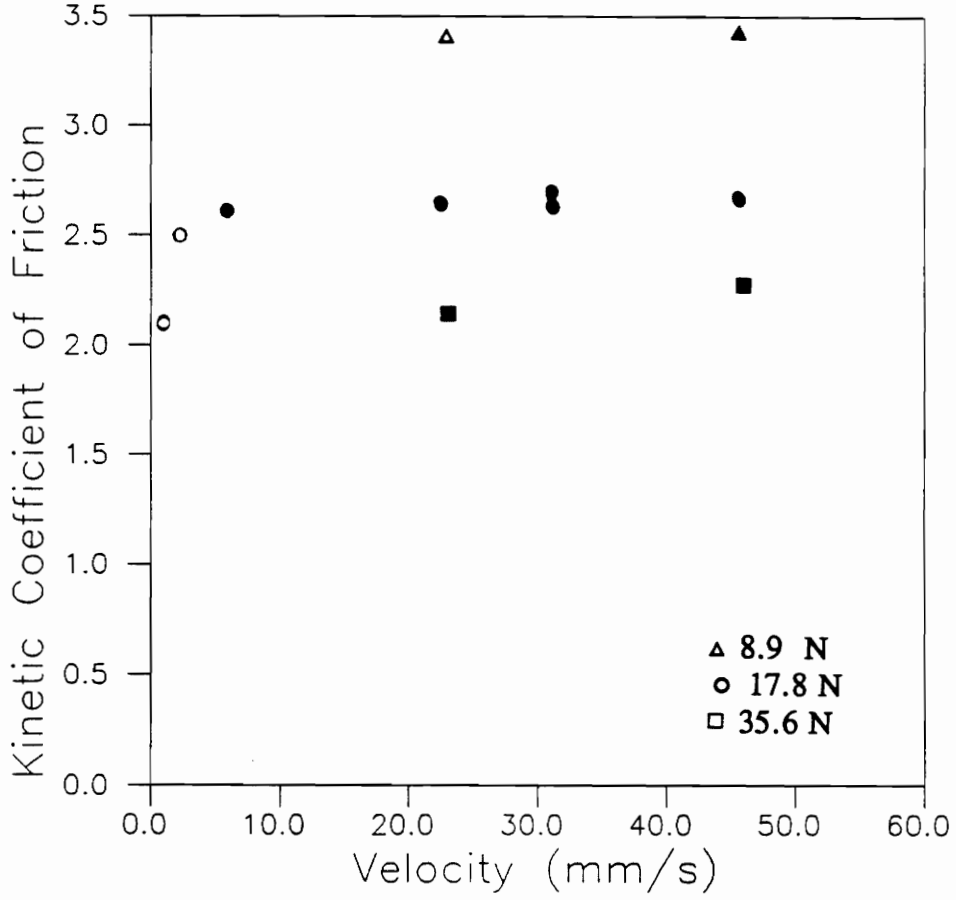


Figure 35. Friction-Velocity Matrix for 5 phr c.b natural rubber against Chromium Oxide with Various Loads.
* Solid symbols indicate oscillatory tests

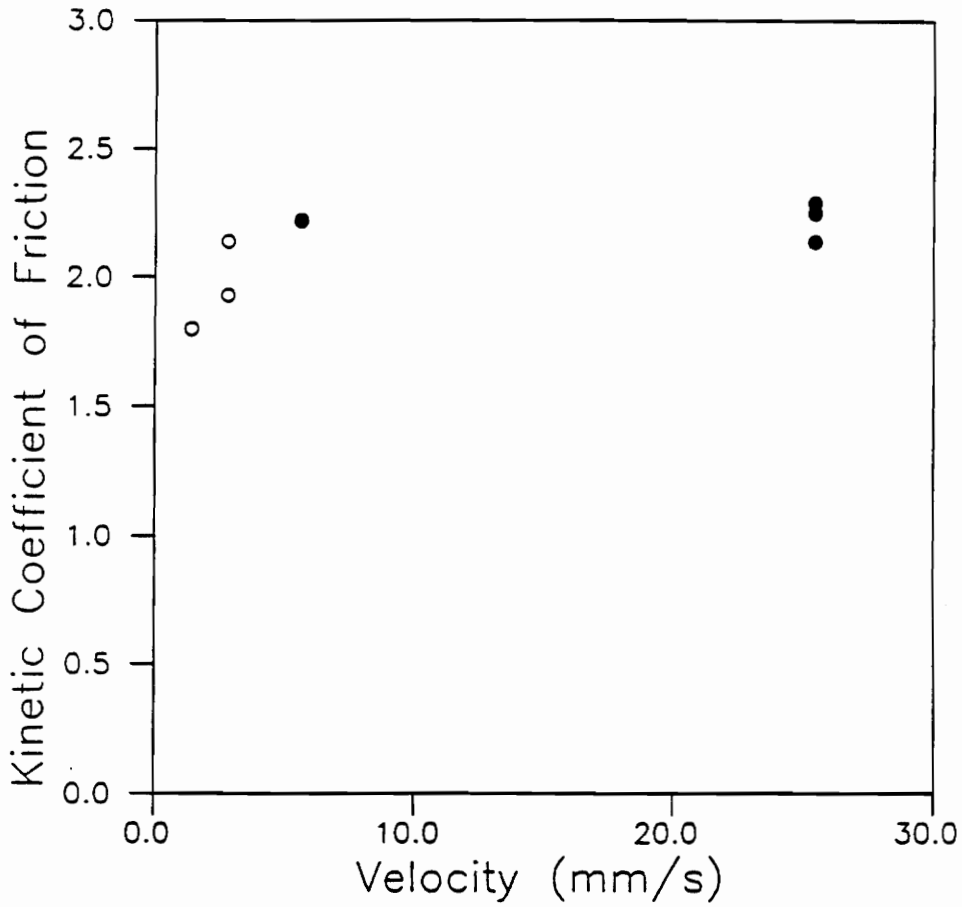


Figure 36. Friction-Velocity Relationship for 5 phr c.b. Natural Rubber against Chromium Oxide (Load = 17.8 N)
* Solid symbols indicate oscillatory tests

rubber specimen for $v$= 2.819, 22.55, and 33.83 mm/s are presented in Figs. 37, 38 and 39 respectively. For this series of tests the frequency of stick-slip locked on to 38 Hz (see Fig.38 t > 1.5 s).

The results of testing against the various counterfaces will now be presented to distinguish between any similarities or differences that may exist. The first set of data that will be presented is low speed sliding ($\approx$1.497-4.05 mm/s). Here a series of tests with varying velocity were run against chromium oxide, glass, cathodic epoxy, and powder epoxy.

For smooth surfaces the friction force should scale with the area of contact and the specific adhesion forces that must be overcome to shear the interface. Therefore, two predictions can be made concerning surface roughness and surface energy (i.e. water contact angle measurements). Since smoother surfaces create a larger area of contact the friction force should increase with decreasing roughness. In the Literature Review it was shown that the work of adhesion, which should be a measure of the friction force, scales with 1 + cos $\Theta$. The first comparison was the friction force recorded for chromium oxide and glass counterfaces. Since glass possesses a lower roughness (5X) and a higher surface energy than chromium oxide, glass should have a higher coefficient of friction. However as can be seen from Fig. 40 comparison of the friction force between the two materials yields very little difference (< 3%). The powder epoxy has a lower surface energy and a quarter of the roughness of the cathodic. However, as can be seen from Fig. 41 the friction-time histories are virtually identical.

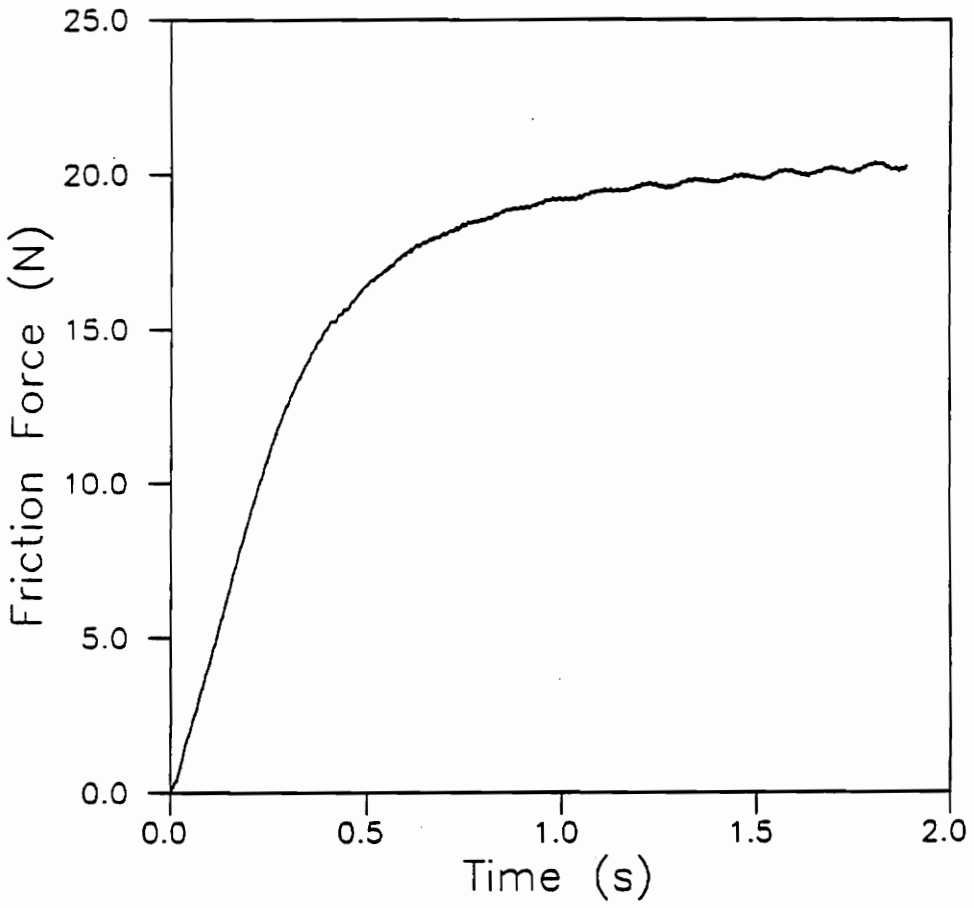


Figure 37. Friction Time History of 5 phr c.b. Natural Rubber against Chromium Oxide (Load = 17.8 N, v= 2.819 mm/s)

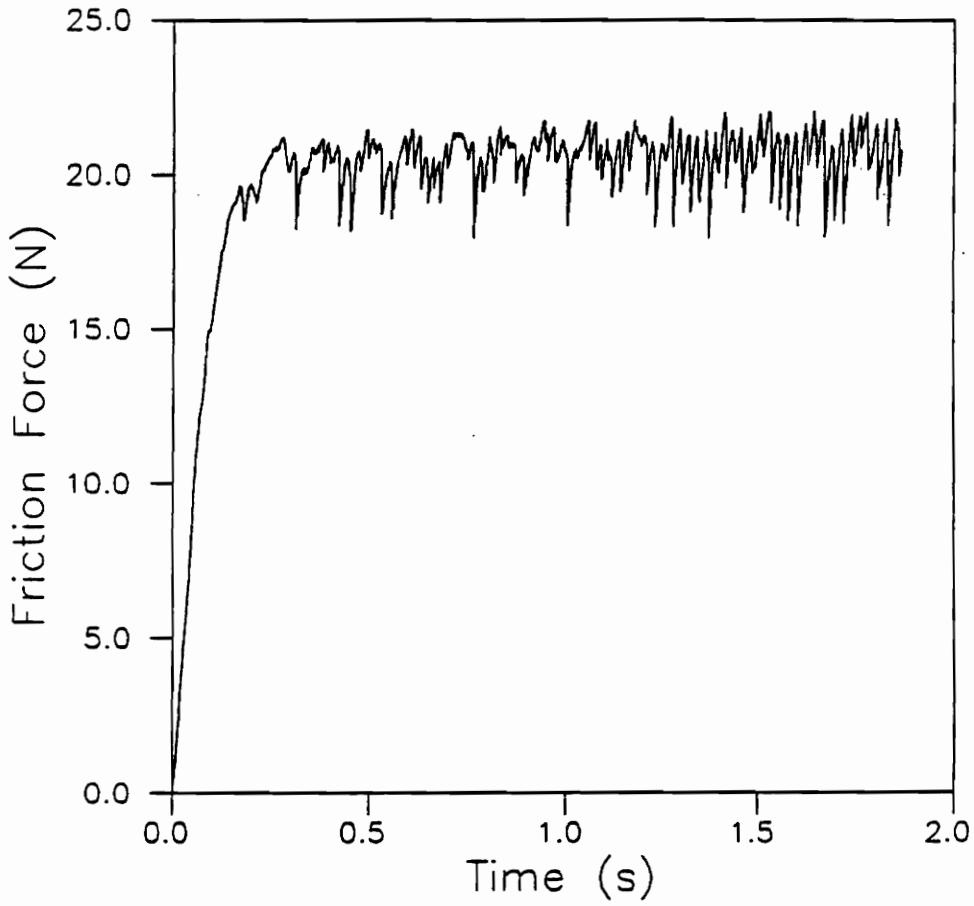


Figure 38. Friction Time History of 5 phr c.b. Natural Rubber against Chromium Oxide (Load = 17.8 N, v= 22.55 mm/s)

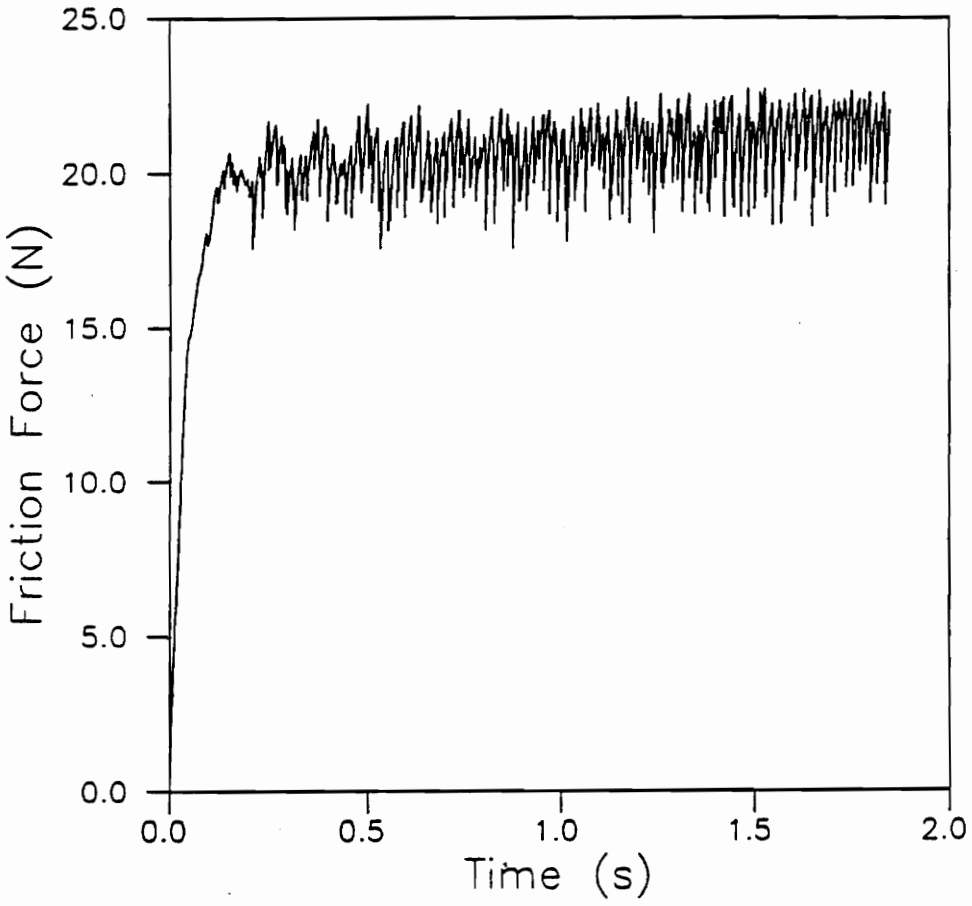


Figure 39. Friction Time History of 5 phr c.b. Natural Rubber against Chromium Oxide (Load = 17.8 N, v= 33.83 mm/s)

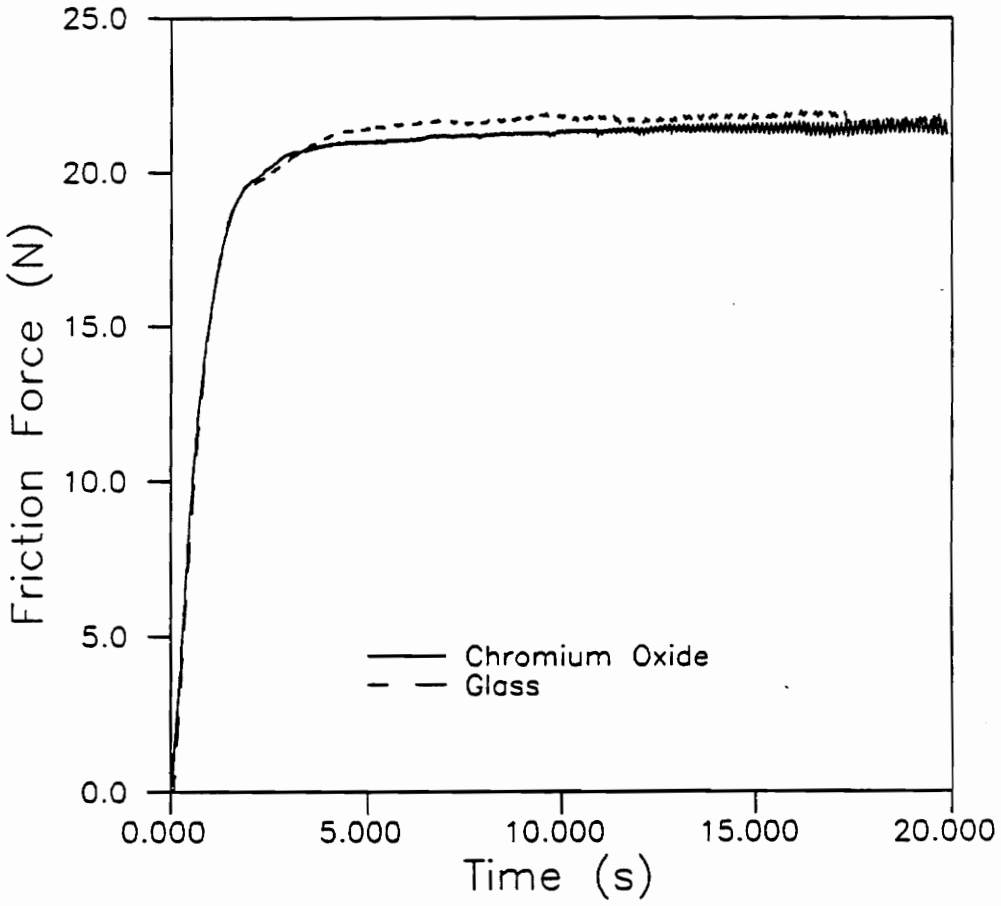


Figure 40. Friciton Time History of 5 phr c.b. Natural Rubber against Chromium Oxide and Glass (Load = 17.8 N, v = 2.819 mm/s).

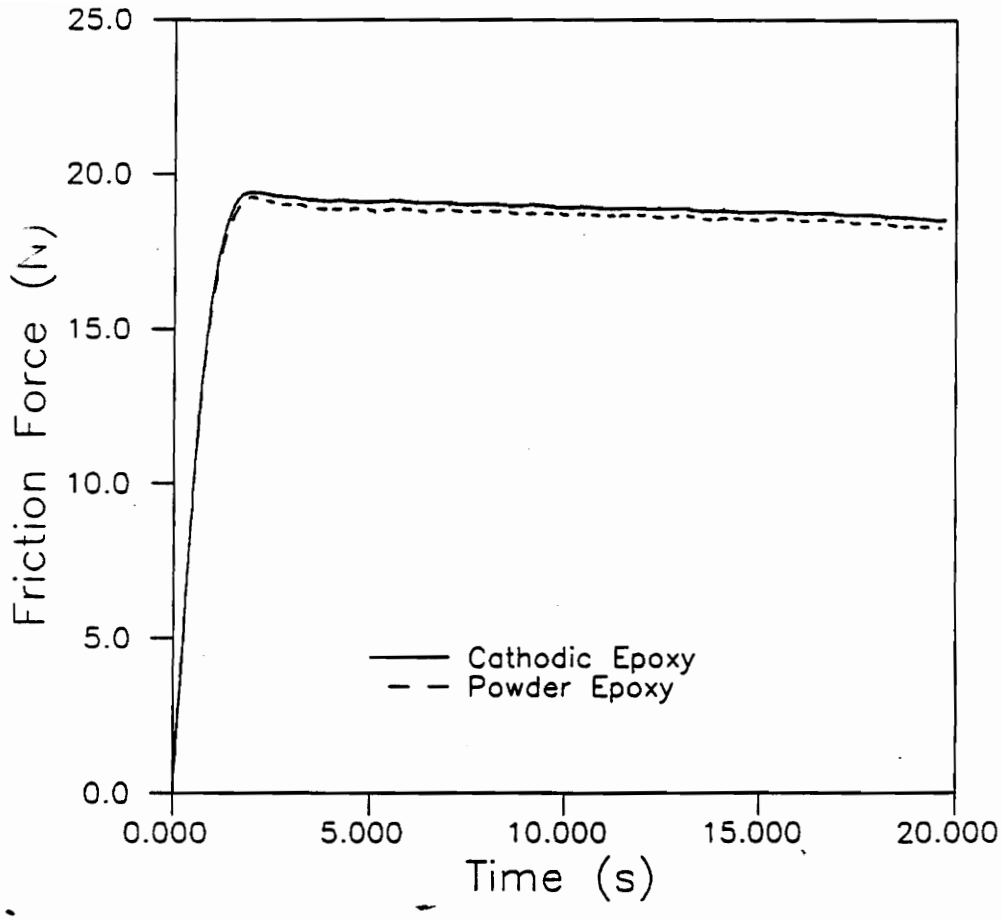


Figure 41. Friction Time History of 5 phr c.b Natural Rubber against Cathodic and Powder Epoxy (Load = 17.8 N, v = 2.819 mm/s).

Comparing chromium oxide from the first set and cathodic epoxy from the second set in Fig. 42 a difference in the coefficient of friction is seen. Figure 43 shows a comparison over the entire velocity range for chromium oxide and cathodic epoxy counterfaces. The chromium oxide starts generating noise at a velocity of 2.819 mm/s, whereas, neither epoxy counterface generated noise over the velocity range tested. However, the coefficient of friction continues to increase for the cathodic epoxy and may eventually cross the threshold value required for the generation of noise.

**Natural Rubber-10 phr c.b.**

The natural rubber specimens containing 10 phr c.b. evidenced greater resistance to wear than the 5 phr c.b. specimens. It was apparent that for sliding purposes, the amount of carbon black filler in natural rubber should be at least 10 phr. Any less carbon black content does not possess the proper wear resistance for multiple passes of a counterface. Of course the reason for choosing various amounts of carbon black was to vary the viscoelastic properties to determine their effect on noise generation, not the effect on wear.

The first set of results that are instructive to investigate are the test matrix of varying load and velocity. Figure 44 shows over the range tested the coefficient of friction increases with increasing velocity and decreases with increasing normal load or pressure. $V_{crit}$ also decreases for increasing load as shown in Fig. 44.

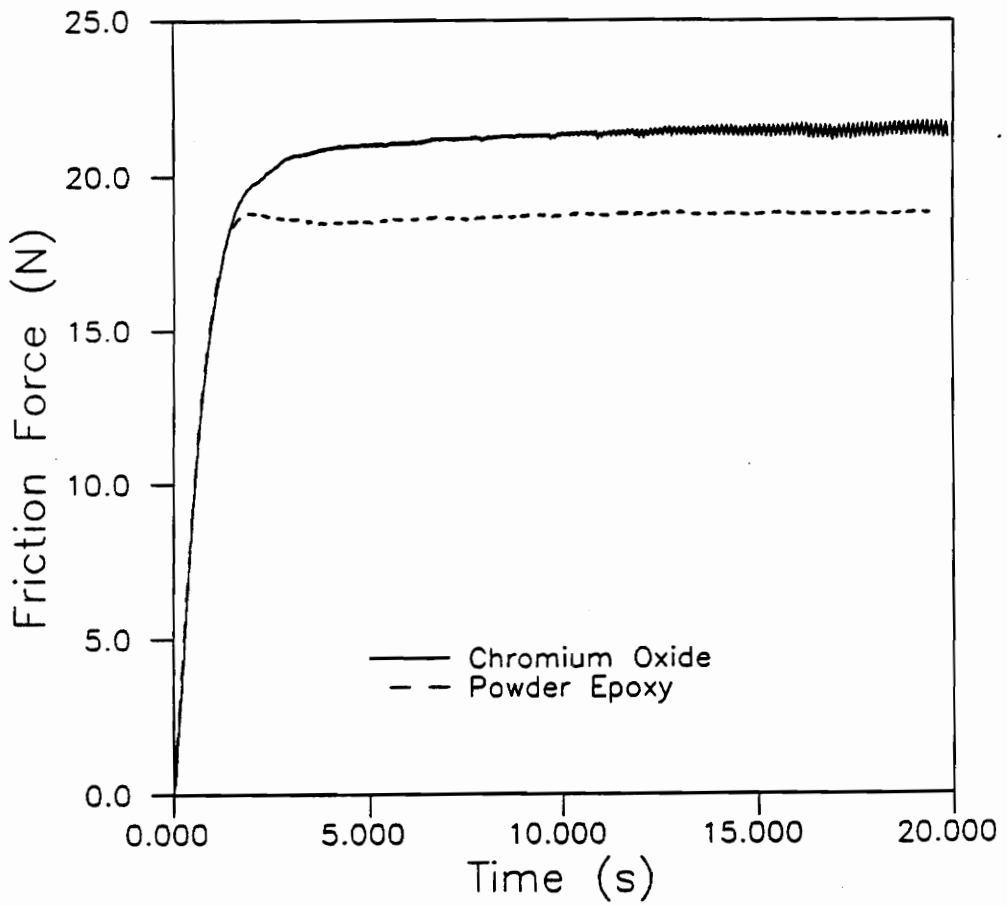


Figure 42. Friction Time Histories of 5 phr c.b. Natural Rubber against Chromium Oxide and Cathodic Epoxy (Load = 17.8 N, v= 2.819 mm/s).

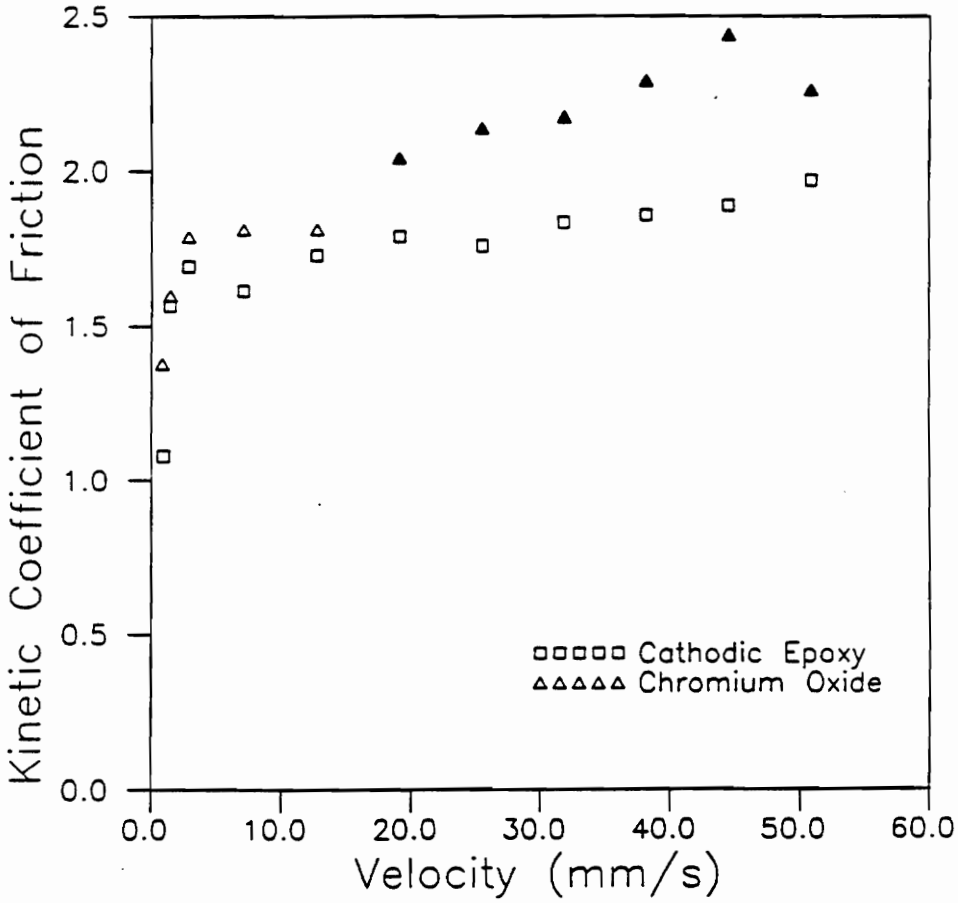


Figure 43. Friction-Velocity Relationship for 5 phr c.b. Natural Rubber against Chromium Oxide and Cathodic Epoxy (Load = 17.8 N)
* Solid symbols indicate oscillatory tests

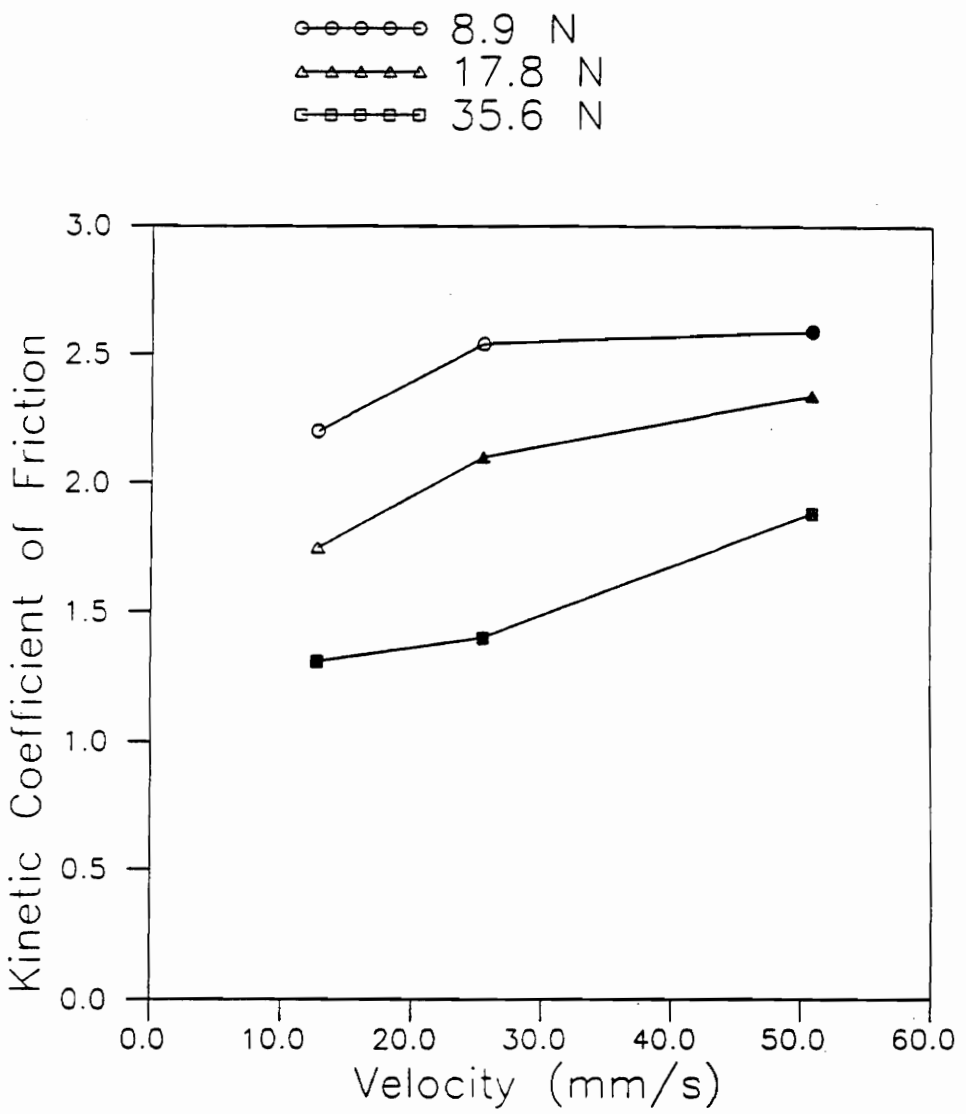


Figure 44. Friction-Velocity Matrix for 10 phr c.b. Natural Rubber against Chromium Oxide for Various Loads.

* Solid symbols indicate oscillatory tests

Figure 45 shows a more detailed look at the friction-velocity relationship for a normal load of 17.8 N against chromium oxide. $V_{crit}$ ($v$= 19.03 mm/s) is slightly greater than $v_{crit}$ ($v$= 2.819 mm/s) for 5 phr c.b. specimen. In addition the coefficient of friction is reduced. Figures 46, 47 and 48 show the time histories of the friction force for v = 1.409, 12.75, and 25.4 mm/s respectively.

**Natural Rubber-20 phr c.b.**

A series of tests were run at 8.9, 17.8 and 35.6 N against chromium oxide to determine the critical velocity of noise generation. Noise was generated at 7.05, 12.7 and 7.05 mm/s respectively for the 8.9, 17.8 and 35.6 N loads. Suprisingly, the 8.9 N test series had a lower critical velocity than the higher loads. This was atypical behavior. In general, increasing normal load decreased the critical velocity. The friction-velocity matrix is shown in Fig. 49 for comparison of the different load levels. The friction-velocity curves for the 8.9, 17.8 and 35.6 N loads are shown in Figs. 50, 51 and 52. The maximum kinetic coefficient of friction for 8.9 N is approximately 1.11 times the coefficient of friction for the 17.8 N load and 1.25 times the value of the 35.6 N load. There is no consistent trend for ranking the minimum values of the kinetic coefficient of friction for the three different normal loads. When the coefficient of friction is plotted against logarithmic velocity, there appears to be a decrease in the minimum coefficient of friction with increasing velocity. The possible exception to this trend is the last two data points for the 8.9 N load.

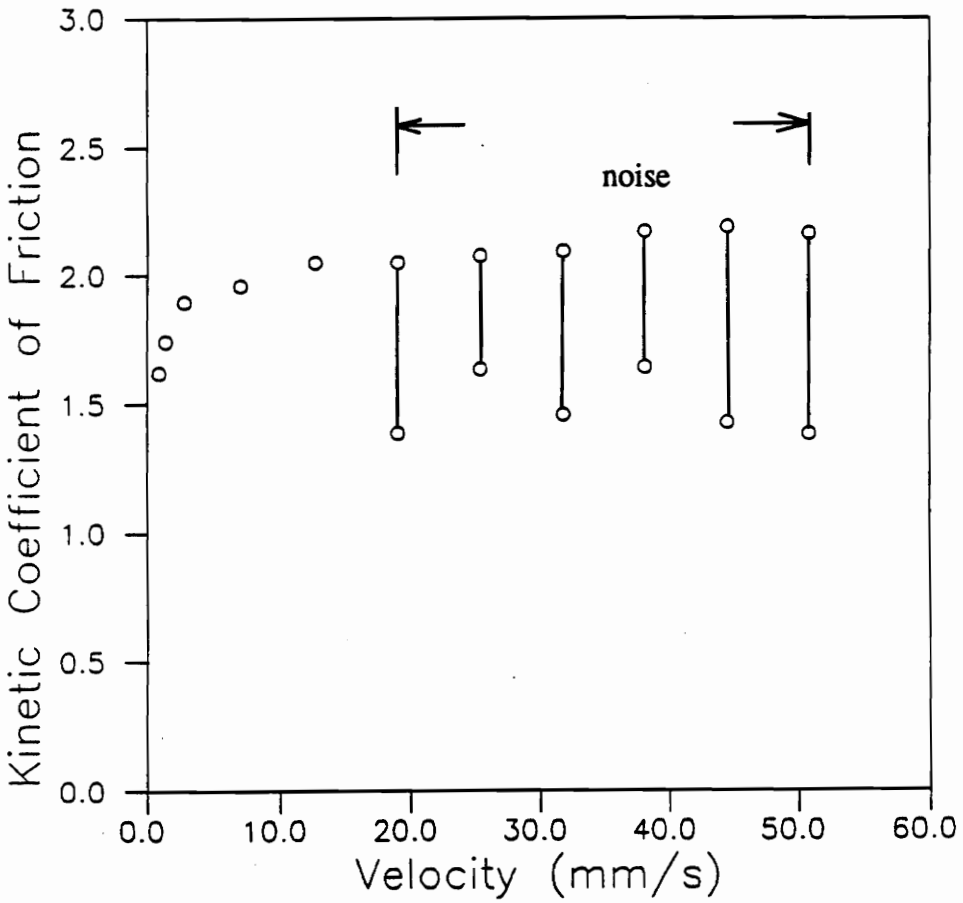


Figure 45. Friction-Velocity Relationship for 10 phr c.b. Natural Rubber against Chromium Oxide (Load = 17.8 N).

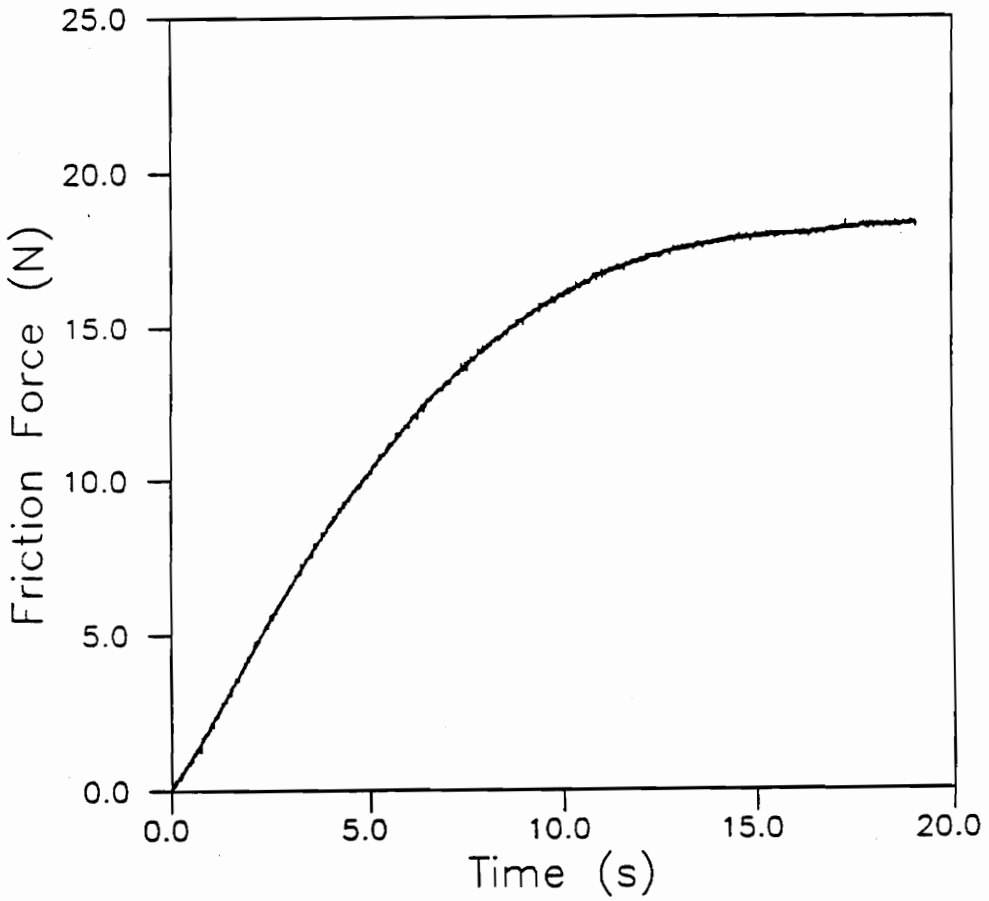


Figure 46. Time History of 10 phr c.b. Natural Rubber against Chromium Oxide (Load = 17.8 N, Velocity = 1.409 mm/s)

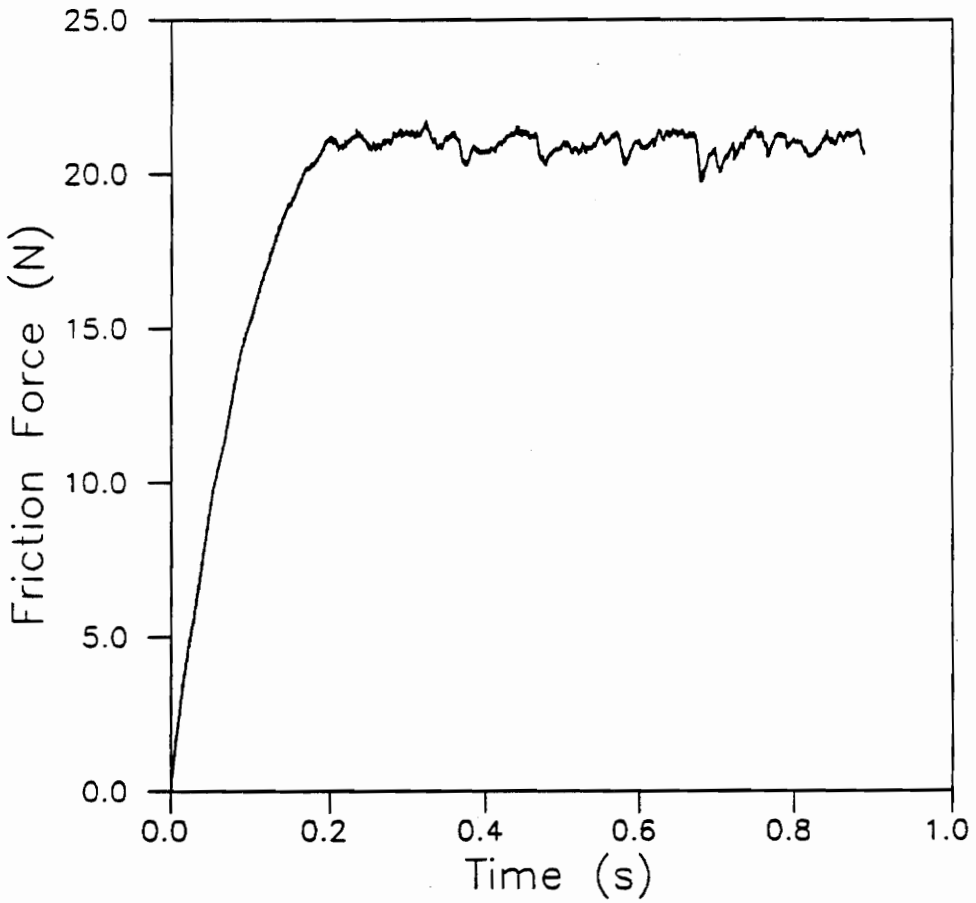


Figure 47. Time History of 10 phr c.b. Natural Rubber against Chromium Oxide (Load = 17.8 N, Velocity = 12.75 mm/s)

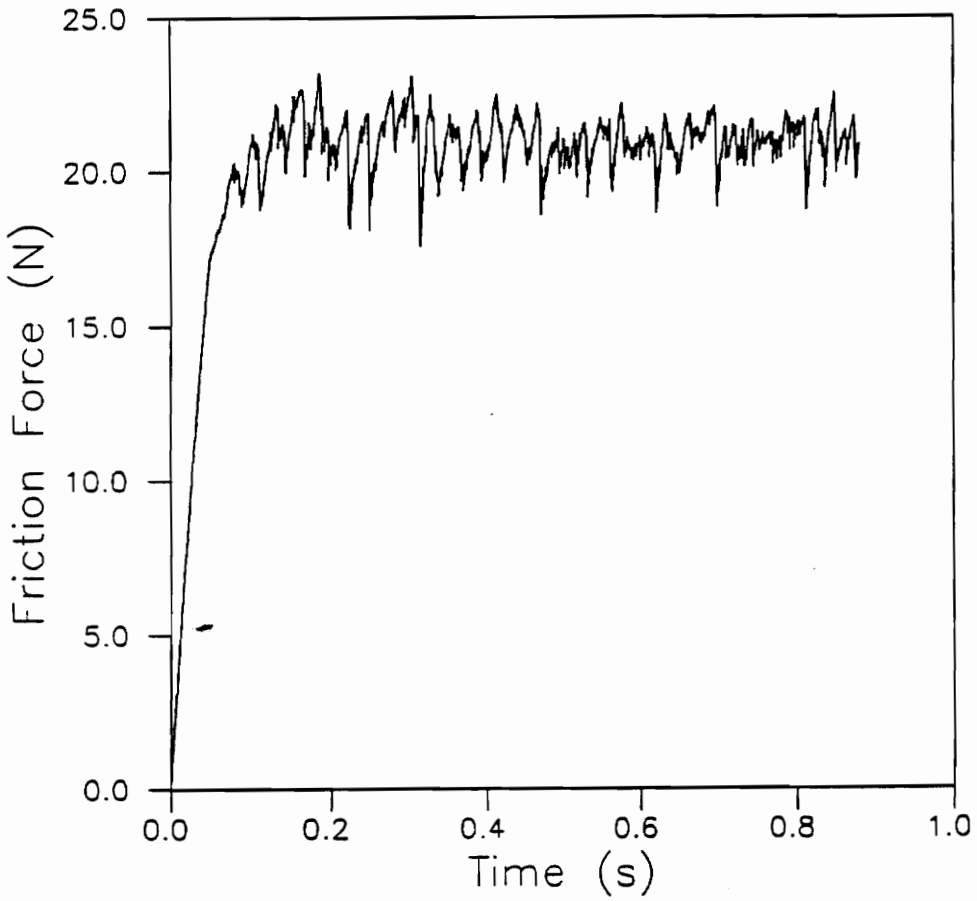


Figure 48. Time History of 10 phr c.b. Natural Rubber against Chromium Oxide (Load = 17.8 N, Velocity = 25.4 mm/s)

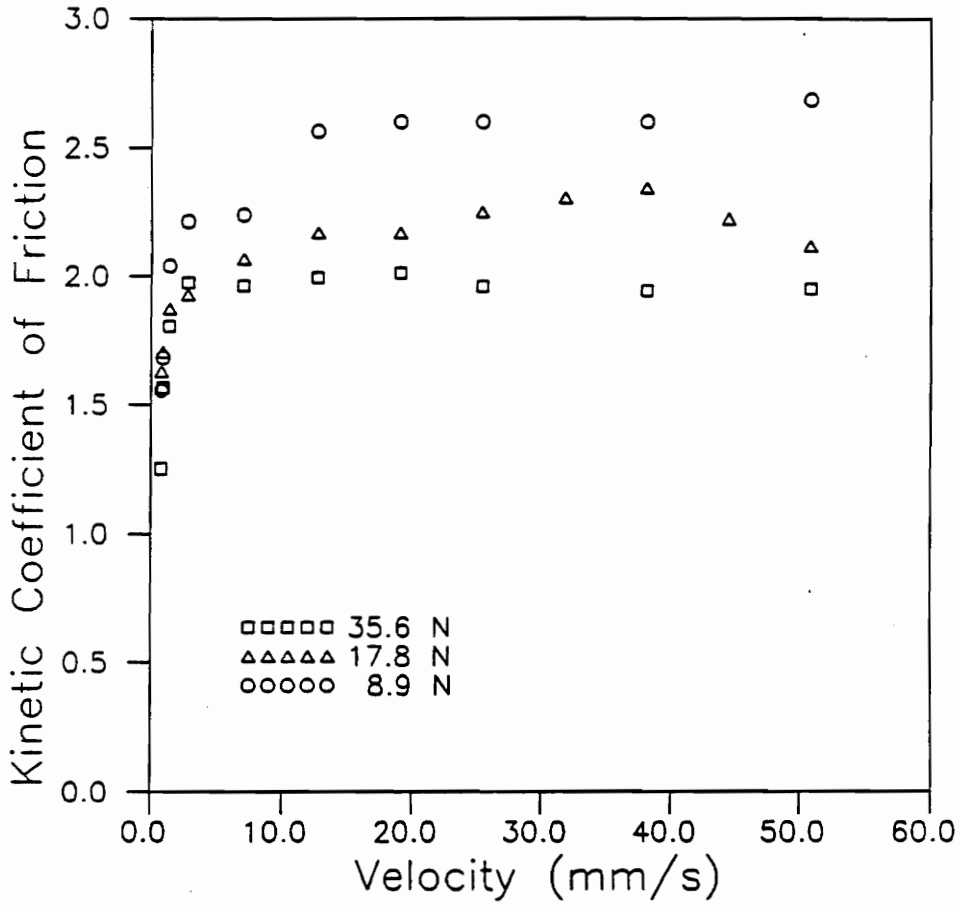


49. Friction-Velocity Matrix for 20 phr c.b. Natural Rubber against Chromium Oxide for Various Loads.

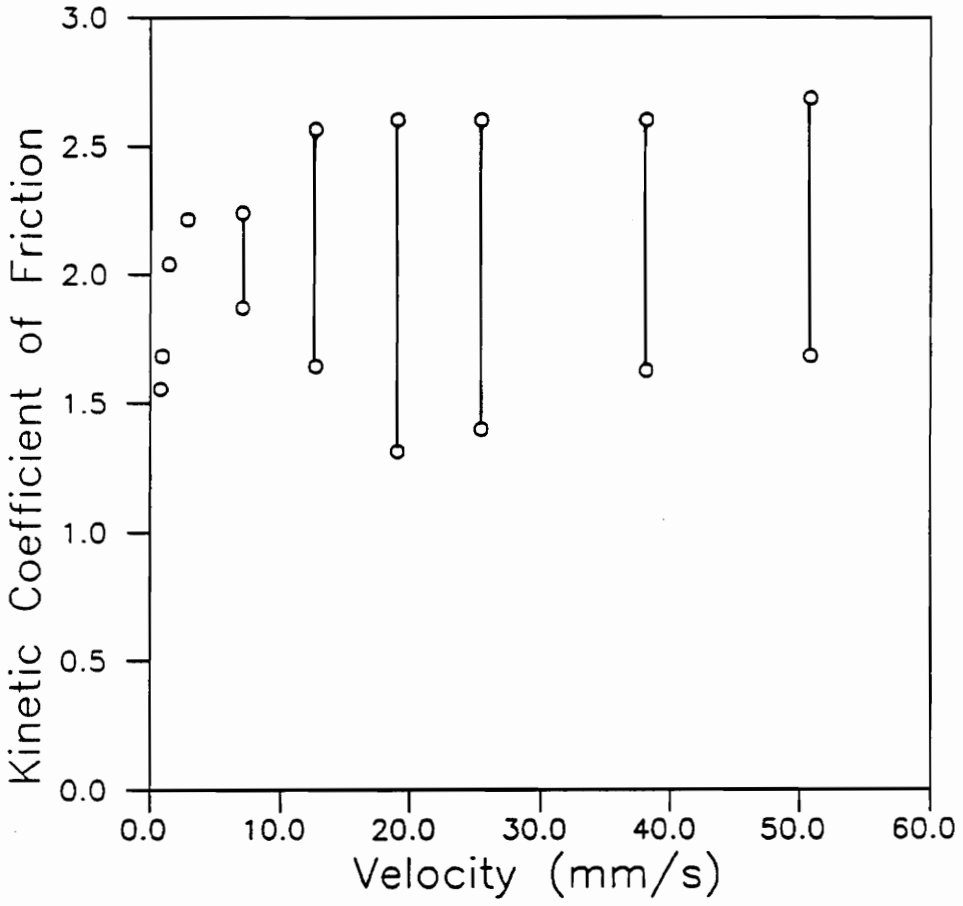


Figure 50. Friction-Velocity Relationship for 20 phr c.b. Natural Rubber against Chromium Oxide (Load = 8.9 N).

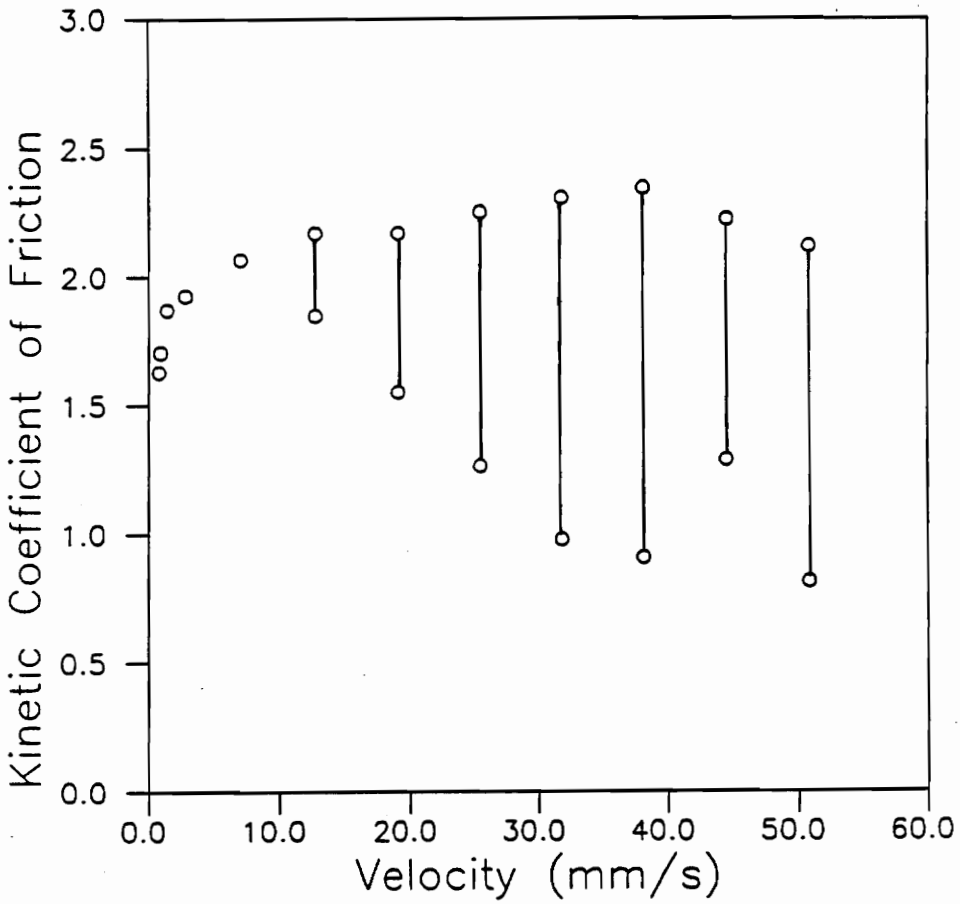


Figure 51. Friction-Velocity Relationship for 20 phr c.b. Natural Rubber against Chromium Oxide (Load = 17.8 N).

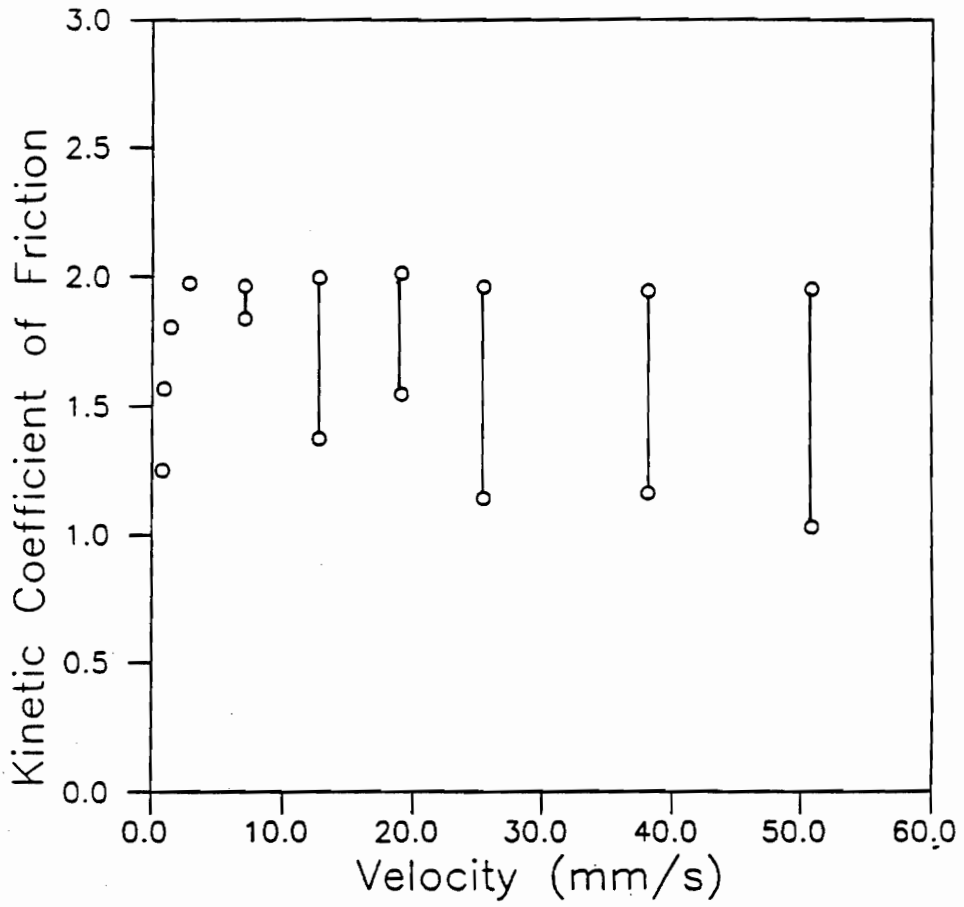


Figure 52. Friction-Velocity Relationship for 20 phr c.b. Natural Rubber against Chromium Oxide (Load = 35.6 N).

The oscillation locked onto a fundamental frequency of approximately 38 Hz for all three load levels. Interestingly, Figs. 50, 51 and 52 show a increase in the oscillation amplitude for $12.7 < v < 31.75$ mm/s. For $v > 31.75$ mm/s it is not conclusive when the figures are considered together, whether or not the amplitude increases or remains the same. Significantly, there is almost a decade of velocity experiencing the oscillatory behavior. If the mean coefficient of friction is considered as the kinematic coefficient of friction there will be a negative slope to the friction-velocity curve. The time histories that are about to be presented contain virturally all of the aspects of harmonic and relaxation oscillations. The first set of data presented will be the results of the 8.9 N load tests.

An example of low load and high speed sliding is shown in Fig. 53. A section of Fig. 53 has been expanded in Fig. 54 to show the slip and subsequent ringing that occurs after the maximum in friction force has been reached.

Figure 55 shows the transition from a condition of predominately low frequency stick-slip of the elastomeric slider to the high frequency ringing of the counterface/test assembly. Figure 56 is an expanded view of range $0.7 < t < 0.8$ s into the test pass. In this particular case the amplitude of the stick-slip event is small enough to allow the high frequency "ringing" to continue throughout the stick phase. For $0.775 < t < 0.800$ s the high frequency oscillation begins to dominate and wash out the slip events.

It was noted early on in the preliminary testing that in many instances some distance (25-75 mm) would have to be traversed in order to generate noise. Figure 57 is an excellent example of this phenomenon. Figure 57a shows the transient harmonic

ringup of the elastomeric slider locking on quickly to the 38 Hz frequency. Around 1.0 s into the test slip starts occuring as shown in Fig. 57b. Figures 57c-d are expansions of representative 0.2 s time intervals of Fig. 57a & b respectively. It is obvious from these expanded traces that initially the system is vibrating harmonically without stick (e.g. $0.4 < t < 0.6$ ) and then transitions into a condition that is dominated by the 38 Hz oscillation but experiences slip on each cycle.

A very interesting phenomenon occurs at the 35.6 N load. At a test velocity of 38.1 mm/s the friction force starts out in the stick-slip mode with the amplitude of oscillation gradually increasing with time as shown in Fig. 58. Approximately 0.6 s into the test run the the amplitude of oscillation becomes relatively constant. The interesting occurence is shown in Fig. 59. The expanded section of time is from the next block of data not shown in Fig. 58, but representative of the test for $t > 0.6$ s. The friction force reaches a maximum value at approximately 38 N and the slider travels for 0.015 s at the 38 N level before experiencing slip periodically. The periodicity of slip does not appear to become random during this phenomenon, but stays as periodic as any of the other test runs not experiencing this phenomenon.

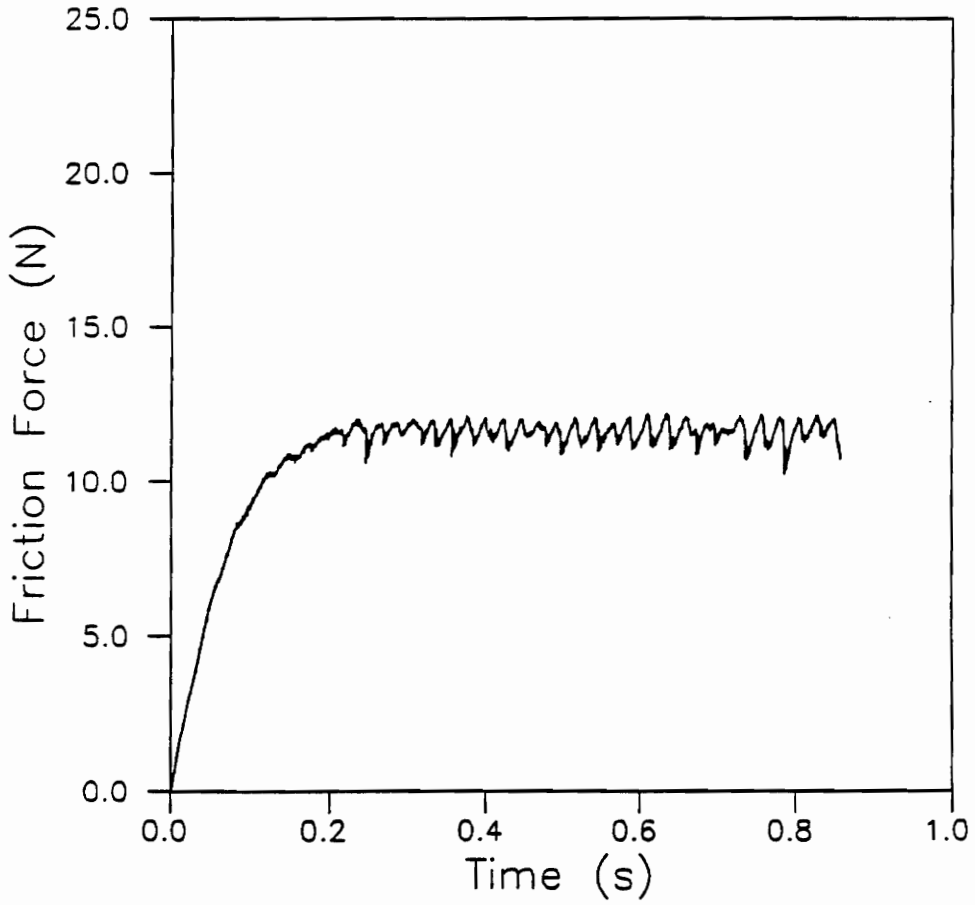


Figure 53. Friction Time History of 20 phr c.b. Natural Rubber against Chromium Oxide (Load= 8.9 N, v= 12.7 mm/s).

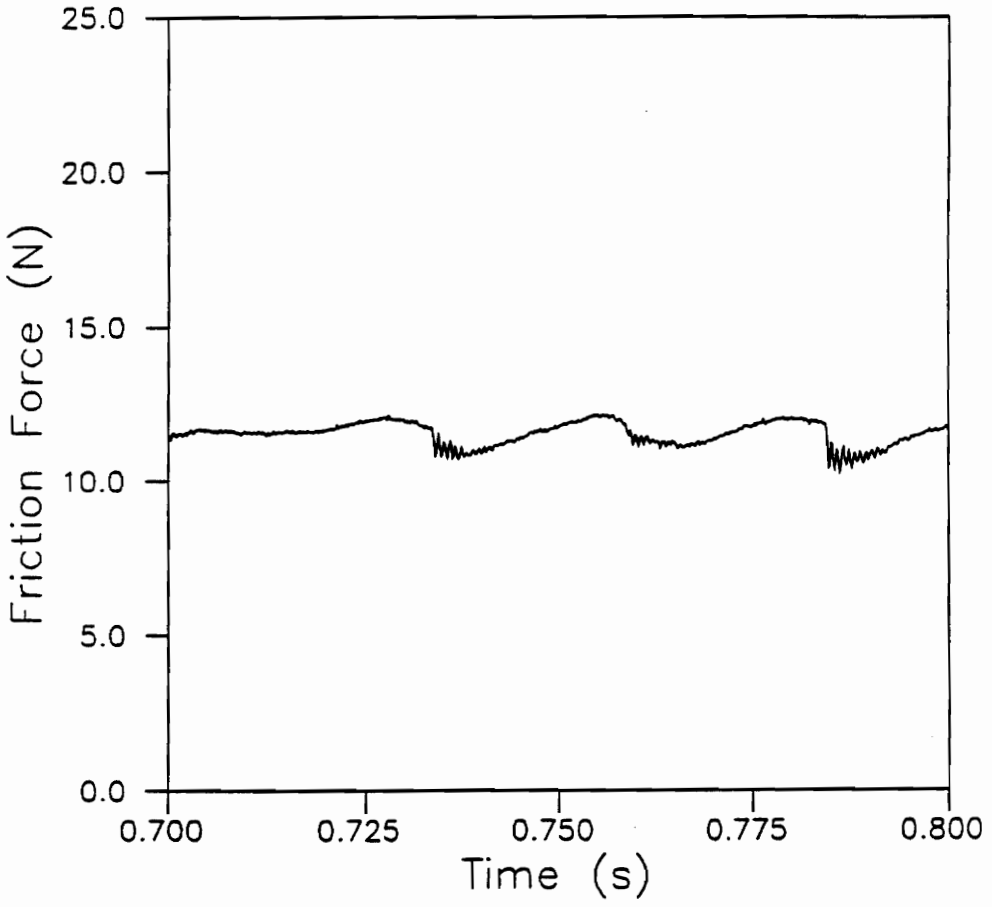


Figure 54. Expanded Friction Time History of Fig. 53 .700 < t < .800 s.

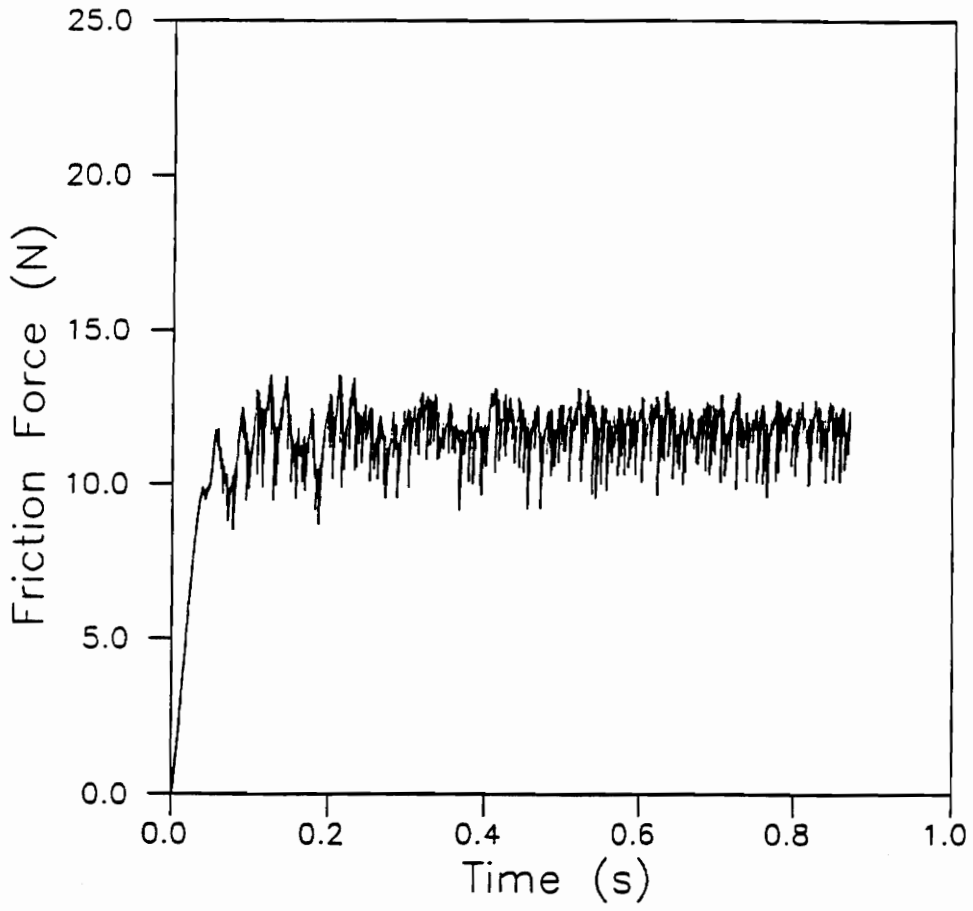


Figure 55. Friction Time History of 20 phr c.b. Natural Rubber against Chromium Oxide (Load = 8.9N, v= 50.8 mm/s).

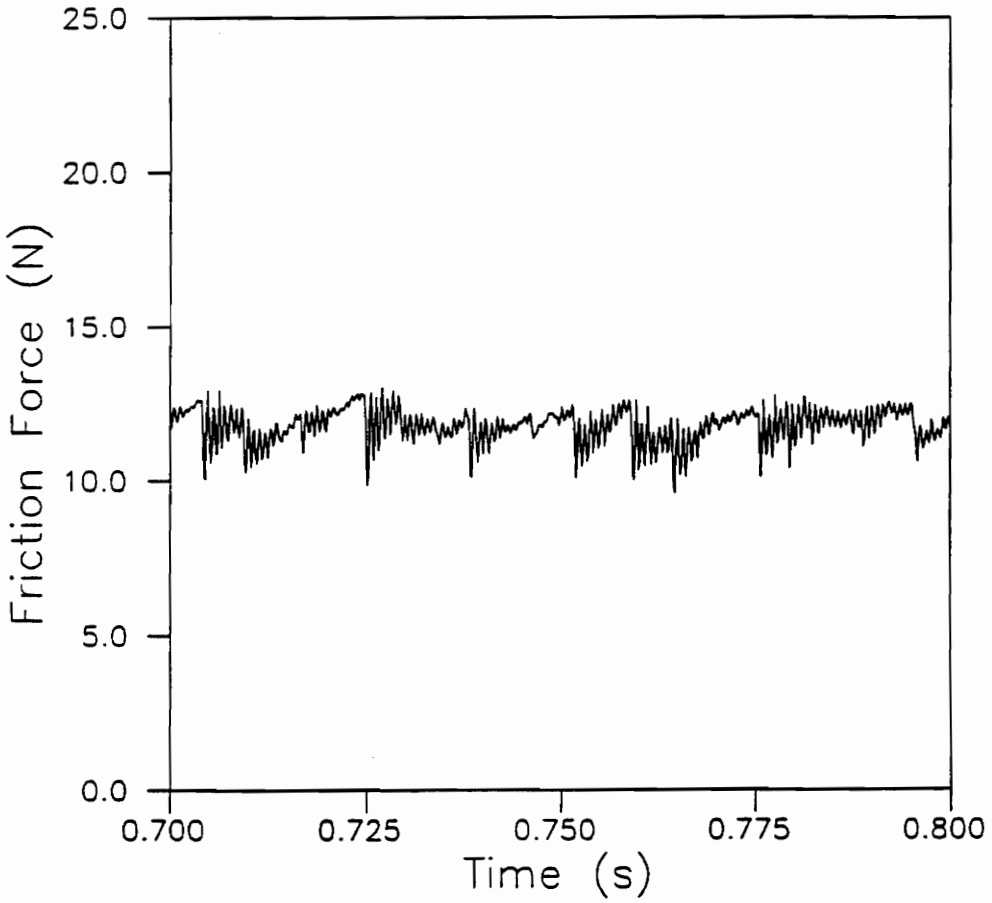


Figure 56. Expanded View of Fig. 55 ( .775 < t < .800 s).

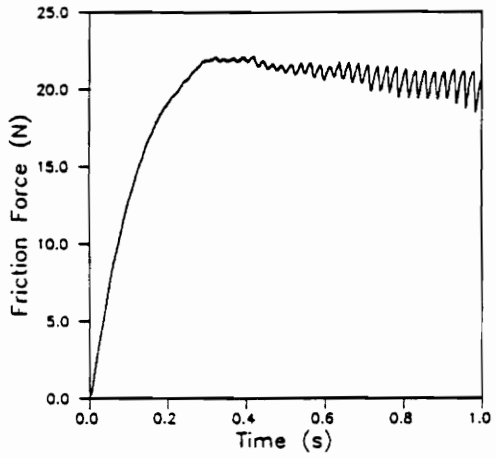


a. First 1 s of Data

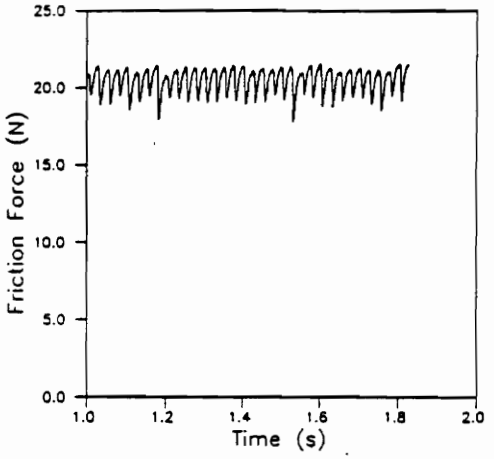


b. Continuation of Data

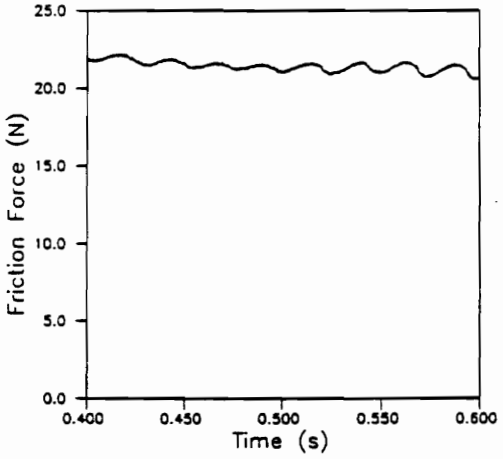


c. Expanded View of a.

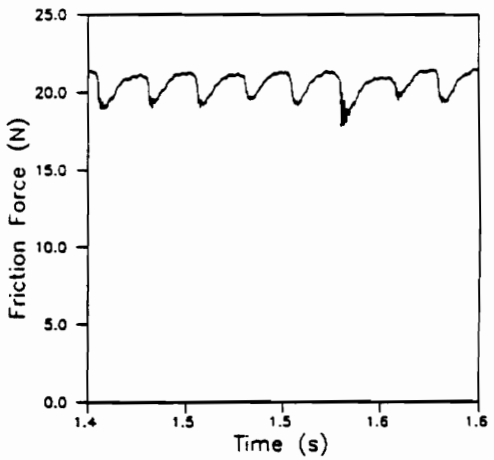


d. Expanded View of b.

Figure 57. Friction Time History of 20 phr c.b. Natural Rubber against Chromium Oxide (Load= 17.8 N, v= 12.7 mm/s).

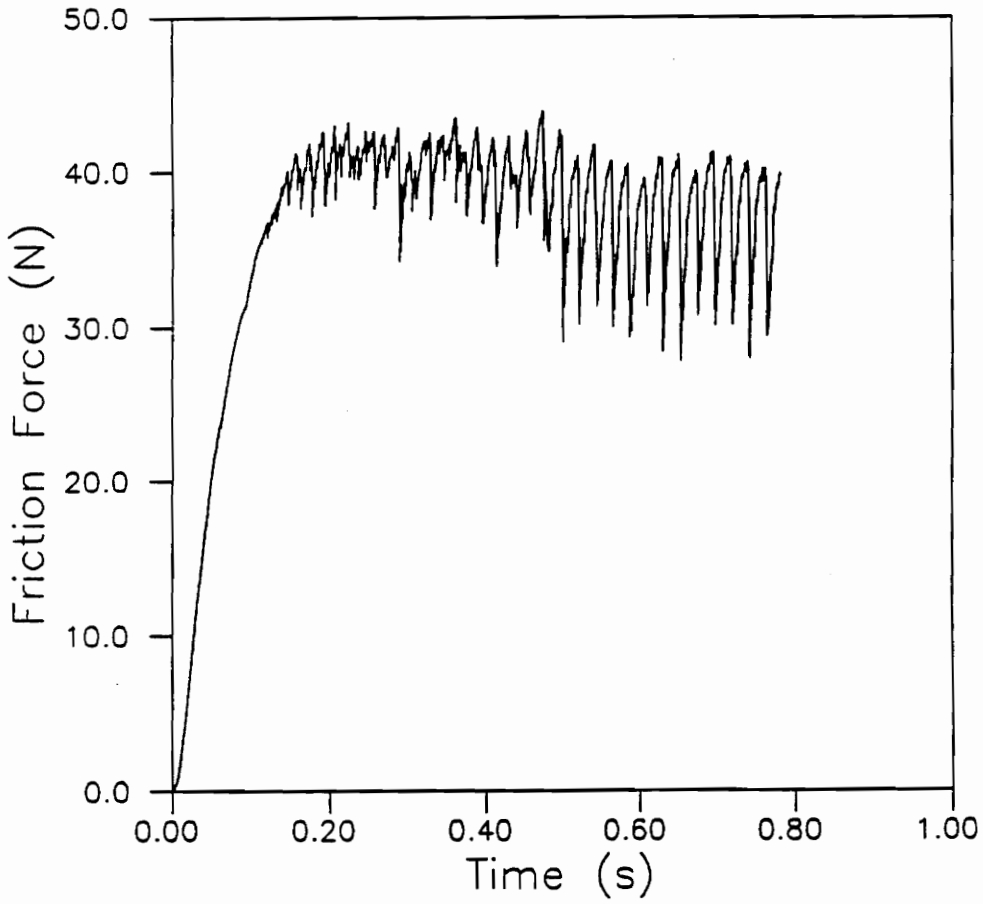


Figure 58. Friction Time History of 20 phr c.b. Natural Rubber against Chromium Oxide (Load= 35.6 N, v= 38.1 mm/s).

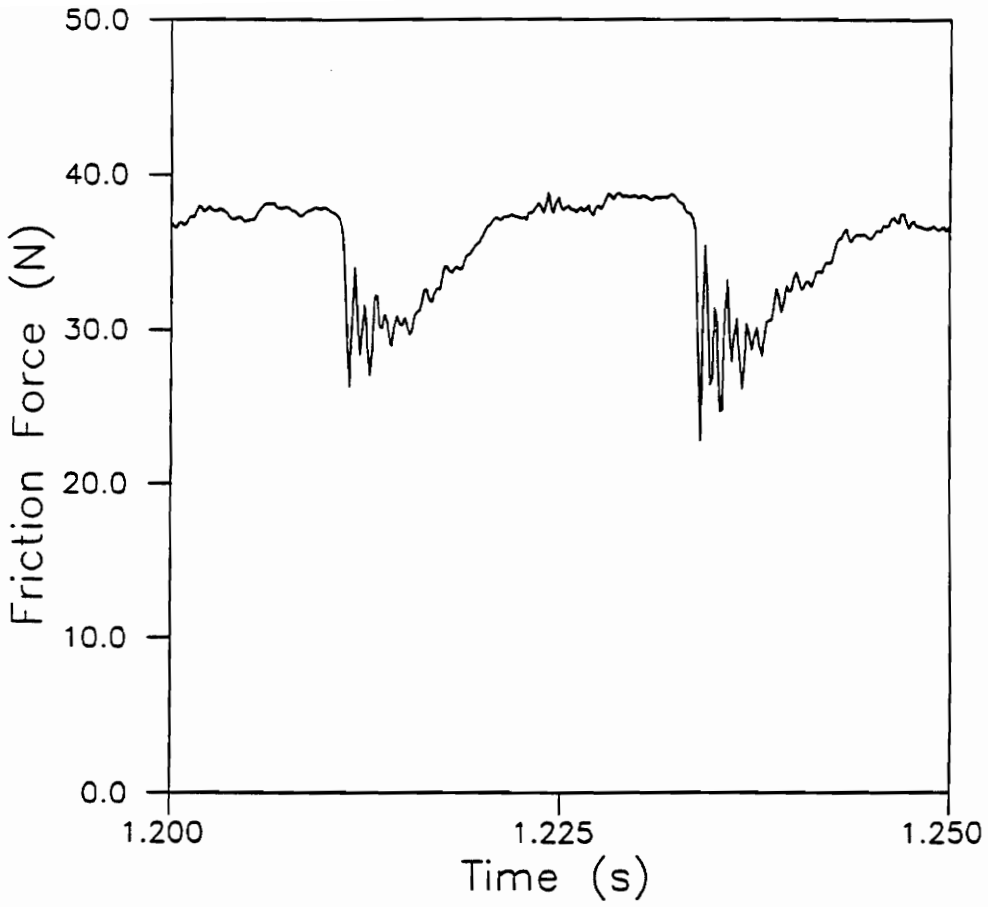


Figure 59. Expanded View of Test Run of Fig. 58 $1.2 < t < 1.25$.

**Natural Rubber-50 phr c.b.**

**Solid Hemisphere**

A series of tests were run at 17.8 N against chromium oxide to determine the critical velocity of noise generation. For this particular series noise was not generated by stick-slip but by harmonic oscillations of the elastomer. The friction-velocity relationship is shown in Fig. 60. In the case of oscillatory behavior the coefficient of friction was determined from the initial value of the friction force, immediately prior to the oscillations. The friction time histories transition from steady sliding as shown in Fig. 61 ($v$= 2.819 mm/s) to oscillatory sliding ($v$> 12.7 mm/s) as shown in Figs. 62 and 63. The classic harmonic oscillations are evident in the time histories of Figs. 62 and 63. In this particular case it appears that it is the elastomer vibrating at its tangential natural frequency, 61.88 Hz. The previous statement is deduced from the observation that the natural frequency in the direction of motion of the test apparatus is approximately 1475 Hz. Figure 62 is a excellent example of harmonic oscillations with the transient ringup to the steady state amplitude as would be predicted by theory. The friction in Fig. 63 has also reached its steady state value, even though it is not obvious from the data presented. The frequency of vibration remained constant with increasing velocity. The mean value of the friction force remained relatively constant over the oscillatory velocity range. The amplitude of the oscillation increased by a factor of 2 from 4.1 N ($v$=12.7 mm/s) to 8 N ($v$= 50.8 mm/s). The harmonic oscillation became audible for $v$> 38.1 mm/s.

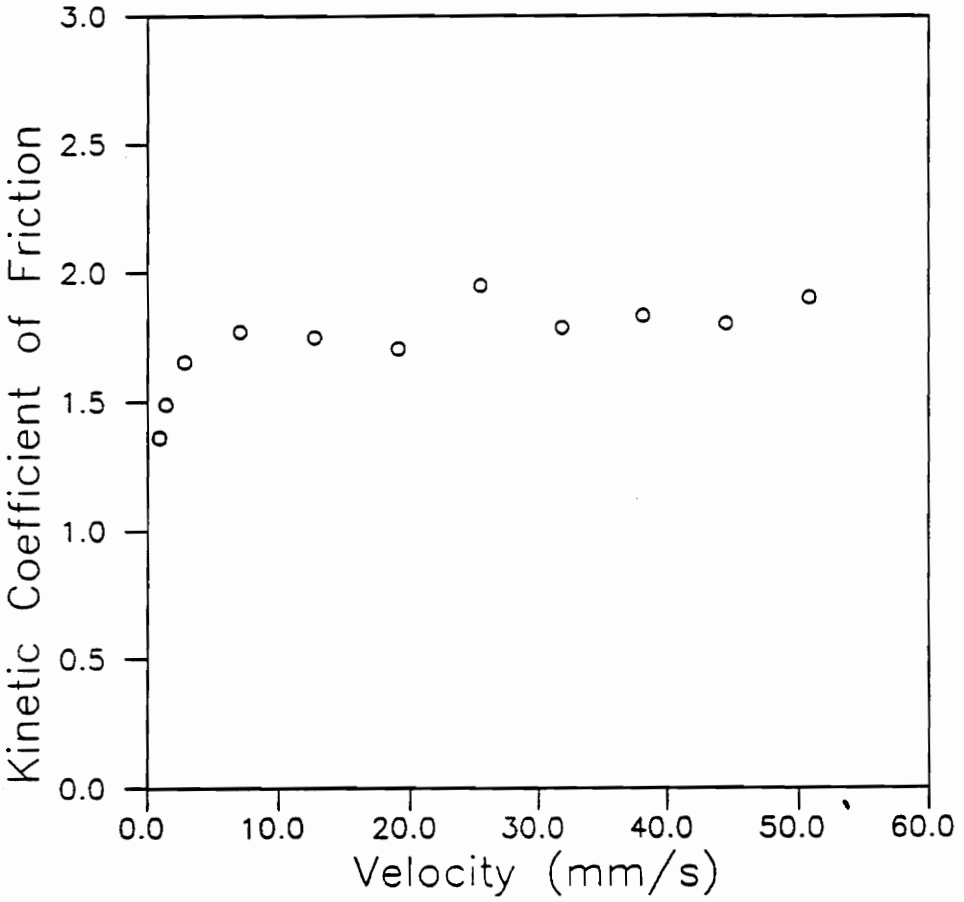


Figure 60. Friction-Velocity Relationship for 50 phr c.b. Natural Rubber against Chromium Oxide (Load= 17.8 N).

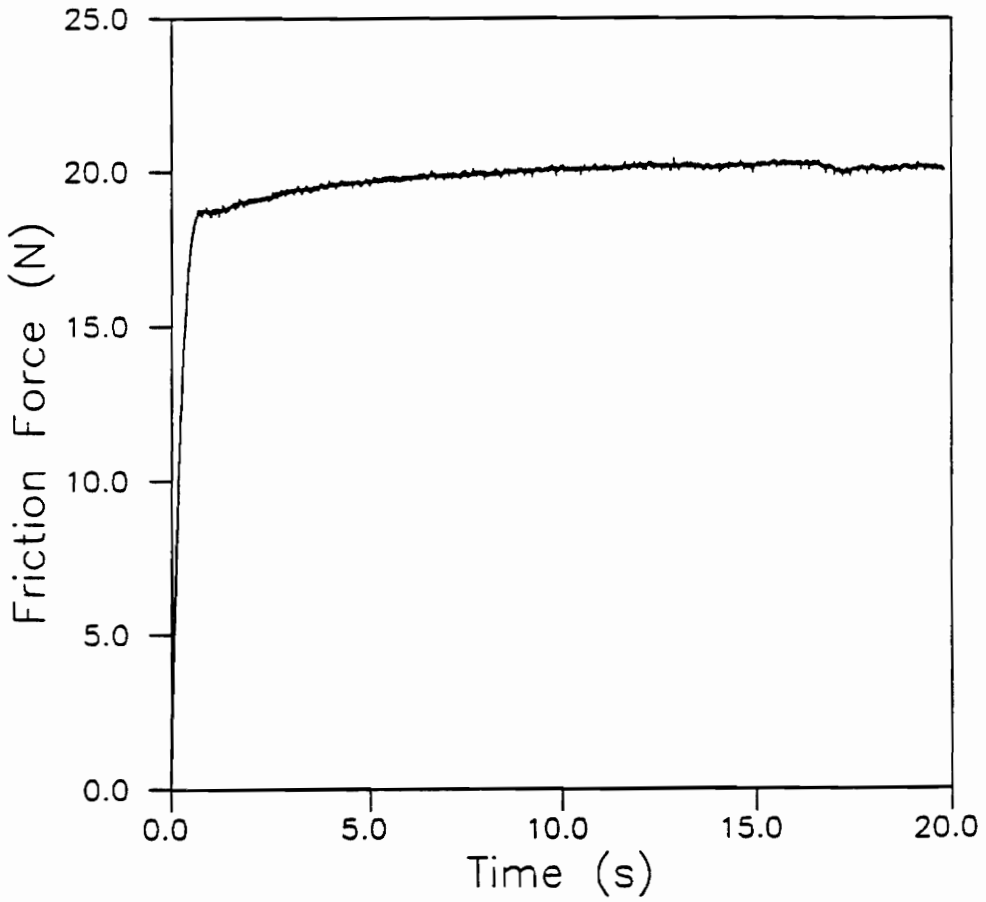


Figure 61. Friction Time History of 50 phr c.b. Natural Rubber against Chromium Oxide (Load= 17.8 N, Velocity= 2.819 mm/s).

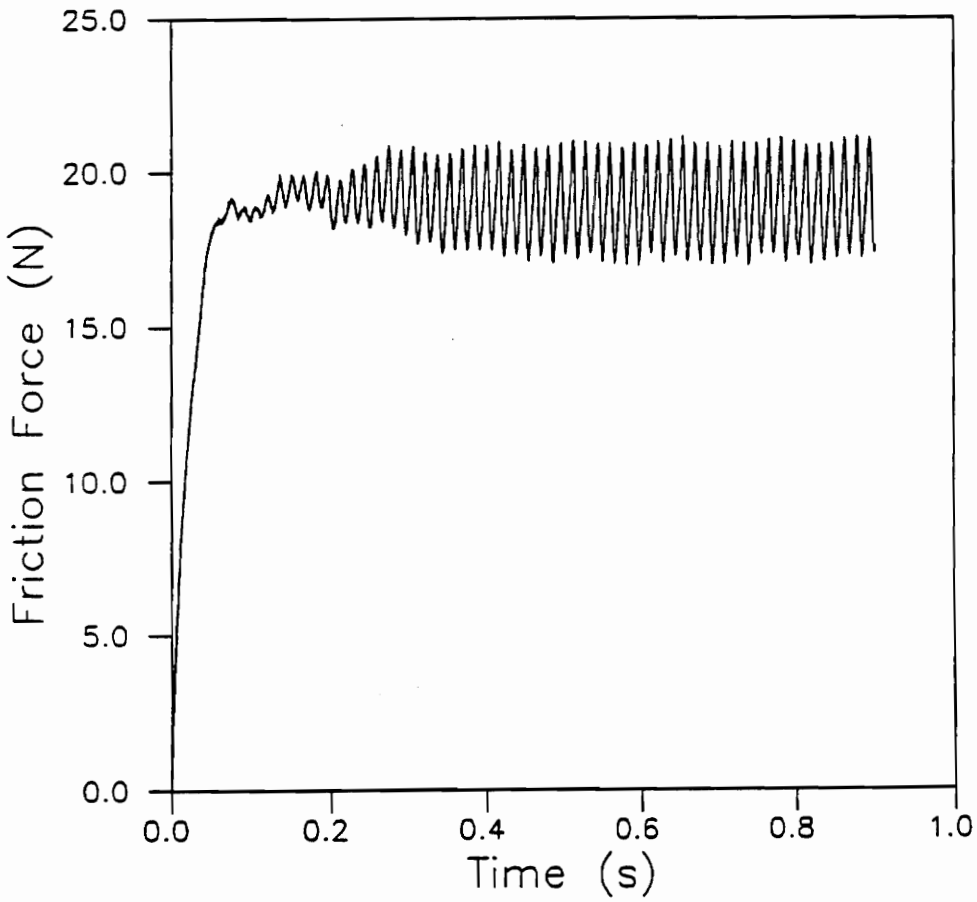


Figure 62. Friction Time History of 50 phr c.b. Natural Rubber against Chromium Oxide (Load= 17.8 N, Velocity= 19.03 mm/s).

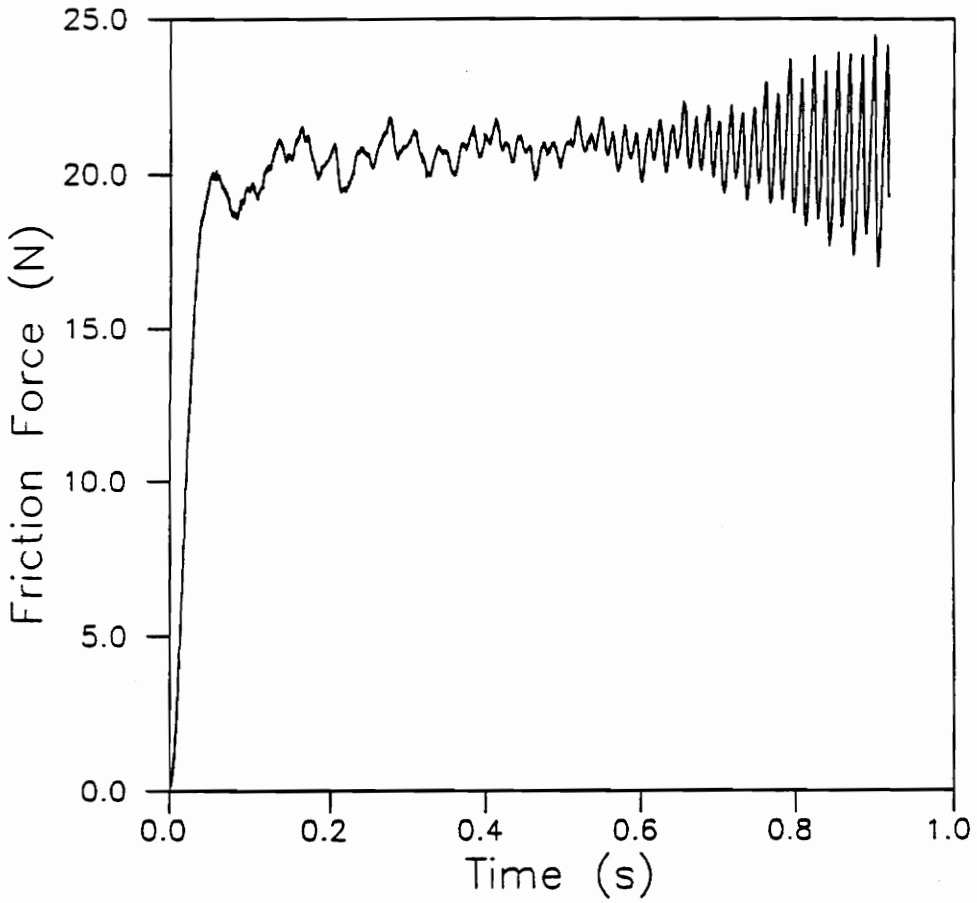


Figure 63. Friction Time History of 50 phr c.b. Natural Rubber against Chromium Oxide (Load= 17.8 N, Velocity= 38.1 mm/s).

### Hollow Hemispheres

In addition to the solid hemispheres, much of the preliminary testing was performed against hollow hemispheres. In general noise would occur more easily for the hollow hemispheres than the solid hemispheres. The test condition at 17.8 N with a chromium oxide counterface was performed with the velocity range to determine the differences between solid and hollow hemispheres. Theoretical predictions based upon viscoelastic models of friction would predict that there would be no difference in the critical velocity of noise generation. In one respect, the theoretical predictions are correct in that both solid and hollow specimens start oscillating within the same decade of velocity. However, unlike the solid specimens, the hollow tests eventually lead to stick-slip. Figure 64 shows the friction-velocity curve for a 17.8 N load. The shape of the friction-velocity curve is the same as that of the solid tests. The stick-slip amplitude is not shown on this friction-velocity curve since the series of tests had sporadic stick-slip or the stick-slip occurred after the initial data had been acquired.

### Butyl

Butyl rubber was the only elastomer on which Schallamach waves were observed. In previous work [26,40,41] it has been noted that tackiness of the elastomer is a implicit prerequisite for the occurrence of Schallamach waves. Butyl was the tackiest of all the elastomers. Tackiness is a function of both modulus and surface forces. High surface

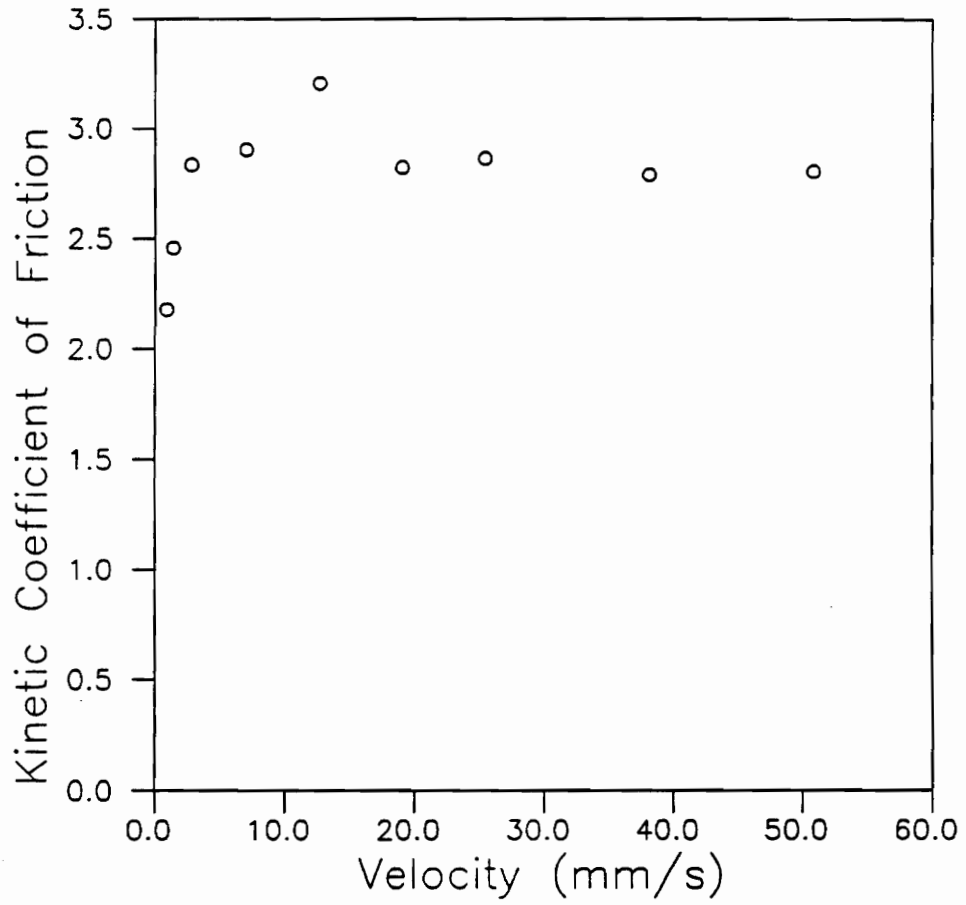


Figure 64. Friction-Velocity Matrix for 50 phr c.b. Natural Rubber Hollow Hemisphere against Chromium Oxide.

attraction between two specimens alone does not make a material tacky. The modulus must also be low to allow the material to deform under the surface attraction and conform to the opposing surface. When the butyl hemisphere was loaded normally to the counterface it took a macroscopically, noticeable negative load for removal from the surface. In addition the removal was accompanied by acoustic emission in the form of a loud "popping" sound. Neither the "popping" sound nor Schallamach waves were present when the butyl slid against glass that had a thin transfer layer of PDMS present.

Formation and propagation of Schallmach waves was not a sufficient condition for generation of audible sound. At very low velocities Schallamach waves were not apparent. Increasing velocity resulted in passing through the first critical velocity, $v_{crit1}$. $V_{crit1}$ was the minimum velocity required for observance of Schallamach waves. In general these waves were on the order of 1-2 mm wide and propagated from the rear of the contact area to the front. Steady-state sliding could occur without any noise generation up to the next critical velocity, $v_{crit2}$. When $v_{crit2}$ was reached a large wave with a size on the order of half to full contact diameter dimensions would pass through the interface. When the size of this wave was approximately equivalent to the contact area diameter the entire contact would be broken and the elastomer would separate from the interface. For large detachments smaller than the contact area the elastomer would respond in a manner similiar to stick-slip. For this case the elastomer would deflect to its maximum deflection at which point the large wave would pass through the interface. As the wave passed the friction force would drop and the elastomer would return to its minimum deflection a process reminiscent of stick-slip.

The filming equipment available at *V.P.I. & S.U.* was not adequate to document this phenomenon with presentable quality. The high speed cameras available did not have the necessary spatial resolution and video cameras did not have the temporal resolution to capture the images. However, visual observation was adequate to describe the phenomenon. Figure 65 shows the progression of detachment waves for a typical time history in which noise similar to stick-slip occurred.

The friction force of the butyl rubber would increase rapidly with time during a single pass. The increase in friction force could be on the order of approximately 10-50% over the initial kinetic friction force. The friction of the other elastomers tested were relatively constant over the short test times ($\approx$ 3-20 s). This rather dramatic increase in friction could lead to the production of the large Schallamach waves noted earlier. After the detachment and stick-slip like motion the friction force was relatively constant for the duration of the test. In contrast, the natural rubber would usually initiate stick-slip immediately upon reaching the maximum kinetic friction force.

The shape of the time history during noise generation was very similar to stick-slip with the following exception. During the stick phase of stick-slip there is a definite linear or nearly linear rise of the friction force with time. However, for noise generated by Schallamach waves the increase in friction force prior to "slip" is minimal, or nonexistent. Figure 66 shows the form of the time history of a typical passing of a Schallamach wave. The similarity with stick-slip is the high frequency ringing immediately following the "slip" event.

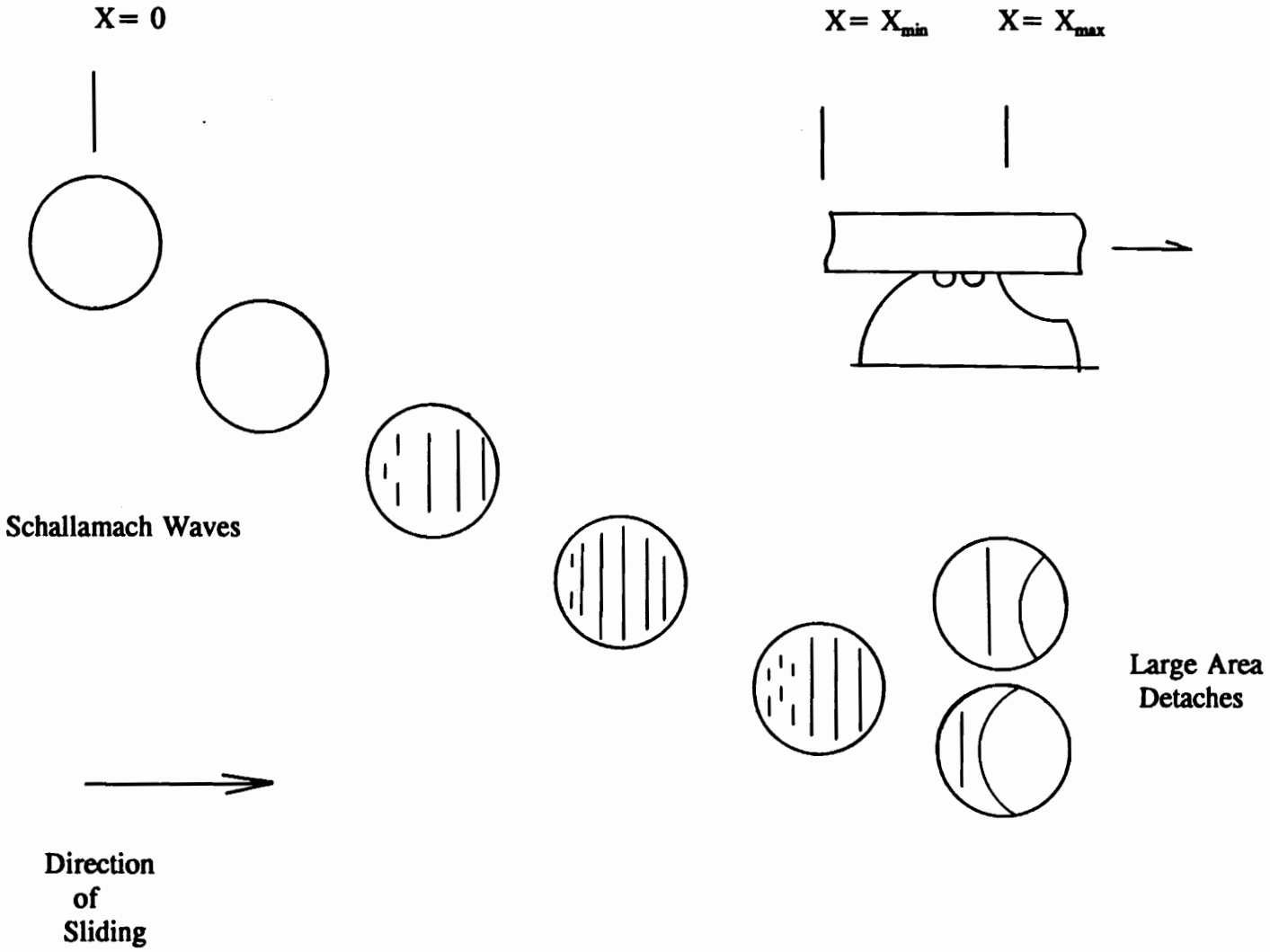


Figure 65. Progression of Detachment Waves for Butyl Elastomer.

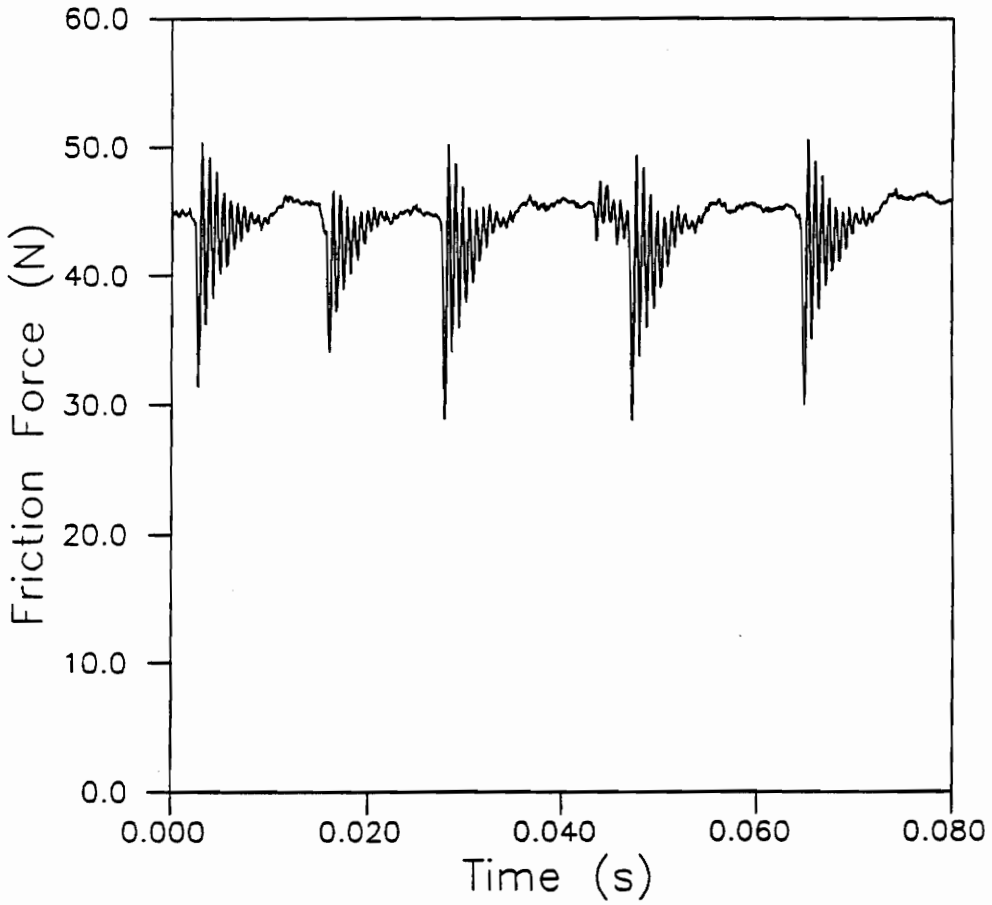


Figure 66. Friction Time History of Schallamach Wave during Noise Production.

## PDMS

It was impossible to generate noise for the PDMS elastomer. In addition, the friction-velocity curve had a break point in the same velocity decade as natural rubber. If the viscoelastic predictions of adhesion are valid the break point of PDMS should have occurred at a velocity approximately 3 decades lower due to the differences in $T_g$ (-73 °C for natural rubber and -123 °C for PDMS). PDMS is notoriously weak in ultimate properties when compared to other elastomers. Figure 67 shows the friction-velocity curve of PDMS for the velocity range tested at 20 and 30 °C. As can be seen from Fig. 67 the coefficient of friction is lower for the higher temperature tests. The magnitude of the coefficient of friction of PDMS is much lower than that of natural rubber. This occurs even though the area for a given load is greater for the PDMS due to the lower modulus.

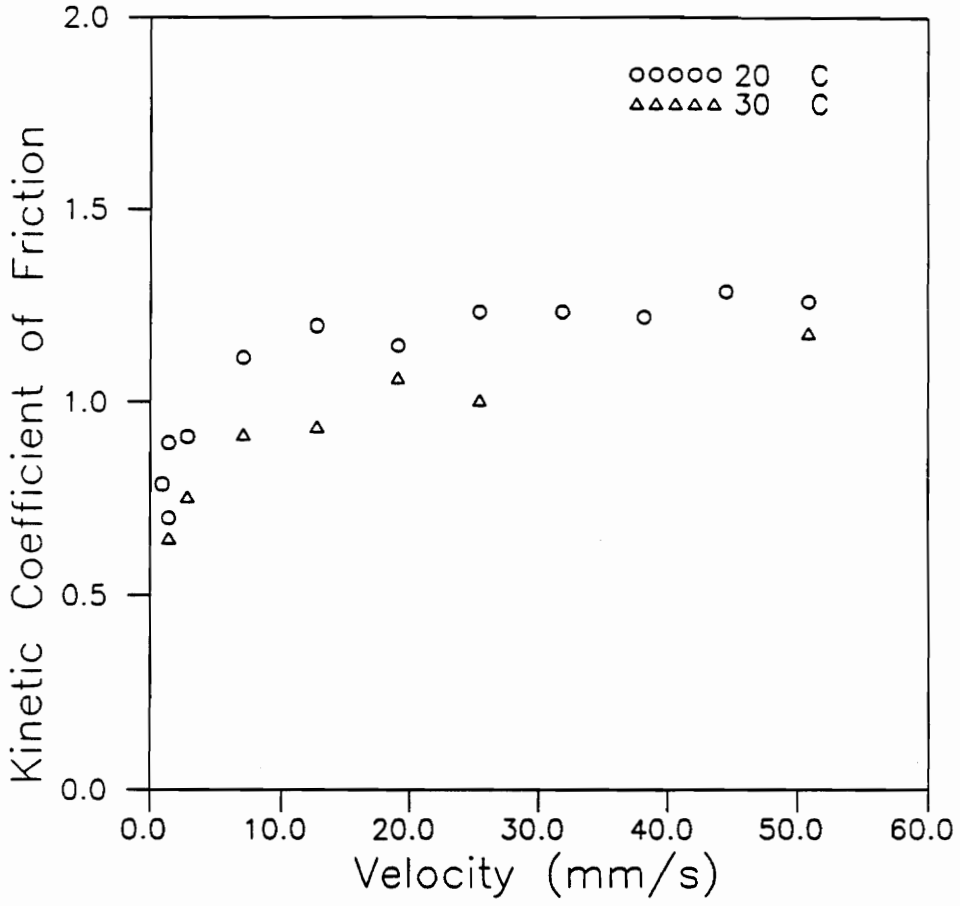


Figure 67. Maximum Kinetic Coefficient of Friction for PDMS against Chromium Oxide (Load = 17.8 N, T= 20 & 30 °C).

### Flourel Fluorocarbon

Initially, the fluorocarbon would not make noise against any of the counterfaces. However, subsequent testing did reveal that the fluorocarbon would make noise under certain conditions. The oscillations created by the fluorocarbon were of much smaller amplitude and higher frequency than those produced by the natural rubber hemispheres. Figure 68 shows the friction-velocity curve for the fluorocarbon elastomer. Once again the same general shape of the friction-velocity curve as seen with the other elastomers is evident for the fluorocarbon. Figure 68 shows that the oscillations did not occur until $v$= 38.1 mm/s. In addition, the system would oscillate harmonically in the tangential direction at 238 Hz prior to and after experiencing a period of stick-slip at the same frequency. This phenomena is illustrated by Fig. 69 and 70.

## Wet Friction Results

### Natural Rubber- 5 phr c.b.

Even though the purpose of this study was to examine dry sliding, a limited number of wet tests were performed. The following results are for the 5 phr c.b. natural rubber specimen sliding against both the chromium oxide and powder epoxy counterfaces. The 5 phr c.b. hemisphere generated stick-slip against the chromium oxide plate, but not the powder epoxy plate in the dry condition. The first set of wet test data is shown in Fig. 71. "Stick-slip" occurs after the peak in the $\mu(v_{plate})$ curve. A repeat

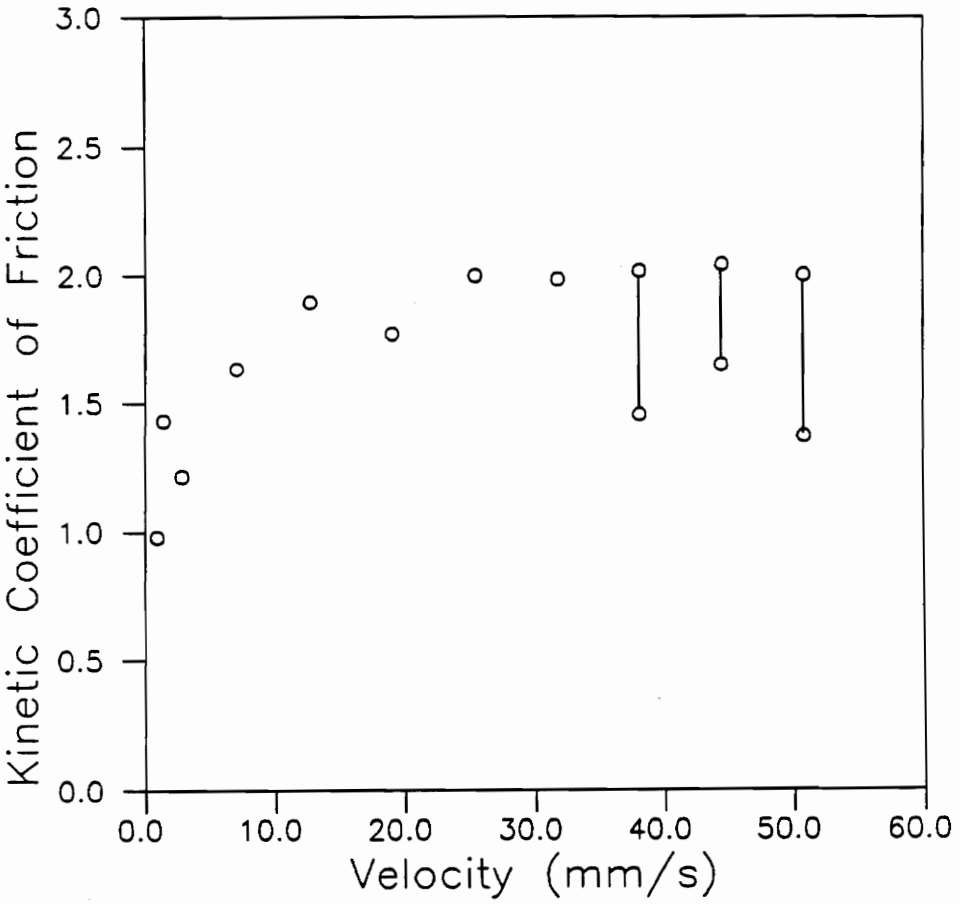


Figure 68. Friction-Velocity Relationship for Fluorocarbon against Chromium Oxide (Load= 17.8 N).

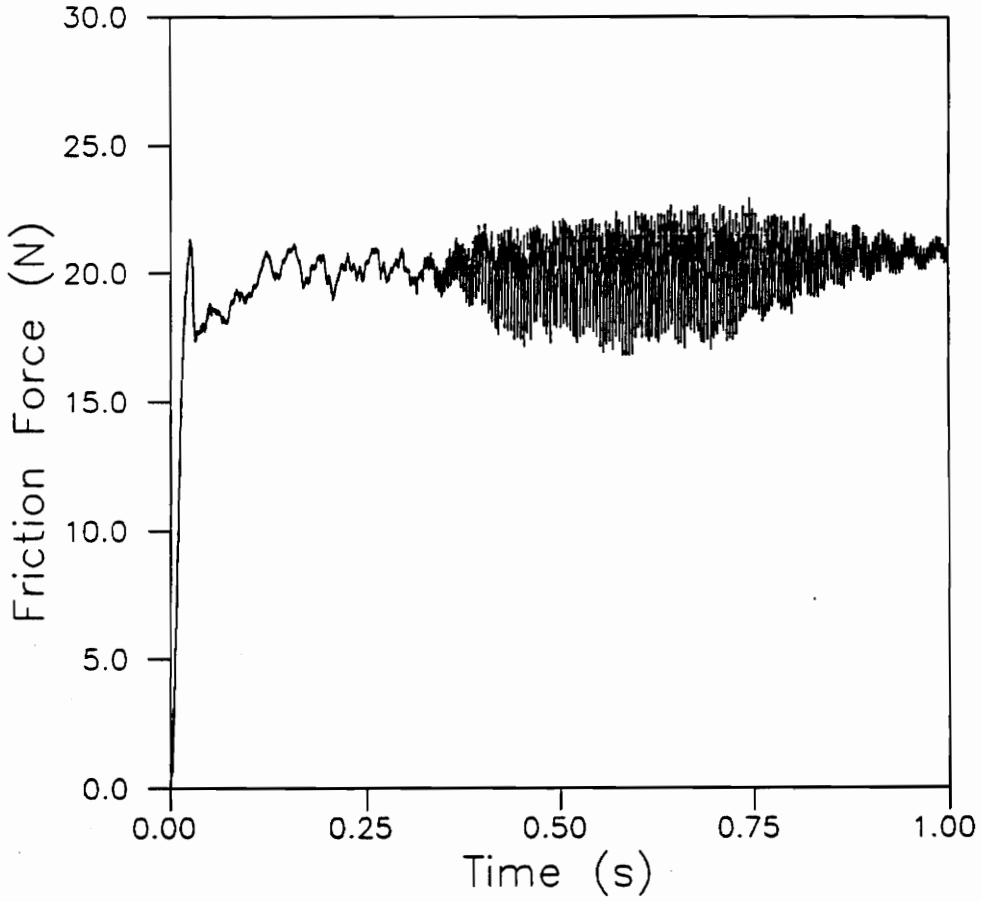


Figure 69. Friction Time History of 50 phr c.b. Fluorocarbon against Chromium Oxide (Load= 17.8 N, Velocity= 38.1 mm/s).

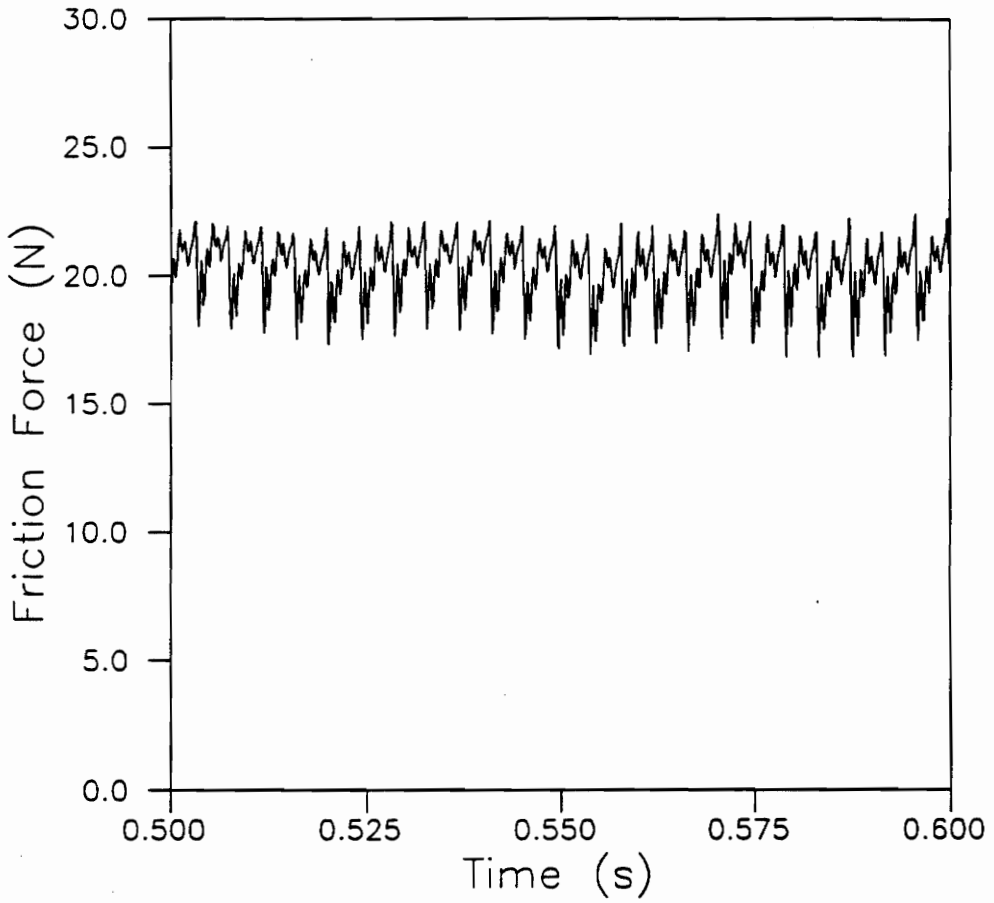


Figure 70. Expanded View of Test Run of Fig. 69 (.5 < t < .6 s).

of this data was performed to verify the general shape of the curve and the value of $v_{crit}$ as shown in Fig. 71. The repeat data set is shown in Fig. 72. The frequency of stick-slip for the original data of Fig. 71 is shown in Fig. 73. There is reasonable agreement between the curves on the peak velocity (1.409 and 2.819 mm/s) and the values of the coefficient of friction at the higher velocities. The peak value is the highest velocity attained before stick-slip sliding occurred. One of the wet $\mu(v_{plate})$ curves is shown in Fig. 74 for comparison to the dry tests against cathodic epoxy. Figure 74 shows that the coefficient of friction for the wet tests is approximately a factor of 2-2.5 less than the dry tests but stick-slip still occurs. Additionally, a few tests were performed against chromium oxide to determine if the water film was breaking down and contact between the elastomer and counterfaces was occurring. The $\mu(v_{plate})$ curve for the wet conditions are compared to the dry conditions in Fig. 75. No transfer film was detected on the chromium oxide after the test run indicating that contact had not occurred between the elastomer and counterface.

The time histories of a series of tests with increasing velocity are shown in Figs. 76, 77 and 78. Figures 76 and 77 show that the wet tests depart from the dry time histories prior to reaching their maximum value. Because of the relative time scale the departure is not discernable for the high velocity test shown in Fig. 78. It is evident

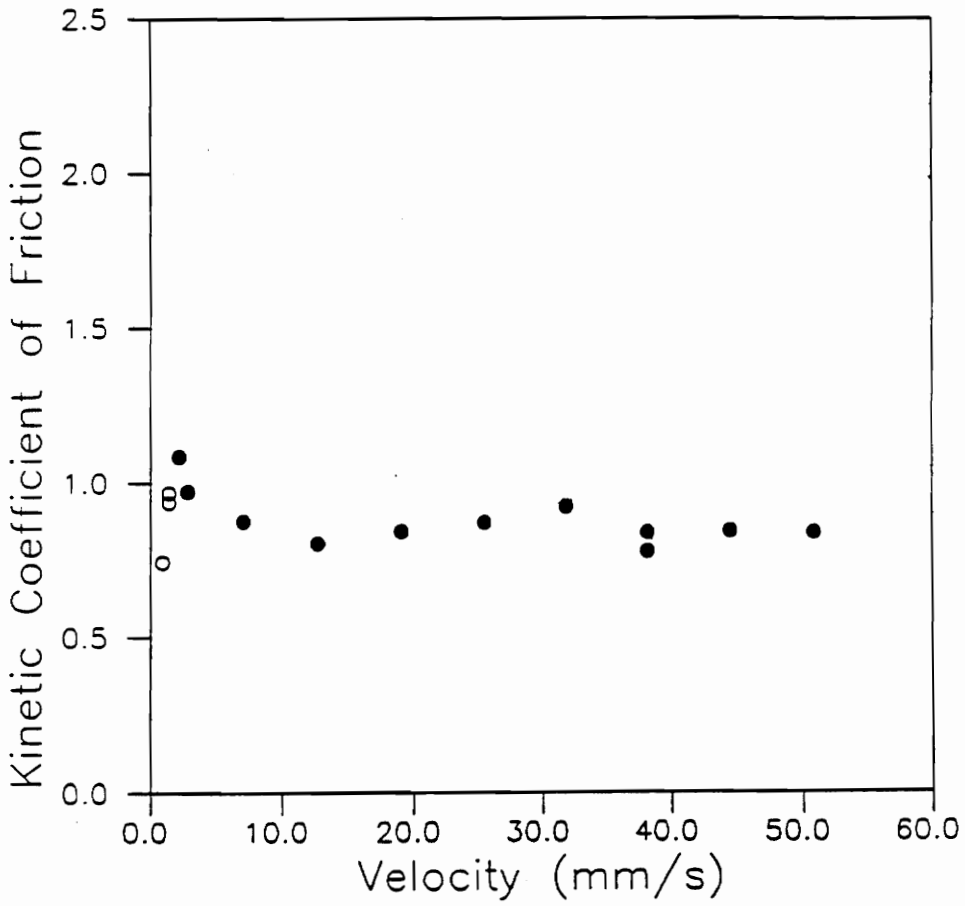


Figure 71. Kinetic Coefficient of Friction for 5 phr c.b. Natural Rubber against Cathodic Epoxy (Load = 17.8 N, Wet).

* Solid symbols indicate oscillatory tests

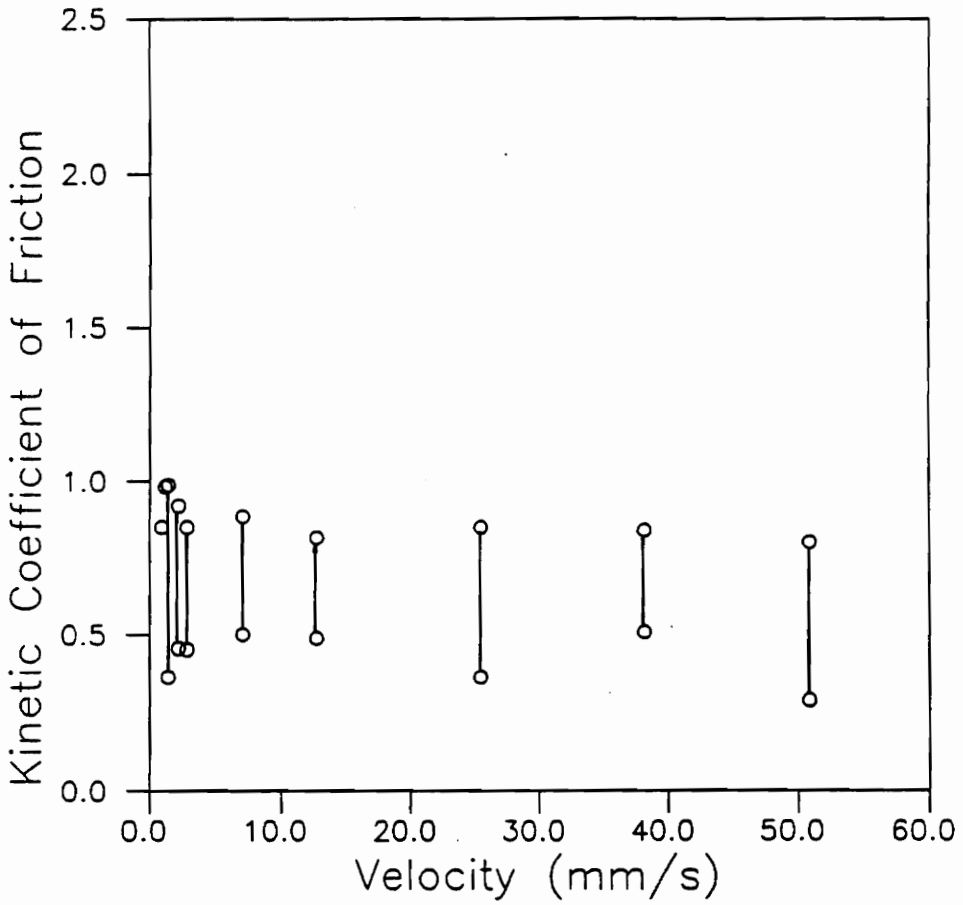


Figure 72. Kinetic Coefficient of Friction for 5 phr c.b. Natural Rubber against Cathodic Epoxy, Repeat Data Set (Load = 17.8 N, Wet).

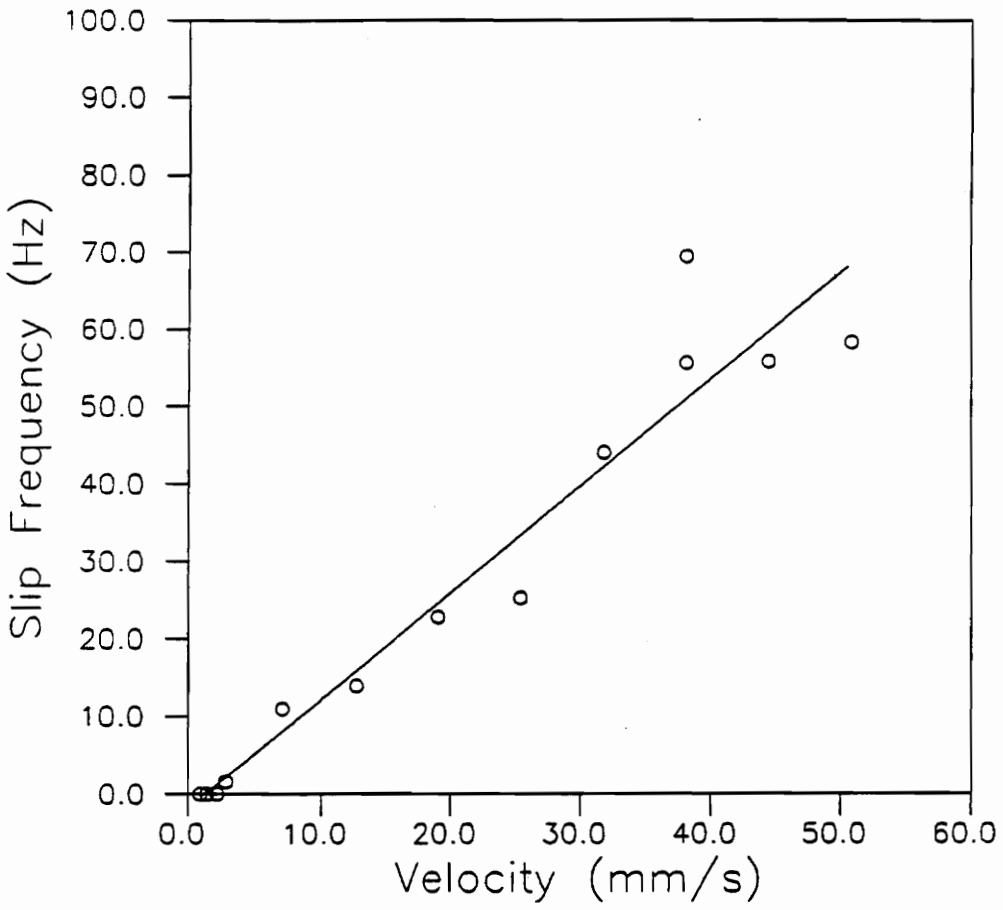


Figure 73. Frequency of slip for Friction-Velocity Data from Fig. 71.

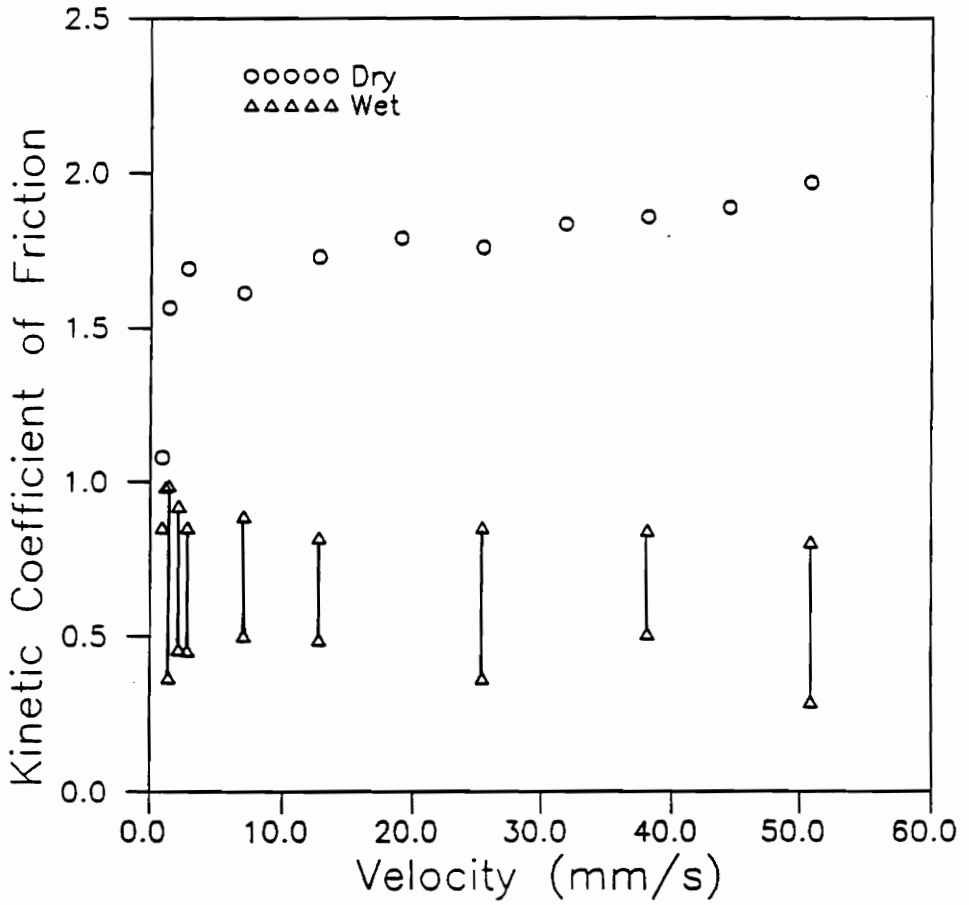


Figure 74. Comparison of Friction-Velocity Curves for Wet & Dry Tests of 5 phr c.b. Natural Rubber against Cathodic Epoxy.

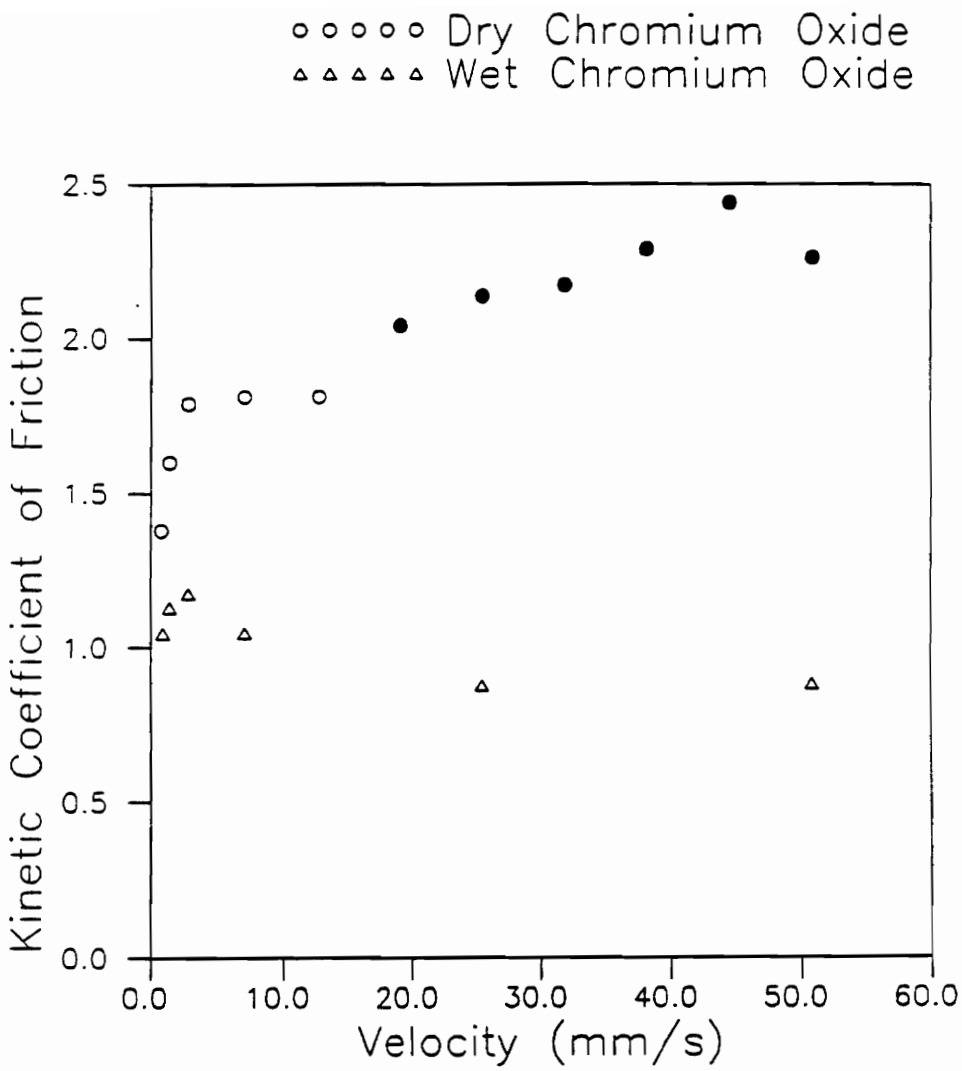


Figure 75. Comparison of Friction-Velocity Curves for Wet & Dry Tests of 5 phr c.b. Natural Rubber against Chromium Oxide.

* Solid symbols indicate oscillatory tests

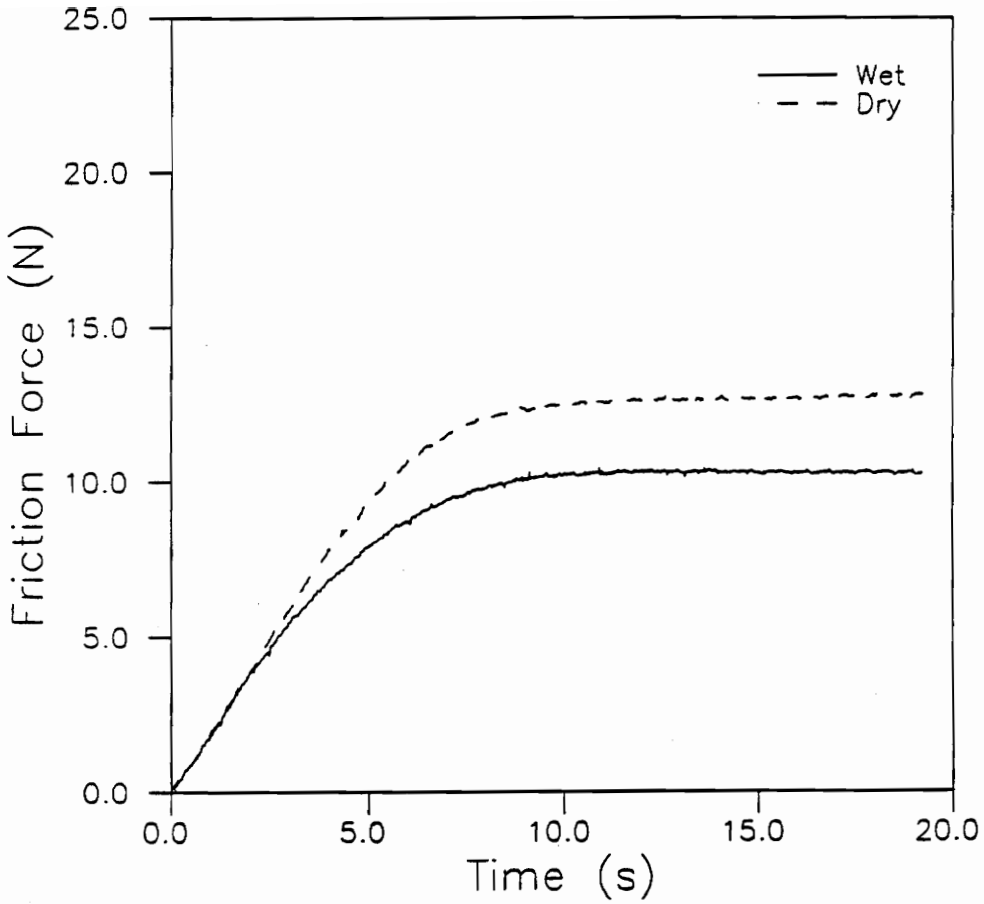


Figure 76. Friction Time Histories of 5 phr c.b. Natural Rubber against Cathodic Epoxy. (Wet & Dry, Load = 17.8 N, v =.919 mm/s)

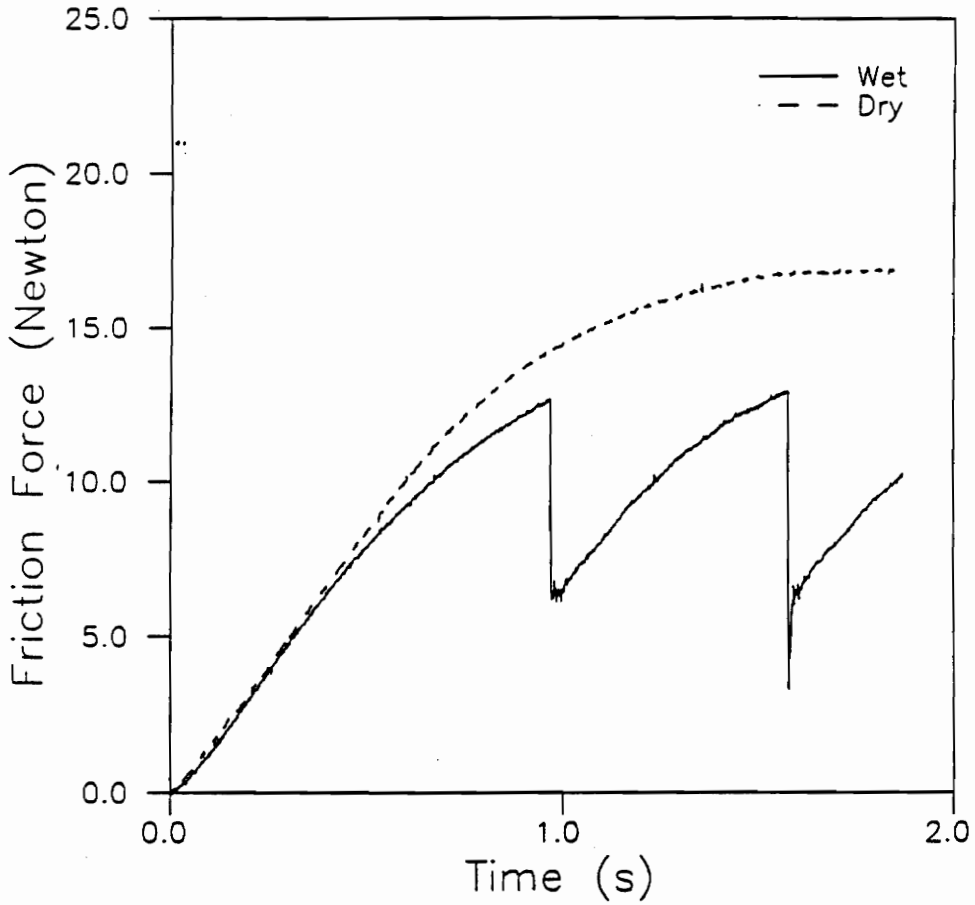


Figure 77. Friction Time Histories of 5 phr c.b. Natural Rubber against Cathodic Epoxy. (Wet & Dry, load = 17.8 N, v = 2.819 mm/s)

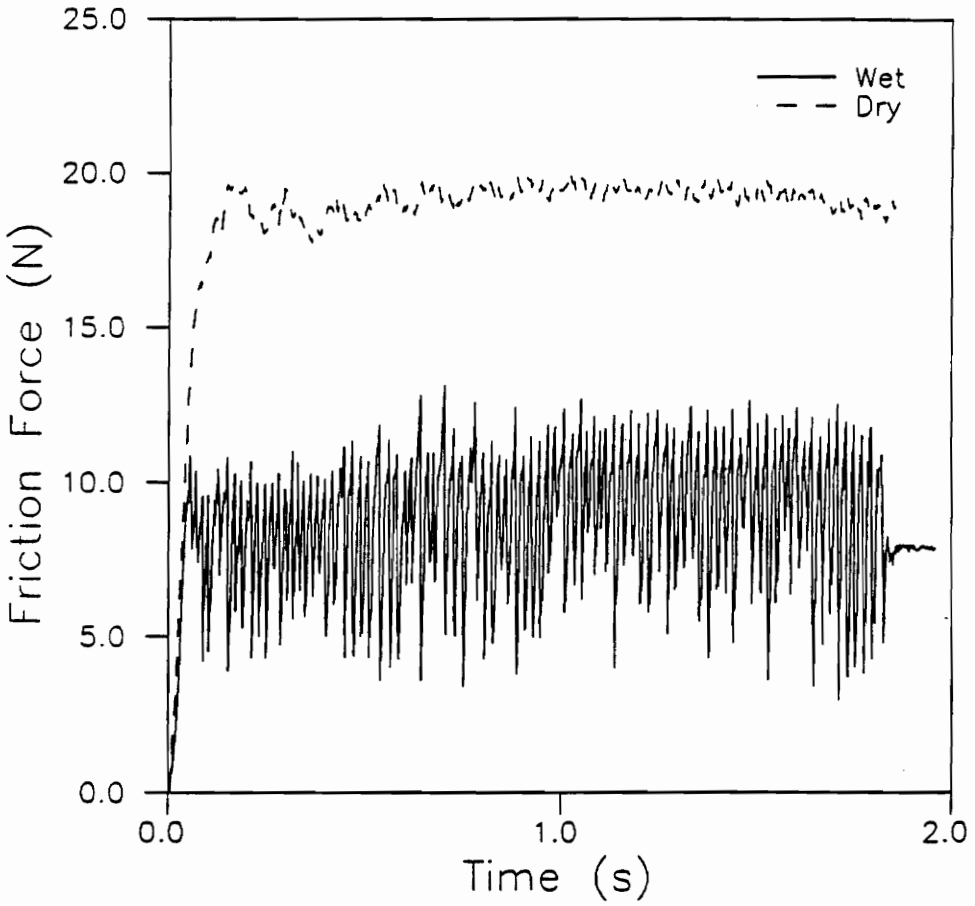


Figure 78. Friction Time Histories of 5 phr c.b. Natural Rubber against Cathodic Epoxy. (Wet & Dry, Load = 17.8 N, v = 38.1 mm/s)

from Figs. 76 and 77 that $v_{rel} > 0$ from the point of departure of the friction force from linearity. Figure 77 can be used to obtain an estimate of $v_{rel}$ at the point of incipient slip. Figure 77 is now shown as Fig. 79 for the determination. As shown in Fig. 79 the slope of the line $v_{rel} = 0$ is $kv_{plate}$. If it is assumed the elastomer is a linear spring in shear, and the measured friction force is proportional to the displacement of the center of the contact area. The following shows how $v_{rel}$ is obtained:

$$F = kx \tag{26}$$

where: $$x = v_{plate}\, t \tag{27}$$

therefore:

$$F = kv_{plate}\, t \tag{28}$$

Since $v_{plate}$ is known the spring constant, $k$, can be determined from the slope, $m$, of the $v_{rel} = 0$ line.

$$kv_{plate} = m = 16.29\ (N) / .961\ (s) = 16.96\ (N/s) \tag{29}$$

$$k = m/v_{plate} = 16.96\ (N/s) / 2.819\ (mm/s) = 6.02\ (N/mm) \tag{30}$$

Once $k$ is known for the hemisphere, the absolute velocity of the hemisphere, $v_{hemishpere}$ (at incipient slip), can be obtained from the slope, $m_b$, at point b.

$$v_{hemisphere} = m_b / k = 6.68\ (N/s) / 6.02\ (N/mm) = 1.11\ (mm/s) \tag{31}$$

Note that both velocities are in the same direction immediately prior to "slip".

Using the slope values obtained from Fig. 79, and the relationship $v_{rel} = v_{plate} - v_{hemisphere}$, $v_{rel}$ is calculated to be 2.819-1.110 = 1.71 mm/s. This value is bounded by the $v_{crit}$'s ( 1.409 and 2.819 mm/s) from Figs. 71 & 72, indicating agreement between the

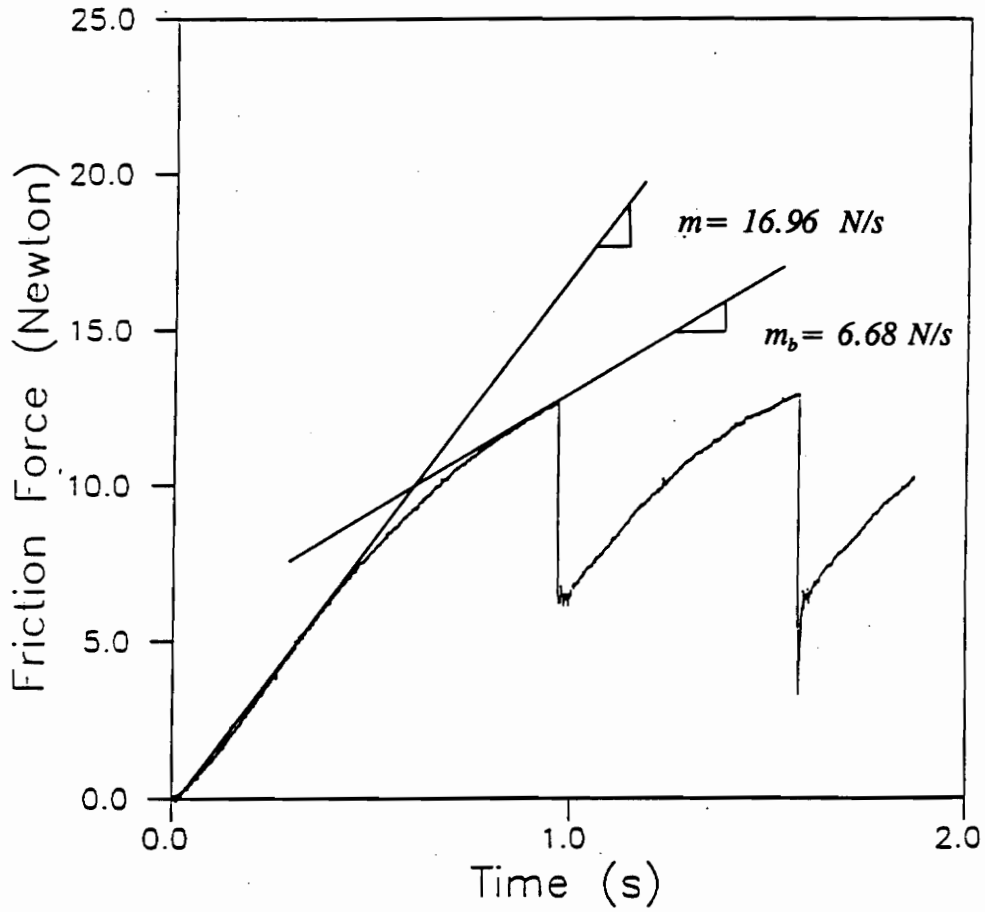


Figure 79. Determination of Relative Velocity from Fig. 77.

critical velocity estimated from friction-velocity curve and the estimate from the friction-time history. The result of the above analysis shows that for wet sliding, the hemisphere goes from a state of small relative slip, to a state of large relative slip.

**Natural Rubber- 50 phr c.b.**

An additional set of wet tests were run with 50 phr c.b. natural rubber against chromium oxide. As can be seen from the friction-velocity curve in Fig. 80 the critical velocity for stick-slip occurs at the same value as that of the 5 phr c.b. specimens. The implication for wet sliding is that the incidence of stick-slip is predominately dependent on the properties of the liquid and not the difference in the viscoelastic properties. The The difference between the maximum and minimum coefficients of friction shows no decrease over the range of stick-slip. Comparison of the wet to the dry tests in Figure 81 shows approximately a 1.8 reduction in friction force for the wet tests. Figure 82 shows the stick-slip frequency for the friction-velocity curve in Fig. 80. As can be seen from Fig. 80 there is the linear relationship of stick-slip frequency to velocity as was evident for the 5 phr c.b. sample (See Fig. 73). Comparison of Fig. 80 to Fig. 73 also shows that the frequency of stick-slip is greater for the stiffer material.

The time histories of three of the test runs are presented in Figs. 83, 84 and 85. Figure 83 shows a remarkable result. The first slip in the stick-slip phenomenon is larger than the subsequent slips. This result is identical to the result obtained for the 5 phr c.b. material at the same critical velocity.

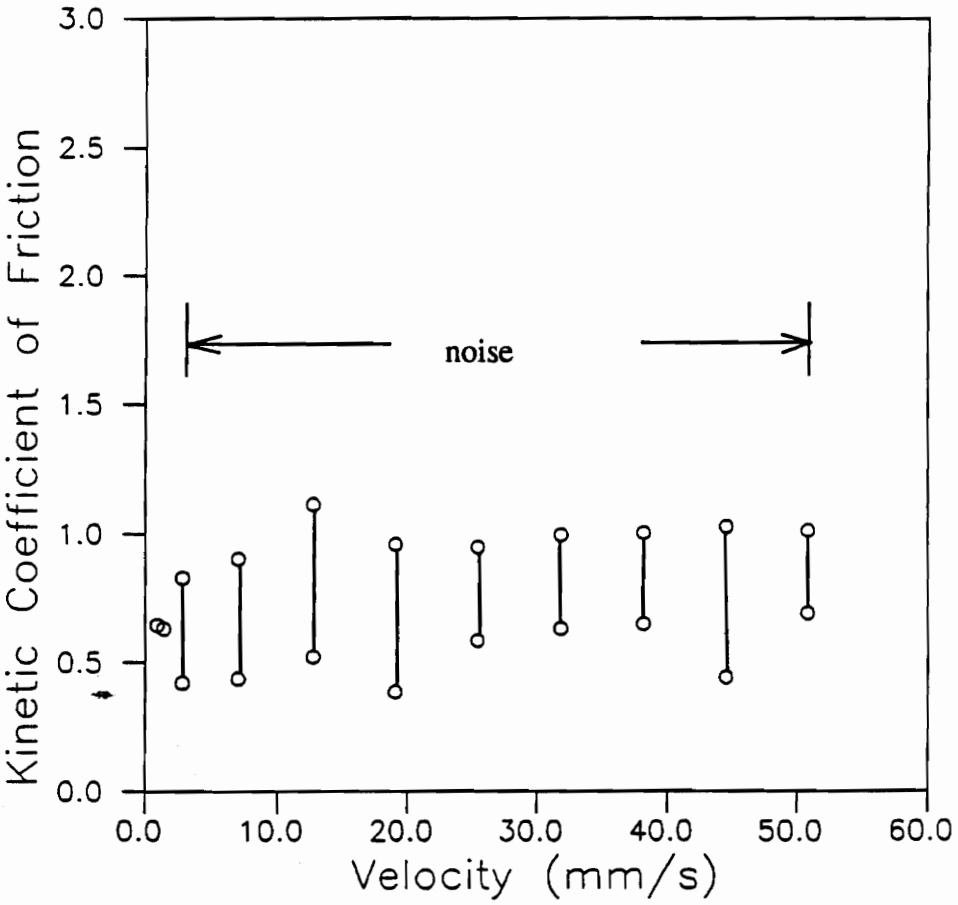


Figure 80. Kinetic Coefficient of Friciton of 50 phr c.b. Natural Rubber against Chromium Oxide (Load= 17.8 N, Wet)

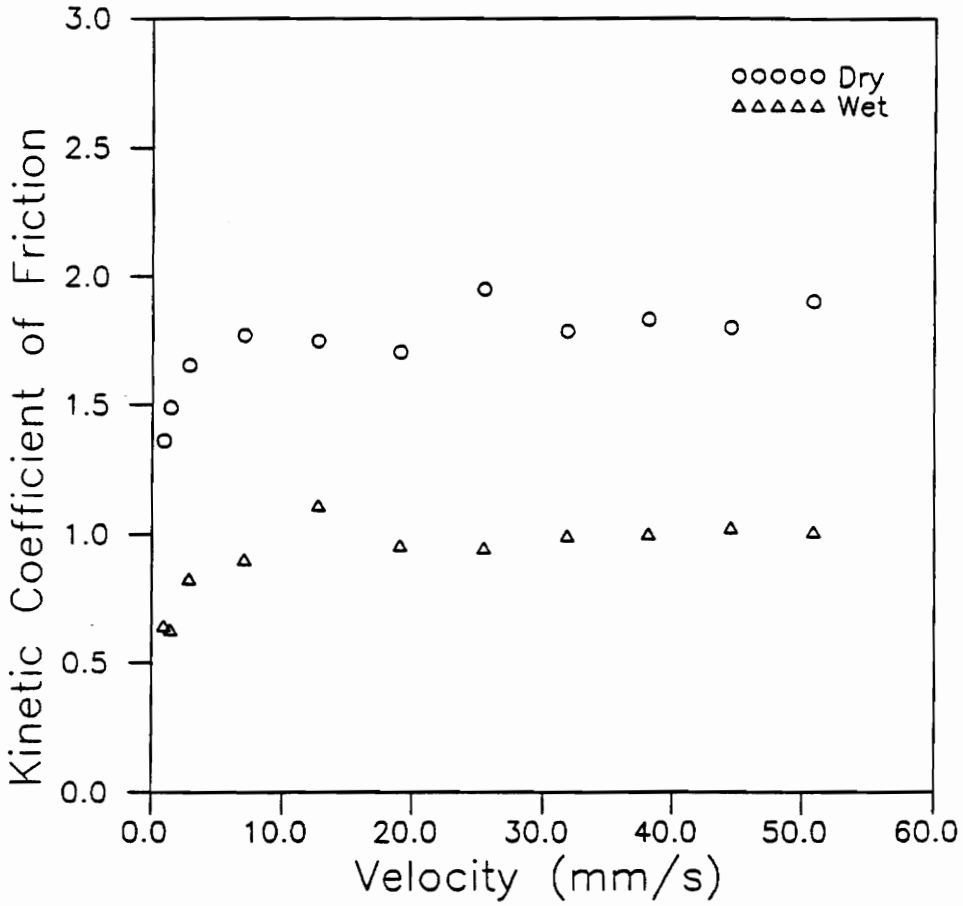


Figure 81. Comparison of Wet and Dry Kinetic Coefficients of Friction for 50 phr c.b. Natural Rubber against Chromium Oxide. (Load= 17.8 N)

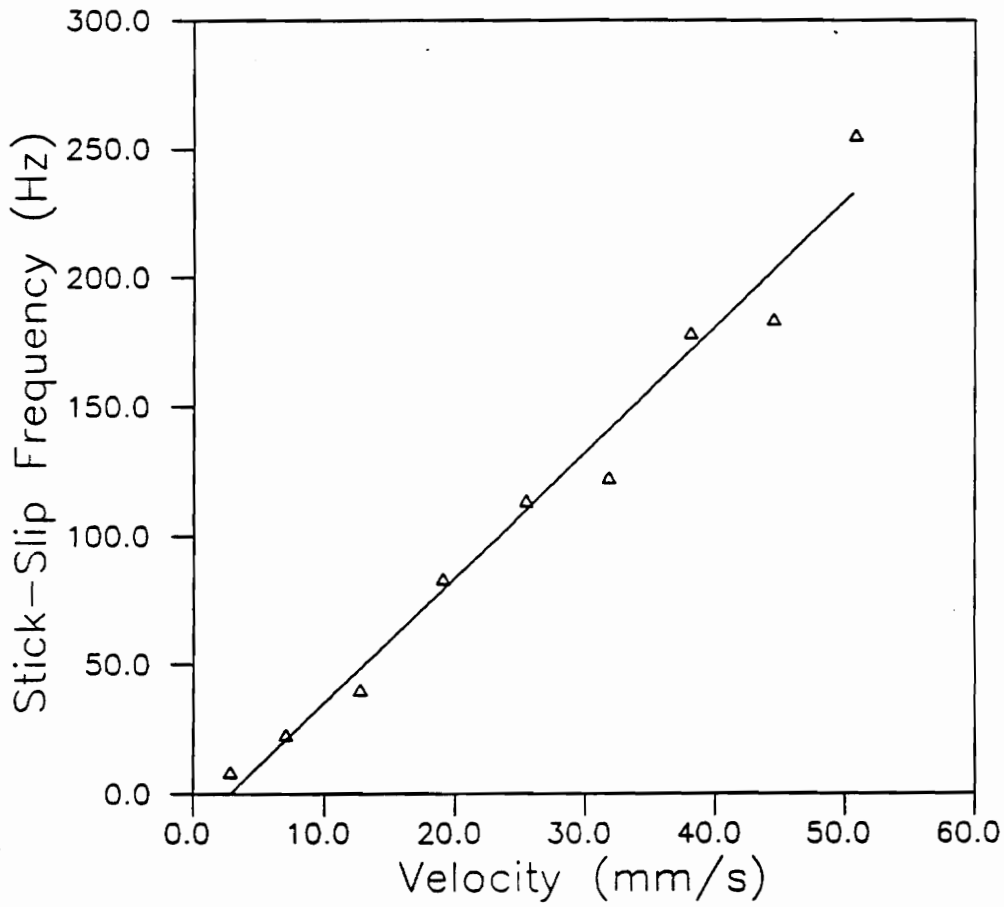


Figure 82. Frequency of Stick-slip for Friction-Velocity Data of Fig. 80.

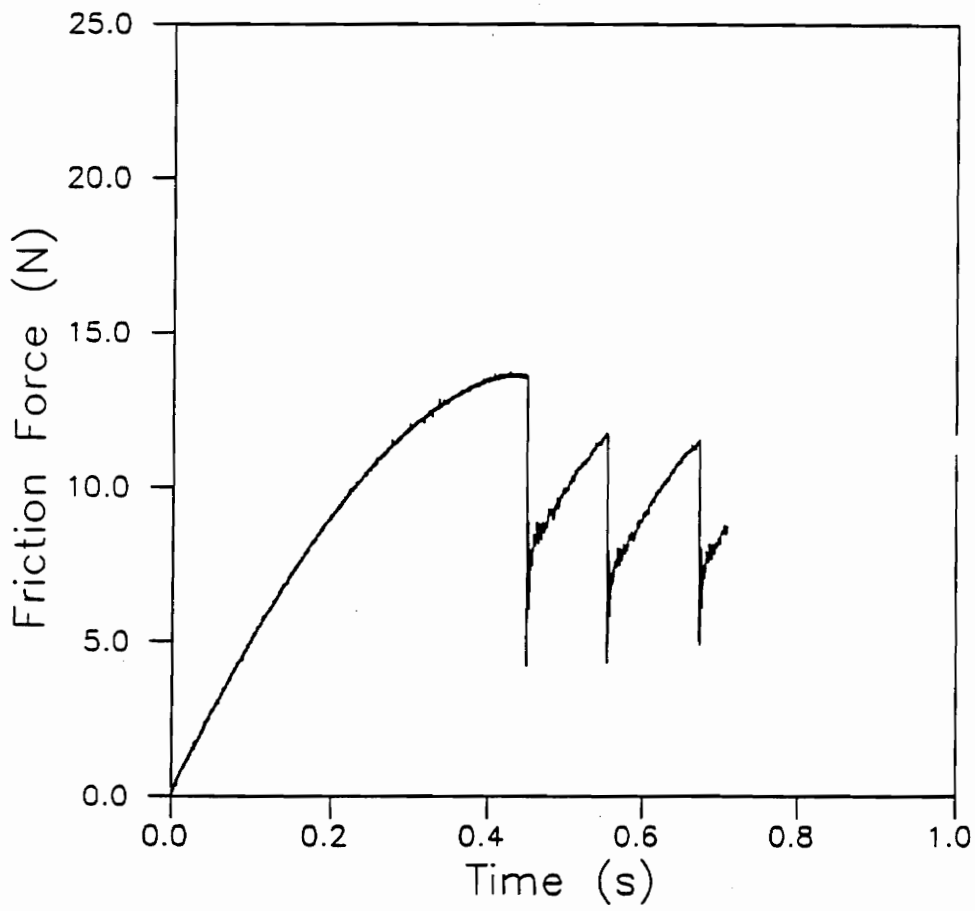


Figure 83. Time History of 50 phr c.b. Natural Rubber against Chromium Oxide. (Load= 17.8 N, Velocity = 2.819 mm/s, Wet)

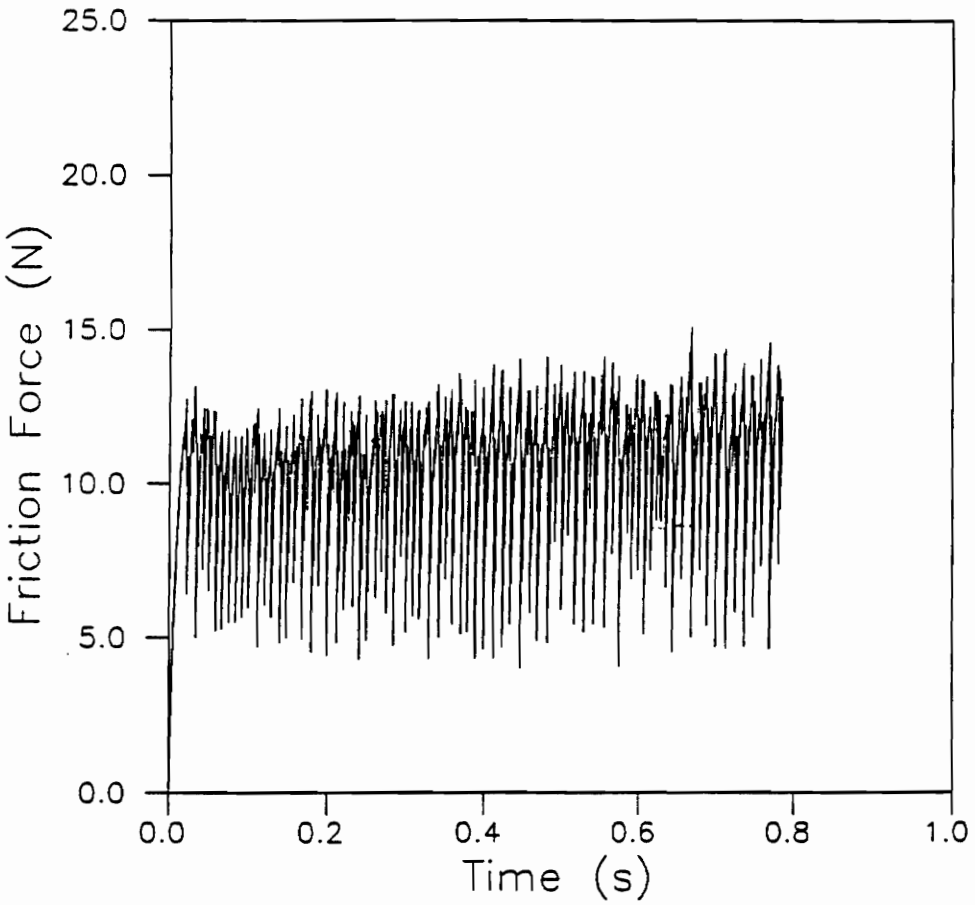


Figure 84. Time History of 50 phr c.b. Natural Rubber against Chromium Oxide. (Load= 17.8 N, Velocity = 19.03 mm/s, Wet)

Figure 85 shows the time histories at the critical velocity for both the 5 and 50 phr c.b. natural rubber hemispheres. Paradoxically, for velocities greater than the critical velocity the friction force at slip for the first slip was equal to not greater than the subsequent slips. Possibly this anamoly is indicative of the change in behavior from steady sliding to stick-slip. However, currently there is no explanation for its occurrence.

### Surface Roughness

Theoretically, increasing the surface roughness of the counterface has two competing effects. Friction was previously described as having two major contibutors, adhesion and deformation. For very smooth surfaces there is little or no deformation due to asperities passing or ploughing through the rubber simply because of their negligible size. Rough surfaces on the other hand, still have an adhesion component, but since the real area of contact is reduced the adhesion becomes neglible relative to the deformation component of friction with increasing roughness. Increased surface roughness (in the range $R_a < 0.200\ \mu$m) appears to have very little if any effect on the friction force and critical velocity. Figure 86 shows a slight increase in critical velocity for aluminum surfaces (with a factor of 2 difference in roughness). Reexamination of Fig. 42, the friction time history for cathodic and powder epoxy shows that the friction levels are indistinguishable, yet there is a factor of 5 difference in roughness.

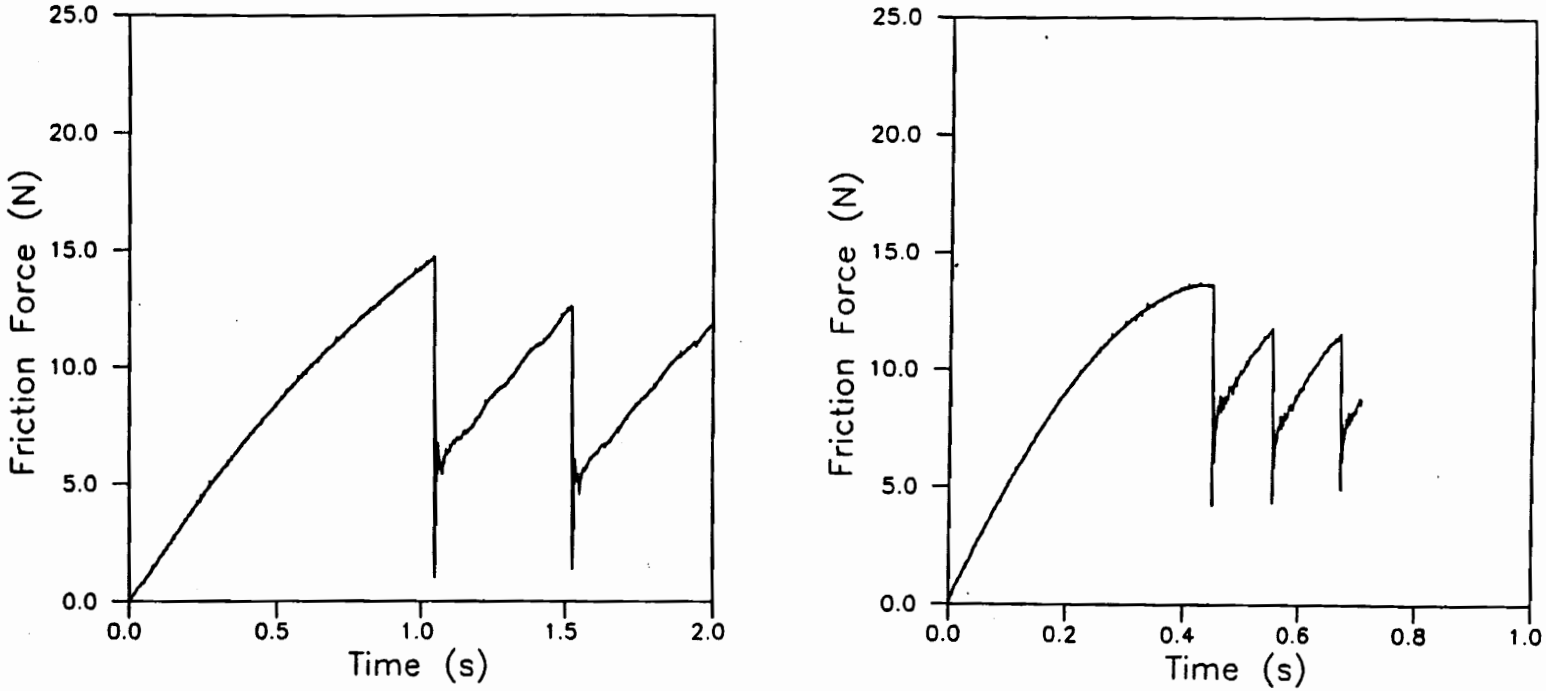


a. 5 phr c.b.

b. 50 phr c.b.

Figure 85. Friction anamoly for tests run at critical velocity for 5 and 50 phr c.b. natural rubber against Cathodic Epoxy (Load= 17.8 N, v= 2.819 mm/s)

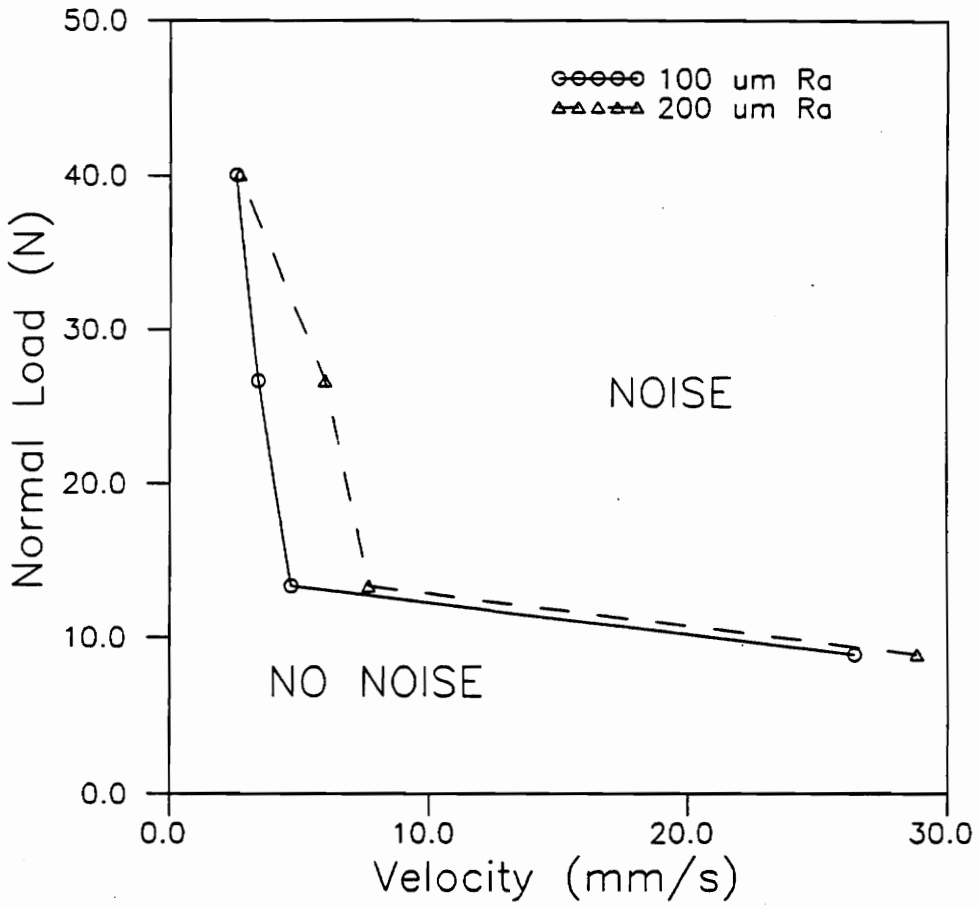


Figure 86. Effect of Surface Roughness on Critical Velocity of Aluminum Counterfaces (Hollow 50 phr c.b. Natural Rubber).

# DISCUSSION

In this study the sliding of elastomers against hard counterfaces was investigated experimentally. After discussion of the experimental results a potential mechanism leading to oscillatory behavior will be discussed. Prior to the discussion of the mechanism which governs dry sliding, the theoretical requirements will be reexamined in light of the experimental results. It has been noted in the Literature Review that the friction-velocity curve must possess double-valuedness of velocity with respect to friction in order for stick-slip to occur. Finally, the theoretical requirements will be related to the tearing of elastomers.

Observations made in the results section for dry sliding show that over the velocity range tested cohesive transfer must be present for the stick-slip phenomenon to occur. The cohesive transfer is in contrast to the previous adhesive theories presented in the literature review. True interfacial sliding without transfer occurred only for the chromium oxide and glass plates when they were cleaned with isopropanol. It is possible that the lack of transfer is occurring due to boundary lubrication from a contaminant film laid down by the solvent wipe.

An attempt will be made later in the discussion to link the stick-slip friction behavior of elastomers to fracture mechanics concepts involved in the tearing of elastomeric sheets. While the discussion of a fracture mechanics approach to stick-slip tearing of elastomer sheets may seem more appropriate to the literature review it is presented in this discussion for the following reason. The fracture mechanics approach

provides a physical mechanism that is transferrable to sliding due to the cohesive nature of the sliding process. Additionally, the argument contains elements of the discontinuous relaxation theory.

### Transfer Film

Implicit in the adhesive theories of friction is the lack of a transfer film. However, for dry sliding, oscillatory behavior occurred only when a transfer film was present. In reviews on the sliding friction of elastomers Roberts [20] and Briscoe [42] have stated that at very low speeds and with very smooth surfaces no transfer has been observed to occur. It was initially suspected by this author that the thickness or presence of the transfer film would indicate that oscillatory sliding occurred. The basis of this prediction was the stick-slip peeling of pressure sensitive tape which occurred above a certain critical speed [43]. Well below the critical speed ($v$ < 4-5 decades lower) the tape peeled uniformly, with cohesive failure of the adhesive. Just prior to and above the critical speed, the failure mode changed to failure at the adhesive-substrate interface.

The strain energy release rate for the peeling of tape as a function of velocity has the double valued velocity required by the theory of relaxation oscillations. Figure 87 shows the experimental results of Maguis and Barquins [43]. There are two important velocities shown in Fig. 87. The first is $v_c$, the onset of stick-slip and the second is $v_2$, the reappearance of steady peeling. It should be noted that the shape of the curve meets

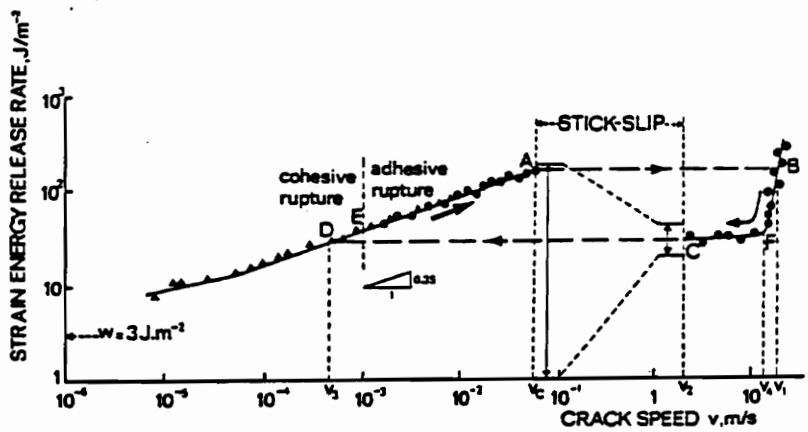


Figure 2. Experimental G(v) curve.

Figure 87. Experimental Results for Peeling of Pressure Sensitive Tape [43].

the requirement for relaxation oscillations. The major difference between peeling of pressure sensitive tape and elastomeric sliding is the location of the propagating crack. In the peeling of tape the crack propagates at the interface of the tape and counterface. In elastomeric sliding the crack propagates within the elastomer which leads to cohesive failure and transfer of the elastomer.

Grosch [8,18] and others [16] assumed that dry sliding of elastomers against smooth counterfaces occurs only adhesively. However, paradoxically, they observed a "viscous smear" on the counterface. Even though an in depth investigation into the transfer film was not performed here, it is obvious from the FTIR and photoacoustic results that the transferred material is the same as the bulk and not just bloomed material. Prior to each of the tests in this series, the hemisphere was wiped with acetone to remove any bloom or loose material. While this procedure is certainly not solvent extraction of the sol fraction, it removed the excess material. The effectiveness of this procedure was indicated by the lack of a transfer film when a hemisphere cleaned with acetone was pressed normally against the plate and unloaded without application of a shear load. Prior to cleaning, the hemisphere would leave a circle of transferred bloom or loose debris.

The presence of transfer film indicates that the sliding process takes place by cohesive failure not adhesive failure for sliding conditions where stick-slip will occur. For conditions where cohesive transfer is not observed (e.g. isopropanol cleaned glass) the contaminant film may act as a boundary lubricant and true interfacial sliding occurs.

The greatest utility of the thickness measurement is the estimation of the order of magnitude of an effective strain rate. The effective shear strain rate, $\dot{e}$, of the material can be defined as follows:

$$\dot{e} = \frac{v}{h} \tag{32}$$

where:

$v$ = velocity of plate

$h$ = effective thickness of strain influence

The transfer layer thickness is used as an estimate of $h$. A reasonable estimate of the thickness range from Figs. 28a-d for natural rubber is 40 - 80 angstroms. Using 50 angstroms with the velocity range of .916 to 50.8 mm/s results in strain rates of .916 ($10^7$) to 50.8 ($10^7$) mm/mm·s. Properties such as rupture strength, etc. of the thin film should be obtained or estimated at these rates to be representative for use in determining the shear strength properties.

The effective depth over which the strain and strain rate influence the elastomer is illustrated by examination of a steady state sliding tests. Figure 88a shows an idealized friction-time history for steady state sliding. Without considering the transition from stick to total slip or sliding, there are only the two distinct phases of strain. Both phases are shown in Fig. 88a. The first stage involves the total elastomer thickness. As can be seen from Fig. 88b the bottom of the elastomer has zero velocity and the top (the point in contact with the plate) has $v = v_{plate}$. Therefore the material sees a strain rate

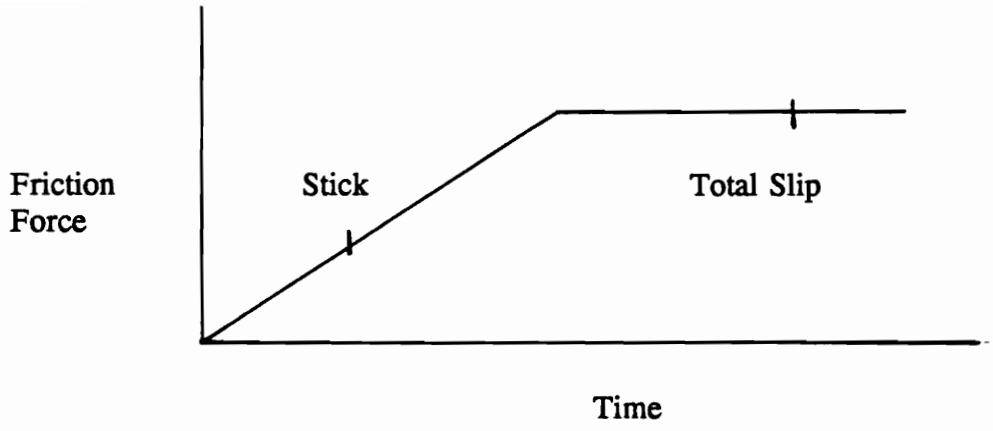


(a) Simplified Friction Time History

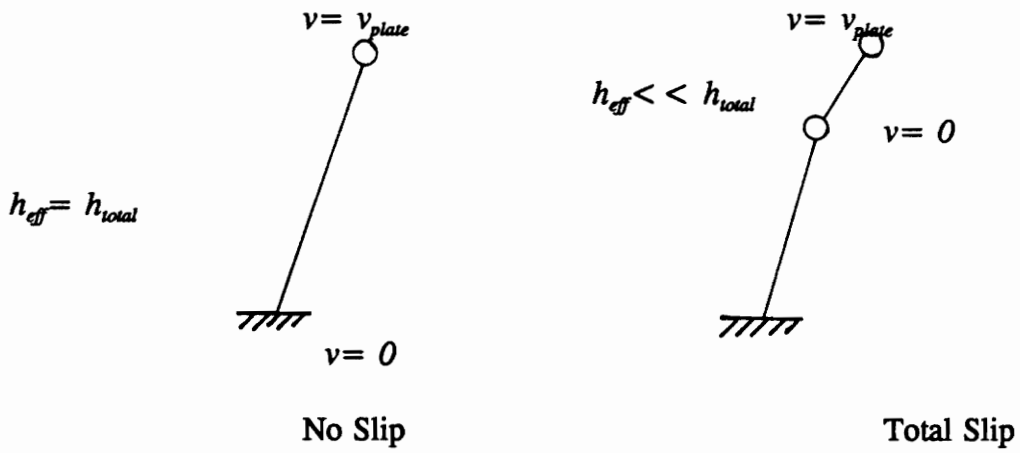


(b) Effective Strain Depth


(c) Strain Conditions Experienced during Total Slip

Figure 88. Effective Strain Rate Depth During Sliding.

equal to $v_{plate}/h_{total}$. During the second state of the friction time history the elastomer has deflected to its maximum deflection and with the exception of minor perturbations due to surface and material inhomogeneties, stays at this maximum deflection. In this case it is obvious that not only does the bottom of the elastomer have zero velocity but so does the bulk of the material. For this situation there is a static strain in the material corresponding to the stress imposed by the friction force. In addition, there is a dynamic component of strain corresponding to the strain rate which operates over an albeit, small finite thickness. Employing this view of the strain effect on the material leads to the estimate of the effective thickness from the transfer film measurements. Figure 88c shows the proposed transfer mechanism. Two chains are shown, one in the unstrained condition. The other chain has been deformed until the force is at the ultimate allowable value. It is proposed that the chains make adhesive contact with the surface and then rupture at the depth obtained from the ellipsometry measurements. Since the elastomer is always exposed to fresh material from the counterface this process is continuous. From Fig. 88c it can be argued that the chains statistically are breaking at their mid-point, but this detail is of little importance. The important point is that the thickness measurements provide an order of magnitude estimate on the effective strain rate depth.

Assuming the simple model of friction as proposed by Ludema and Tabor [15], the friction force during steady sliding should scale with the rupture strength (although, they note that there is a factor of 10 reduction from the theoretical prediction of the magnitude of the friction force to experimental results!). Additionally, Ludema and Tabor [15] assumed that the shear rupture properties are proportional to the tensile

strength. Tensile rupture properties obtained by Smith [44] for styrene-butadiene are shown in Fig. 89. As can be seen from Fig. 89 the tensile rupture properties reach a maximum value at a strain rate of approximately $10^6$ - $10^8$ mm/mm·s. Increased values of strain rate beyond $10^6$ do not significantly increase the rupture strength. Since the order of magnitude of the transfer film thickness remains relatively constant the strain rate scales linearly with imposed sliding velocity. Based upon the presence of the transfer film this researcher believes that the Ludema and Tabor model is more representative of the dry sliding process than the molecular kinetic theories. Since the thickness of the transferred film remains relatively constant (i.e. 40 -80 angstroms), the strain rate is proportional to velocity. Therefore, the thickness measurements provide validation of the levelling off of the maximum coefficient of friction with increasing velocity in terms of the strain rate dependence of the rupture properties. Note that the test geometry of elastomeric slider on a hard flat counterface eliminates the stiffening effect of the storage modulus and a corresponding decrease in the area of contact. If the area of contact is independent of the velocity, the Ludema and Tabor theory predicts (from strain rate dependence shown in Fig. 4) the shape of the friction-velocity curves observed in this research.

The strain rate dependence of the shear strength also becomes important in unsteady sliding, particularly stick-slip. In the Experimental Results section it was noted that there was a deviation from linearity (or the $v_{rel} = 0$ line) in the friction time trace (see Fig. 33). Therefore, during the micro-slip of the stick phase of stick-slip sliding the strain rate can transition from 0 to $v_{rel}$*(at incipient slip)*$/h$. In this case, the maximum

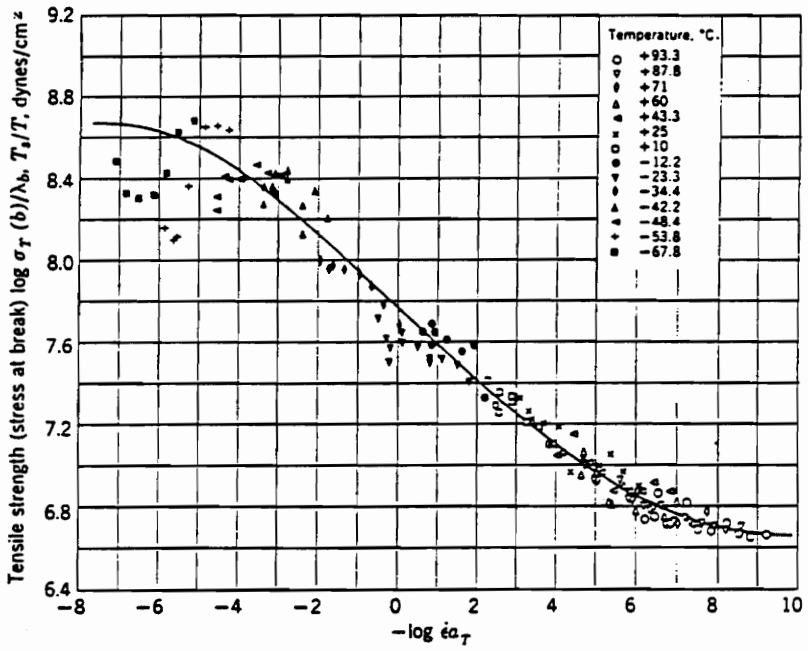


Figure 89. Tensile Rupture Properties for Styrene-Butadiene Elastomer [45 from 44] ($T_s$= 20 °C).

strain rate is less than but of the same order of magnitude as $v_{plate}/h$. The transition from 0 to $v_{rel}$*(at incipient slip)* accounts for the increase in friction during micro-slip of the stick phase.

Further proof that the mode of sliding against clean surfaces is dominated by cohesive and not a rate (or temperature) activated adhesive process is one of the observations from the experimental apparatus section. In the heated test subsection it was noted that the hemisphere had to remain against the heated counterface for approximately 2 minutes to maintain a constant level of friction during the test. If the sliding of elastomers is indeed dominated by polymer chains attaching, releasing, and reattaching to the surface, only heating the counterface should reduce the level of friction. However as was previously observed, inadequate heating of the elastomer surface would revert the coefficient of friction to the value obtained at $T = 20$ °C.

## Dry Friction Results

### Natural Rubber

More exhaustive testing was performed on natural rubber elastomers for the following reasons. First and foremost, natural rubber generated noise by stick-slip, the mode that is most likely to occur under operating conditions. The Schallamach waves observed for butyl rubber and the poor tear strength (in its unfilled state) make it an unlikely candidate for replacing natural rubber. PDMS did not yield stick-slip. Therefore extensive testing would yield very little information for analyzing the noise

threshold. Additionally, in another apparatus designed to simulate the stabilizer bar configuration [46] it was also confirmed that PDMS would not generate noise.

Increasing carbon black raises the glass transition temperature which is equivalent to shifting the frequency of the maxima (at constant temperature) of the loss modulus and tan $\delta$ to a lower value. Therefore, the molecular kinetic theories and others predict the critical velocity for stick-slip should shift to lower frequencies. However, increasing carbon black increases the amount of hystersis which should shift the peak to higher frequencies. The results of the hollow 50 phr c.b. natural rubber hemispheres imply that this shift may due to increasing stiffness, and not necessarily the result of a shift in the viscoelastic properties.

**Butyl Rubber**

The butyl sliding results differ slightly from those obtained by other investigators [26,47,48,40]. Their research shows waves of only one size traversing the interface while the results presented here have shown that for noise generation there are two different size waves that occur. The theoretical instability theory formulated by Biot [49], does not predict the size of the wave. In Biot's model a semi-infinite half space was analyzed and a uniform distribution of the strain in the direction of stress was assumed. However, the stress and/or strain distribution on the contact area of a slider or counterface are not uniform and vary in form according to the Hamilton-Goodman [50] relationship for a moving sphere on a plane as shown in Fig. 90. It is obvious the most likely place to generate the buckle or wave is at the peak of the compressive stress.

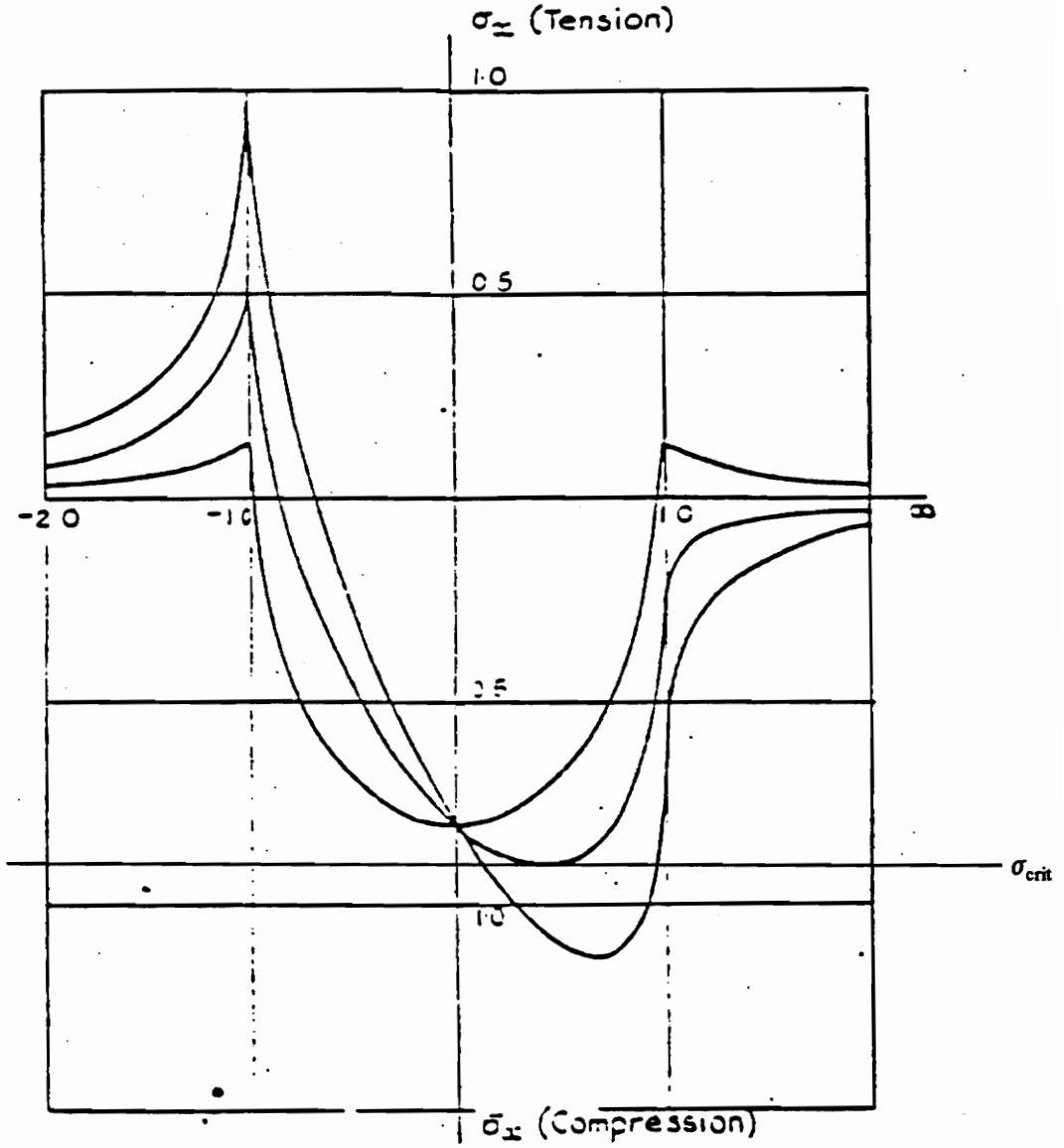


Front Edge Rear Edge

———> Direction of Sliding Plate

Figure 90. Hamilton-Goodman Stress Distribution [50].
Normal Stress Parallel to Flat Counterface and in the Direction of Sliding.

Biot [27] developed the following relationship to predict the onset of the instability.

$$\lambda_{crit} \geq .444 \tag{33}$$

where: $\lambda = l/l_o$
$l$ = final length of stressed material
$l_o$= initial length of stressed material

This theory does not predict the size of the buckle nor does it take into account the viscoelastic nature of the formation and propagation. However, it does give an idea of the magnitude of the friction force required to yield the critical compressive stress via the Hamilton-Goodman stress distribution for sliding contact. Returning to Fig. 90 it can be seen that as the coefficient of friction increases, regardless of the reason, the maximum compressive stress on the front half of the contact area increases. After it reaches the value predicted by Biot [27] the Schallamach waves should occur. Additionally, the slope of the stress distribution would tend to propagate the waves away from the maximum compressive stresses in the direction of the maximum tensile stresses.

### PDMS

PDMS did not generate noise under dry sliding conditions. At first this was surprising since PDMS has the lowest modulus of the specimens tested. Noise was anticipated based upon the previous observations that hollowed hemispheres were more prone to noise generation than solid hemispheres. However, PDMS is also the weakest of the elastomers tested.

PDMS has the lowest glass transition temperature of any elastomer (-127 °C). In addition to the low $T_g$, PDMS remains noncrystalline to low temperatures due to the low melting temperature ($T_m \approx$ -40 °C) [51]. This results in a rubbery plateau which extends to very low temperatures. The lack of fillers and noncrystallinity of the PDMS relate to the fracture mechanics argument which will be developed later. Since neither of these are present there is no mechanism to have a higher energy release rate than propagation rate. However, the lack of stick-slip at the higher velocities may be due to the weak rupture properties which may result in no difference between the initiation and propagation energy release rates.

### Fluorocarbon

Initially, it was not possible to make the fluorocarbon make noise against the various counterfaces. The reason appeared to be the stiffness of the elastomer in the tangential direction. However, as the test results show it is possible to generate noise with the fluorocarbon elastomer. Once again the same shape of the friction-velocity curve is obtained. Specifically, the curve flattens out in the 10-20 mm/s velocity range. Unlike, the natural rubber results the fluorocarbon generates noise well after (20 mm/s) the flattening of the curve has been passed. The oscillations and subsequent stick-slip are at a frequency 4-5X the oscillatory frequency of the natural rubber specimens. This increase is to be expected due to the increase in stiffness.

### Wet Tests

It is obvious the mechanism of sliding is not the same for the wet and dry tests. In the dry tests noise was always accompanied by transfer. In the wet tests no transfer was evident. The lack of transfer to the counterface implies that contact between the elastomer and the counterface never occurred. The results of the wet tests are in agreement with those of other researchers [10,11,12,13]. In their work, the researchers were only able to generate noise with their test apparatus and elastomers when wet. The counterface materials probably could not create the necessary adhesion to cause cohesive failure of the elastomer.

Interestingly, since the presence of water prevented contact and should have acted as a lubricant, the implication is that other possible lubricants (such as the silicone paste) could in fact worsen the noise problem. Once again we return to the theoretical argument that it is the shape of the friction-velocity curve that is important, not the maximum value it attains. The same lack of dependence on the maximum coefficient of friction has been implicit in all the previous theories of stick-slip generation. For example, the negative slope argument did not imply anything about the maximum value of the friction force.

Perhaps one of the most interesting results of the wet tests is the same critical velocity for both the 5 and 50 phr c.b. natural rubber hemispheres. Bhushan's [10] results show the critical velocity for stick-slip increasing with increasing amount of hysteresis of the elastomer. Increased amounts of carbon black increase the amount of

damping or hysteresis of the rubber. Therefore the 50 phr c.b. hemisphere should have a higher critical velocity than the 5 phr c.b. hemisphere. However, the results obtained in this study show that the critical velocity is independent of the amount of carbon black. In addition, if the natural rubber results are considered alone, it appears the lubricant (i.e. water) determines the critical velocity.

However, when the PDMS results are considered the critical velocity is no longer the same. There is a fundamental difference between the PDMS and natural rubber elastomers as far as the wet tests are concerned. Finally, the surface energy can be brought into the discussion. Because of the technique used to "wet" the elastomers the difference surface energies became important. A Kimwipe was laid on the elastomer and removed immediately prior to the test run. Remember that the water contact angle is perhaps the easiest way to determine surface energy of a material. For this study the water contact angle was used to rank the surfaces, not to determine the absolute surface energies. In Table 2 it is seen that natural rubber has a water contact angle of 82° and PDMS has a water contact angle of 104°. A water contact angle of zero means that water will "wet" the surface (i.e. spread and cover). A water contact angle greater than 90° means that water will bead on the surface. Even though the water contact angle of natural rubber is not zero it is less than the water contact angle of PDMS. When the Kimwipe was removed from the natural rubber a complete film of water was left on the hemisphere's surface. When the Kimwipe was removed from the PDMS the water beaded and there was a tendency for the water to migrate away from the contact area upon application of the normal load.

Since the wet tests were unable to be performed in a flooded condition, the critical velocity for the PDMS tests may not be representative. Also, the test method avoided any hydrodynamic effects due to the lack of excess liquid.

Unlike the dry tests, where the maximum friction force experienced during stick-slip remains constant or increases slightly during increasing velocity , the maximum friction force reached during stick-slip for the wet tests decreased after the critical velocity was attained. Therefore, even though the calculation of the relative velocity at slip was on the order of the critical velocity, the higher velocity tests did not experience friction forces as high as that of the test run at the critical velocity.

It is obvious when compared to dry tests against the same counterface, e.g. Fig. 77, the wet tests experience a small amount of bulk or gross relative slip during what is commonly referred to as the "stick" phase. During this time the displacement and absolute velocity of the hemisphere is in the direction (positive) of motion of the plate. The hemisphere then goes into the commonly observed slip phase, which does not differ from the slip phase as encountered in metallic or dry elastomer stick-slip, where the slider has a negative absolute displacement and velocity. Therefore, this phenonema is more accurately described as "slip-more slip" instead of "stick-slip".

If the theoretical requirements for harmonic oscillations or stick-slip are considered, it is apparent it is the shape of the friction-velocity curve that "drives" the system into oscillatory sliding. The main point and fundamental difference between wet and dry sliding is that a miminum coefficient of friction is not required for stick-slip in wet sliding. From the friction-velocity curves generated for wet sliding a negative slope

is seen after the critical velocity is reached. Indeed the theoretical and experimental implication is that any contaminant, liquid or solid that results in a negative slope to the friction-velocity curve will result in oscillations.

Not surprisingly, wet tests produced noise more readily than dry tests (e.g. at lower velocities and loads) and with greater amplitude of oscillation. Of course, anyone who has ever owned a pair of tennis shoes could have made this observation!

At first glance it may appear that wet tests are unrelated to the dry tests. Insofar as the wet tests have no evidence of contact between the hemisphere and the counterface the previous statement is true. However, the wet and dry tests are related in the following manner. If the governing differential equation is considered, it is obvious that the mass, stiffness and material damping of the system remain the same. The $f(v_{rel})$ forcing function changes. The theoretical prerequisite for oscillations depends on the shape of the friction-velocity curve not on the mechanism that yields this shape. The friction-velocity curve for 5 and 50 phr c.b natural rubber against chromium oxide and cathodic epoxy all evidence a negative slope at the critical velocity. Admittedly the slope then becomes essentially zero at the higher velocities ($v > 17.3$ mm/s).

**Surface Energy and Surface Roughness**

Unlike the results reported by Savakoor [32], there was no relationship between surfaces with different surface energies and the coefficient of friction. Even though theory predicts that the work of adhesion and hence the coefficient of friction should be

proportional to 1 + cos Θ, this was not observed in this study. With the exception of Savakoor's work, most researchers have found that the sliding friction of elastomers and other polymers has little if any dependence on the water contact angles. The observed discrepancy is illustrated by comparison of the glass results cleaned by acetone and isopropanol.

Isopropanol was originally used as the solvent for cleaning the glass, primarily because it was used virtually in all the past research on sliding elastomers [8,18]. However, this was not a particularly good idea! The isopropanol cleaned glass did not yield noise, while the acetone cleaned glass did yield noise. The reason for this was obvious. The elastomers did not transfer to the isopropanol cleaned glass while they did transfer to the acetone cleaned glass. The elastomers had lower friction on the isopropanol cleaned glass. Additionally, ellipsometry measurements of the chromium oxide counterface with cleaned with isopropanol and acetone showed no transfer and transfer of elastomer respectively.

True interfacial and/or boundary lubricated sliding occurs when the counterfaces are cleaned with isopropanol. The interfacial sliding occurs even though, in the case of glass, the water contact angle and thus the surface energy of the isopropanol cleaning is greater than the acetone cleaned chromium oxide which implies that if transfer occurs for the chromium oxide it should also occur for the isopropanol cleaned glass.

The above points to the fact that surface energy is a poor indicator/predictor of friction levels. It is possible, in the case of glass, to have a high surface energy contaminant film present that possesses low shear strength, which results in a lower

coefficient of friction than the proportional prediction of 1 + cos Θ from the theory.

### Theoretical Friction-Velocity Relationship

Researchers in the past have implied that a negative slope of the friction-velocity curve is all that is necessary for stick-slip motion to occur, but the theory states there must be an additional upswing to the curve beyond the negative slope to provide the necessary prerequisites for relaxation oscillations to occur. Theoretically, a negative slope can only lead to harmonic oscillations not stick-slip. Various investigators [38] have stated the way to eliminate stick-slip motion is to operate on the positive slope of the friction-velocity curve. While this is certainly mathematically true, can it be determined beforehand that a sliding pair possesses a positive slope to the friction-velocity curve in the desired operating range of velocity and load?

Historically [8,18,9,10,15,16], it was assumed the friction-velocity relationship determined by a series of independent friction-time tests was directly related to the friction-time relationship in the slip phase of a single test. However, this assumption bears closer examination. The literature is not clear on what value is used as the kinetic coefficient of friction when frictional oscillations occur. It appears that in most cases the average value of the friction force is used in obtaining the kinetic coefficient of friction at the imposed counterface velocity. Using the average value as the coefficient of friction for oscillatory sliding is dubious. At this juncture a few remarks concerning this inference are in order. In sliding where there is random fluctuations of the friction

force, the average value is without question the most appropriate estimate of the friction at the imposed sliding velocity. There is not a 100% assurity that this is the value used in constructing the friction-velocity curves in the literature! The inference comes mainly from Grosch's [8] statement that the same maximum friction force was reached in all the tests that experienced stick-slip. If the above statement can be taken at face value it implies that he (Grosch) must have used the average values in constructing his famous bell shaped friction-velocity curve (see Fig. 8). Barquins and Roberts [16], thought that their results with the same rubber and wavy glass disagreed with Grosch's, in the decrease of friction with increasing velocity. However, if the data presented in Fig. 10 for the stick-slip region is replotted as average values instead of maximum and minimum it is seen that there is indeed an obvious "negative" slope to the friction-velocity curve. The following discussion will show that in most, if not all, cases the use of the average value leads to erroneous conclusions about the true friction-velocity relationship.

First the results of the wet tests, which show stick-slip, will be examined. From the wet test results presented in the Experimental Results section we will assume that $v_{rel} > 0$, but $v_{rel} < v_{plate}$, in the stick phase of a stick-slip time trace. Immediately preceding slip, $v_{hemisphere}$ is positive. Now, the hemisphere, excluding inertial effects, slips backward with varying $v_{hemisphere}$ which is negative. The magnitude of $v_{rel}$ becomes greater than $v_{plate}$. Actually, for any backward slip (i.e. $v_{hemisphere} < 0$) $| v_{rel} | > v_{plate}$.

What conclusions can be drawn from this? First, $v_{rel}$ does not have to equal $v_{plate}$, except instantaneously when passing through this velocity. The implication here, is the friction-velocity relationship determined from the series of time histories is not adequate

to determine the $\mu(v_{rel})$ curve. Indeed, the relative velocity at which slip occurs may be the same at all velocities beyond $v_{crit}$.

To determine the true $\mu(v_{rel})$ relationship it is necessary to measure the friction force and relative velocity during slip. The proper way to do this is to measure the absolute velocities of both the plate and hemisphere while simultaneously measuring the friction and normal forces. The normal force must be recorded simultaneously since it has been observed in this work and others [52], [53] that a normal displacement accompanies the slip phase. Unfortunately, this was impossible for the current experimental setup.

In reality the velocity in the friction-velocity curves (in Fig. 36, for example) that have been generated are not $v_{rel}$ but $v_{plate}$ over the range of velocities tested. The only time the velocity is $v_{rel}$ is when there is steady state sliding. During stick-slip the relative velocity ranges from zero or very low velocity to much higher velocities. The relative velocity only passes through the plate velocity never staying at that velocity for any appreciable time. This results in the following interpretation of the friction velocity curve. In region I shown in Fig. 91 $v_{rel}$ is equivalent $v_{plate}$. In region II the maximum $\mu$ is plotted versus the plate relative velocity. The true friction-velocity relationship beyond $v_{crit}$ cannot be determined from the historical method of plotting $\mu$ against $v_{plate}$. It has also been shown in the results section that $v_{rel} \neq 0$ at incipient slip (particularly for the wet tests).

In region I of Fig. 91 the force-time relationship for a given data point on the curve is shown in Fig. 92. $V_{rel}$ transitions from zero to $v_{plate}$. This transition may occur

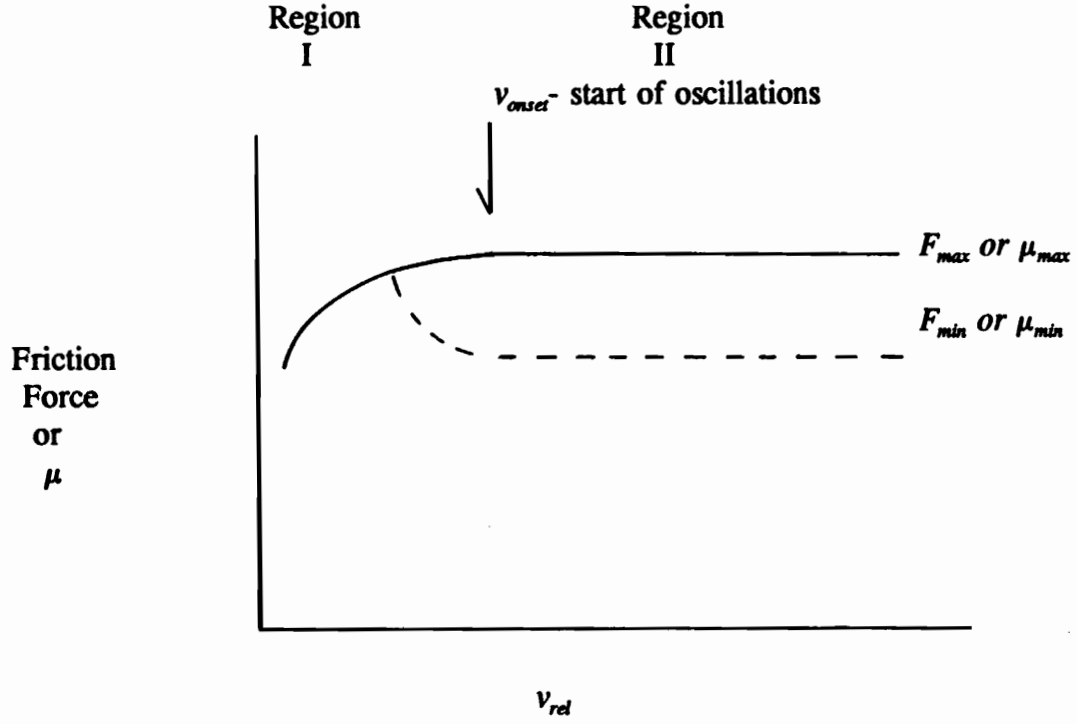


Figure 91. Generalized Friction-Velocity Curve.

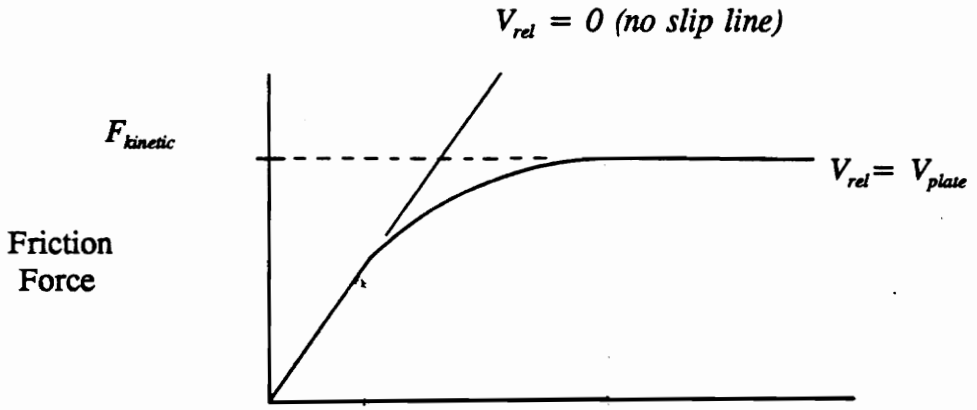


a. Friction Time History.

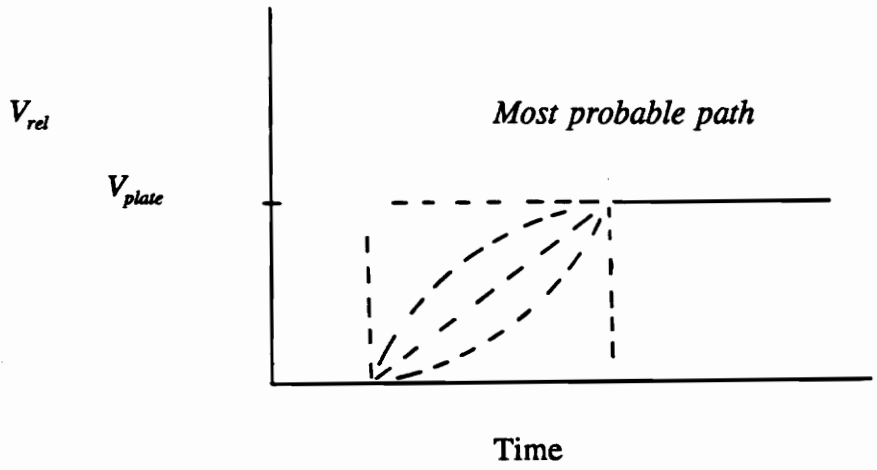


b. Transition from Stick to Slip.

Figure 92. Generalized Time History for Steady-State Sliding.

suddenly (i.e. instantaneously) or this may occur gradually. Hypothetical representations of $v_{rel}$ are also shown in Fig 92. An argument can be made for each path shown in Fig. 92. It is often difficult to determine if $v_{rel} = 0$ during the complete "stick" phase of dry sliding. Johnson [51] shows the deviation from the theoretical $v_{rel} = 0$ curve can occur by slip on the outer annulus of the contact area for a sphere on sphere configuration, when the interfacial shear stress, $\tau > \mu\sigma_{normal}$ as shown in Fig. 93. In this case $v_{rel} > 0$ for the annulus but, obviously $v_{rel} = 0$ for the central circular portion of the contact area. However, for the experimental results presented earlier it does appear that $v_{rel} \neq 0$ prior to incipient slip for the center of contact.

The production of relaxation oscillations (stick-slip) or harmonic oscillations (squeal) depend on the true $\mu(v_{rel})$ relationship. This does not mean the coefficient of friction-velocity curve must follow a required relationship because there is the additional and perhaps independent variation of the normal load. Since normal load changes result in a corresponding friction force change, through coupling by the coefficient of friction, a double valued friction velocity relationship can occur solely by normal oscillations.

### Comparison of Metallic and Elastomeric Sliding Systems

If the theoretically required shape of the friction-velocity curve is re-examined similarities between metallic and elastomeric stick-slip become apparent. Both systems require a double-valued friction force with respect to relative velocity. In a sense the friction-velocity relationship for elastomers is the same as for metals except that it is

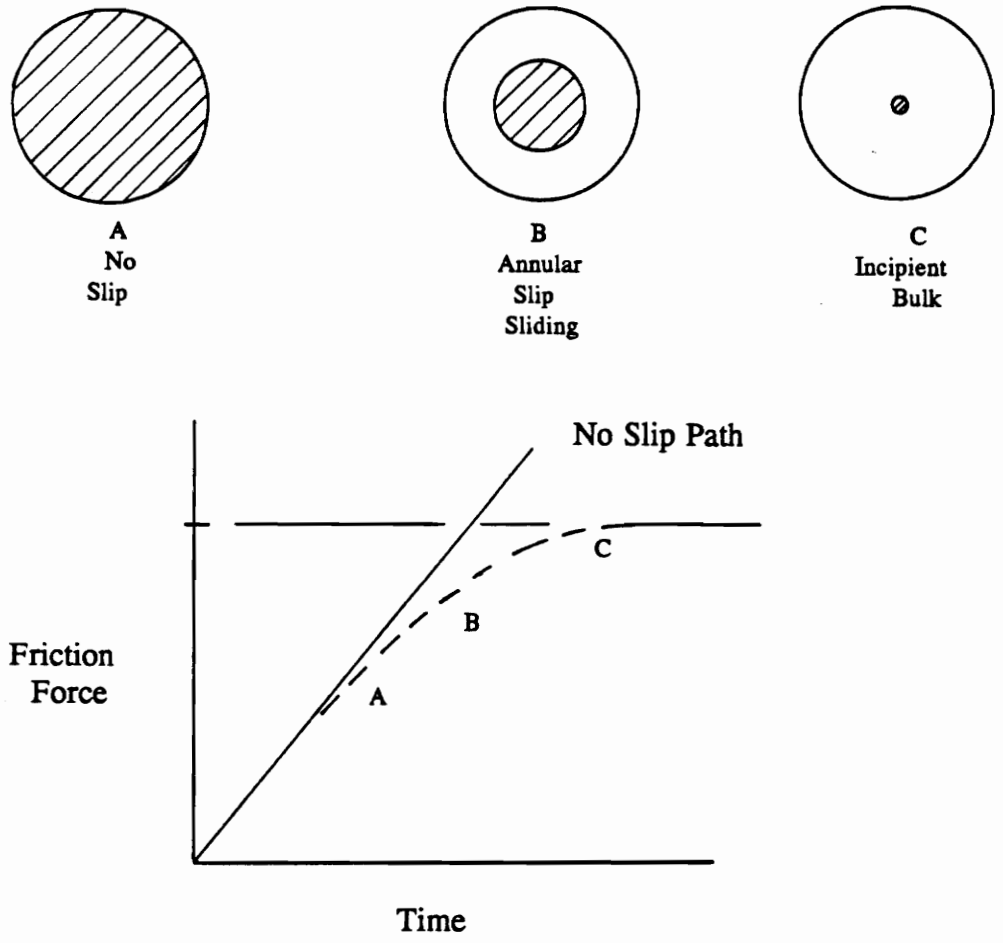


Figure 93. Deviation from Theoretical Force-Deflection Character by Annular Slip.
* Shaded region represents no slip area

shifted in relative velocity. Instead of stick-slip occurring below a critical velocity, it occurs above a critical velocity. Figure 94 shows the proposed similarities in the friction-velocity curves with the exception of initial rise of friction prior to $v_{crit}$ for the elastomeric system.

Now the differences between the two sliding systems should be examined in detail. Figure 92 shows that for steady sliding elastomeric systems transition from stick (i.e. $v_{rel} \approx 0$) to slip ($v_{rel} = v_{plate}$) slowly . Whereas, the transition for metallic systems is considered instantaneous. Herein lies the fundamental difference between sliding metallic and elastomeric systems. As stated in the previous paragraph, and which can also be seen from Fig. 94, the proposed friction-velocity relationships are virtually identical in shape or form with the exception of the initial rise in friction with velocity for the sliding elastomers. Therefore, stick-slip sliding should cease for velocities above $v_{min}$ for both the metallic and elastomeric systems. In metallic systems, the amplitude of stick-slip decreases as $v_{rel}$ is increased from $v_{crit}$ to $v_{min}$, (the velocity where F is a minimum). It is hypothesized this occurs for the following physical reason. The transition from stick to slip in metallic sliding is very fast and happens from a systems viewpoint, virtually instantaneously. Therefore the stick-slip process for $0 \leq v \leq v_{min}$ starts at points such as B, E, and A on the friction-velocity curve as shown for paths a-d in Fig. 95. The increased test velocity results in a reduced amplitude of oscillation until steady sliding commences at $v = v_{min}$ which has also been observed experimentally [38,54]. The reduction of amplitude is illustrated in Fig. 95.

In general, it has been observed in this research and others [8,18,16,15], the

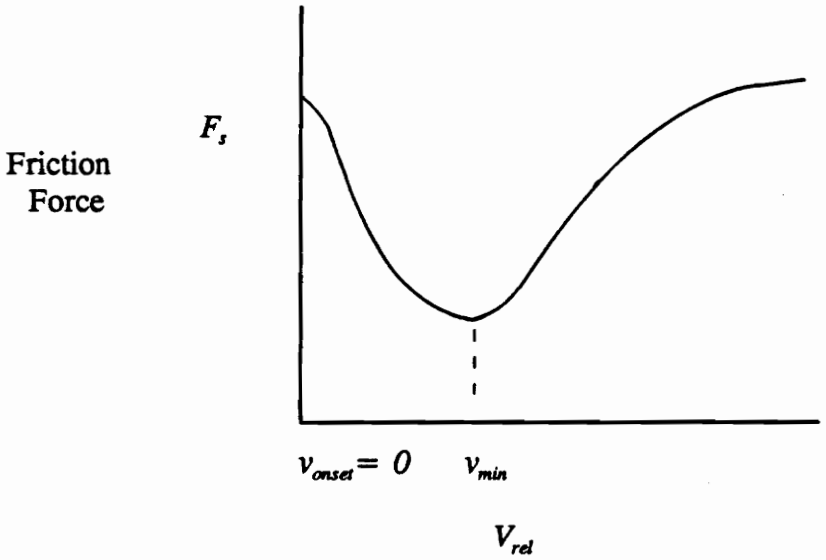


94a. Metallic Sliding

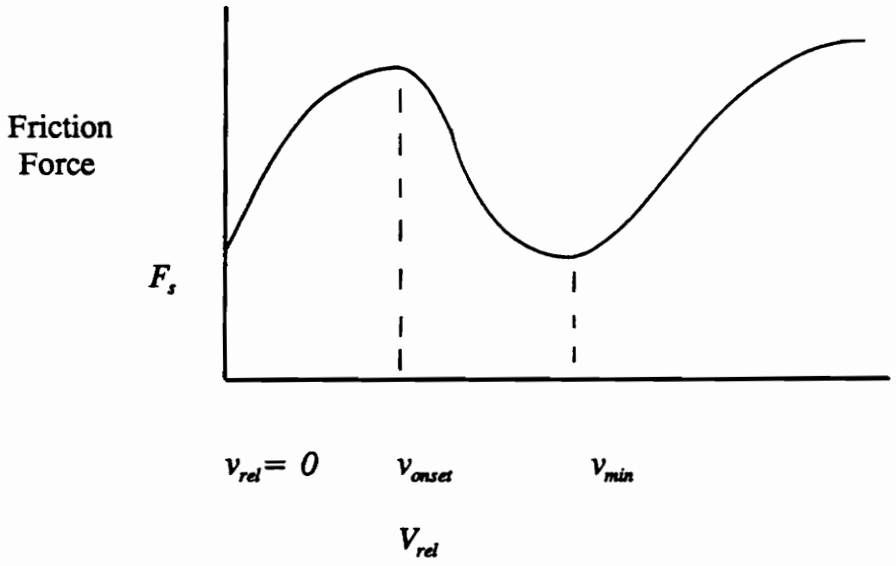


94b. Elastomeric Sliding

Figure 94. Friction-Velocity Relationships for Elastomeric and Metallic Sliding.

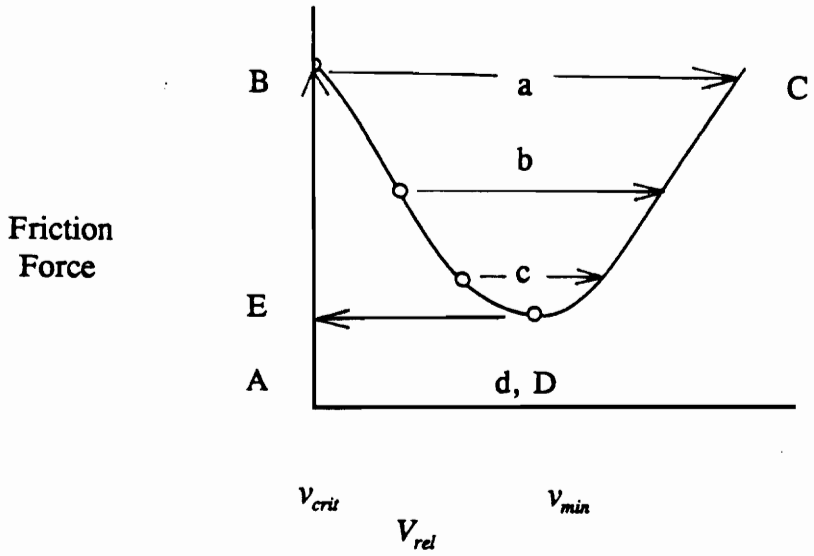


95b. Friction-Velocity Curve with Paths

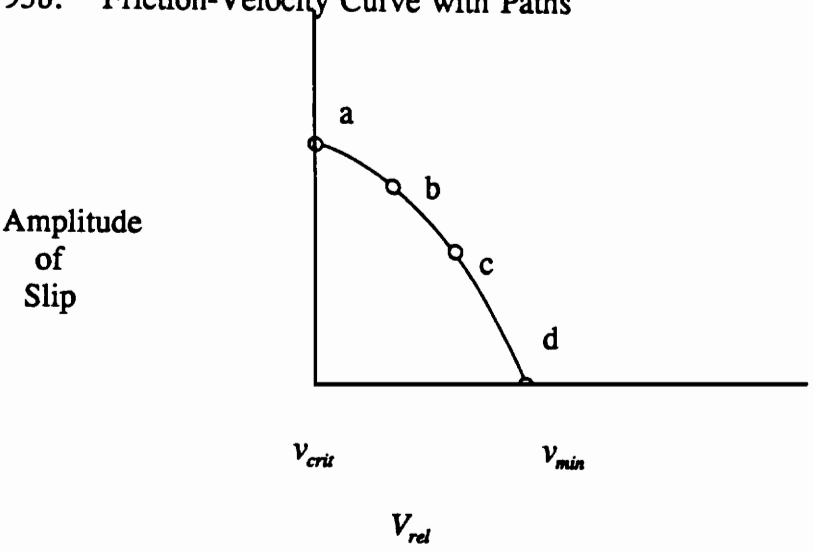


95b. Amplitude

Figure 95. Reduction of Stick-Slip Amplitude for Metallic Sliding [adapted from ref. 55].

occurrence of stick-slip motion neither diminishes in amplitude with increasing relative velocity nor does it vanish in elastomeric sliding. The proposed reason for this difference from metallic stick-slip follows. In metallic sliding $v_{rel} = 0$ for the majority of the stick portion of sliding. The transition from $v_{rel} = 0$ to $v_{rel} \approx v_{plate}$ occurs very quickly as mentioned previously. However in elastomeric sliding $v_{rel} \neq 0$ during the "stick" phase. The transition from $v_{rel} = 0$ to $v_{rel} = v_{crit}$ is smooth and gradual.

Examination of a hypothetically "true" friction-velocity relationship (not the historically constructed one) in detail, while taking into account the assumed slip throughout the "stick" phase yields an explanation for the observed continuation of stick-slip for plate velocities beyond $v_{min}$. Figure 96 show the hypothetical friction-velocity relationship. Essentially Fig. 96 can be viewed as Fig. 15 with the "stick" phase expanded to account for relative slip between the mating elements.

The same reasoning (theory of relaxation oscillations) presented earlier for stick-slip sliding for elastomers as well as metals applies to Fig. 96 at $v_{rel} = v_{onset}$. However, the fundamental difference between the two sliding systems becomes crucial. It is proposed for elastomeric systems the "stick" phase for $v \geq v_{onset}$ traverses from points *A* to *B* as shown in Fig. 96. Because the transition from stick to slip is relatively slow, unlike the virtually instantaneous transitions for metals, the slip phase of motion starts at approximately point *B* each time, as a first approximation, with $F = F(v_{onset})$ and $v = v_{onset}$. Unlike metals, the section *B-D* is never intersected as in the paths *b* and *c* of Fig. 95. Therefore the amplitude of stick-slip does not diminish and vanish with increasing velocity as in the case of metallic sliding. This is observed in the experimental results

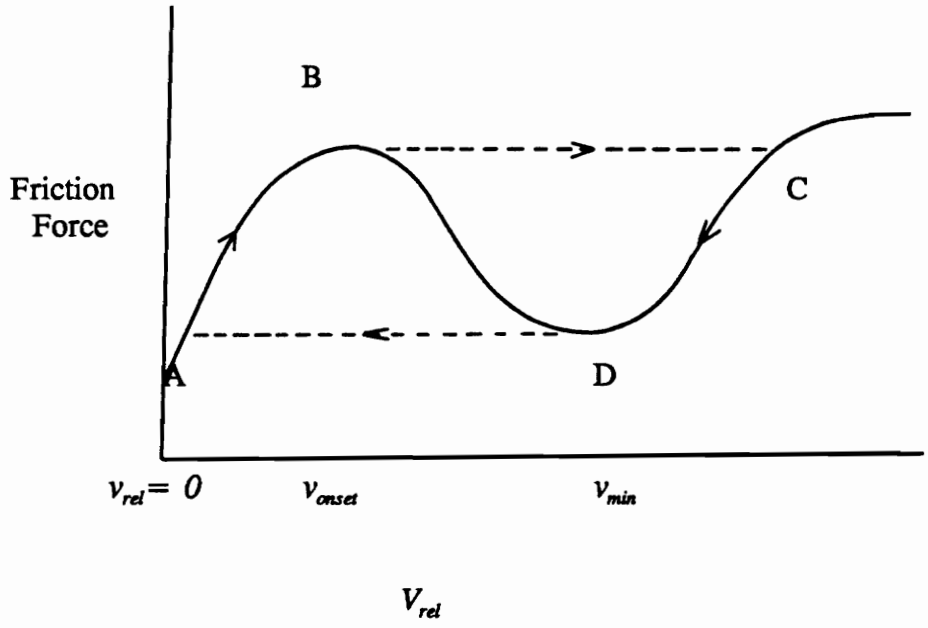


Figure 96. Theoretical Friction-Velocity Relationship for Elastomeric Sliding.

(for example see Fig. 52).

A few comments on the highly idealized case that was just presented are in order. The first implication that bears examination is that the maximum force should remain constant with increasing velocity for this proposed stick-slip model. However, experimental results show this is not the case. The theoretical model proposed here does not take into account the probable shifting of $v_{crit}$ to higher velocities with increasing plate velocity. The result of the velocity increase is to increase the strain rate imposed on the elastomer. Employing Ludema and Tabor's [15] argument of increasing shear properties with increasing strain rate it is seen that $F_{max}$ should increase with increasing $v_{crit}$.

### Fracture Mechanics Approach

Approaching the problem from the materials viewpoint, the dry sliding process can be viewed as a fracture event. Figure 97 shows the crack propagation at the interface (or at a shallow depth in one of the materials) of two different materials. Steady state sliding appears as two infinite materials with the crack propagating at constant speed. Stick-slip occurs when the energy release rate to initiate the crack is higher than the energy release rate of propagation. At this point there has not been a distinction between a crack propagating at the interface or a crack propagating in one of the materials. Indeed, either phenomena could conceivably result in the requisite shape of the friction-velocity curve necessary for oscillatory motion to occur (e.g. the viscoelastic peeling of pressure sensitive tape occurs adhesively). The central idea to the viscoelastic theories

Figure 97. Representation of Sliding Event as Crack Propagation.

of adhesive friction was to develop the experimentally observed shape of the friction-velocity curve.

Stick-slip type behavior has been shown to occur in the tearing of elastomeric sheets with a state of pure tension (Mode I crack) at the crack tip or a state of pure shear (Mode III) at the crack tip [55,56]. Unsteady tearing resembles the stick-slip friction oscillations in many respects. In regions of a positive slope to the energy release rate the motion is steady with no large excursions in either tearing force or velocity. In regions of negative or zero slope the tearing force and velocity fluctuate between well-defined bounds.

The strain energy release rate for rubber loaded in tension may be written as follows [57]:

$$G_c(\dot{a}) = \frac{P^2}{2B}\left(\frac{C_1}{a_1}\right) \tag{34}$$

where:

$P$ = fixed load

$B$ = crack width

$C_1$ & $a_1$ are constants

Figure 98a shows the form of the strain energy release rate curve for a material that will undergo stick-slip tearing. The striking similarity to the required theoretical friction-velocity curve required for stick-slip sliding is obvious. Indeed, the same discontinuous arguments that hold for stick-slip sliding will also hold for tearing of elastomer sheets. As is noted on the curve there are two stable regions bounding an unstable region.

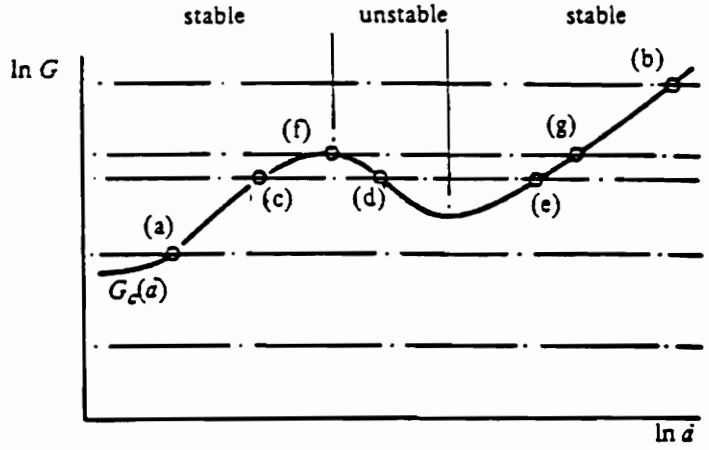


a. Energy Release Rate for Unstable Crack Growth
G= strain energy release rate
da/dt= tear rate

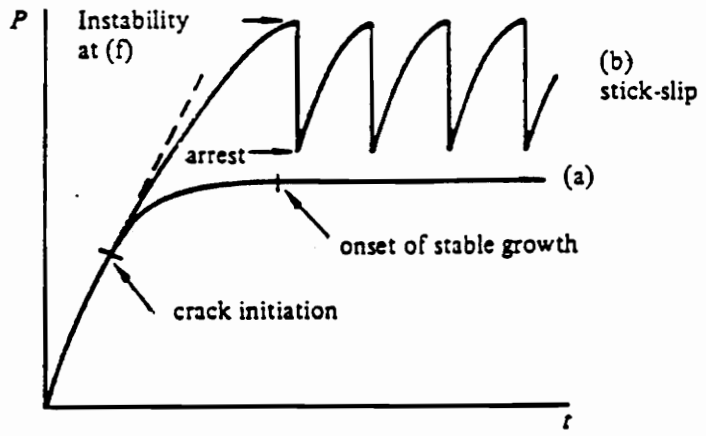


b. Generalized Time History of Stable and Unstable Crack Growth.
P= Load (proportional to stress)

Figure 98. Stability of Crack Growth in Tearing of Elastomers [57].

Employing the same reasoning as before we see that points *a, c, e, g,* and *b* are stable points where a crack will propagate at a fixed load and speed. Points *f* and *d* are unstable and both the force and velocity will fluctuate. Figure 98b shows the two possible modes of crack growth in the time domain. Interestingly, the stable crack growth shows a crack initiation stress or load less than the stress for stable propagation value, evidencing much similarity to the deviation of the friction force from the $v_{rel} = 0$ line.

Figure 98 shows the energy release rate as a function of velocity for the tearing of crystallizable natural rubber. In Fig. 98a, point *a* is in a region of positive slope which corresponds to steady sliding since the initiation rate is the same as the propagation rate. Point *d* is in a region of negative slope of the curve and corresponds to a condition where the elastomer is crystallizing at the crack tip which results in a higher initiation release rate than propagation rate. Crystallization has been shown to occur in transparent rubber viewed under polarized light [56]. However, crystallization is not the only mechanism that will lead to higher initiation rates. Any mechanism that causes the initiation energy release rate to be greater that the propagation rate will lead to stick-slip tearing. This could include viscoelastic effects that cause the initiation release rate to be larger than the propagation. Indeed, any mechanism that effectively blunts the crack tip can result in higher initiation rates. Examples of this are fillers in a cross-linked elastomer or hard phases in a thermoplastic elastomer. Figure 99a & b show for the tearing of rubber there is no obvious negative slope to all of the curves, with the exception of the -20 °C curve in 99b, in the regions of stick-slip. The results shown in

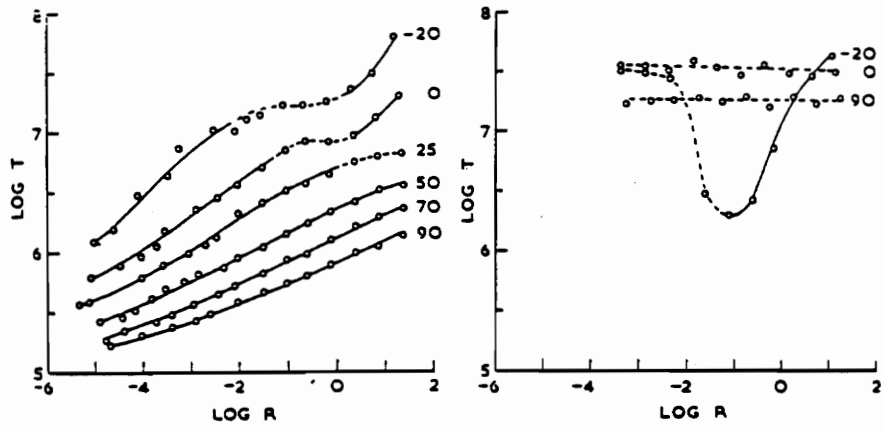


a. GR-S Vulcanizate
Varying Temperatures (°C)

b. Natural Rubber Vulcanizate
Varying Temperatures (°C)

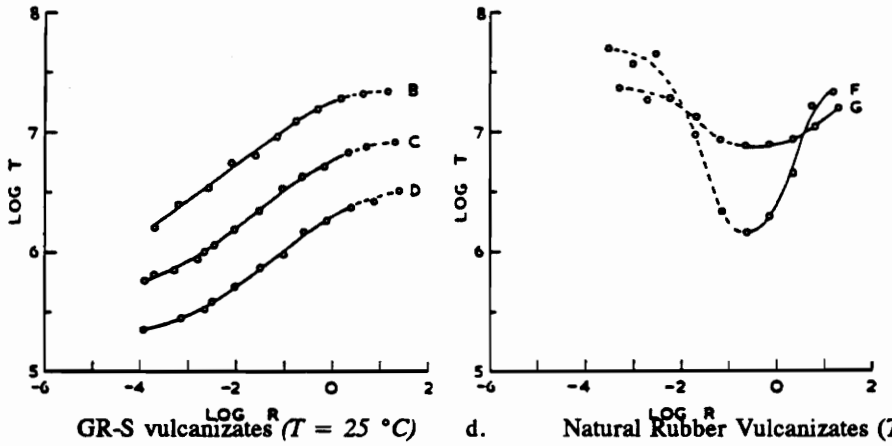


c. GR-S vulcanizates *(T = 25 °C)*
B-lowest, C-medium, D-highest degree of crosslinking

d. Natural Rubber Vulcanizates *(T = -20 °C)*
F-lowest degree of crosslinking
G-highest degree of crosslinking

Figure 99a-d. Energy Release Rate of Natural Rubber during Tearing [58].
T - Average Tearing Energy Release Rate (ergs/cm$^2$)
R - Tear rate (cm/s)
- - - Stick-slip, ——— Steady Tearing

Fig. 99a-d were obtained with testing that resulted in a tensile state of stress at the crack tip. Fig. 99a, b, & c show the reappearance of steady tearing in regions of the positive slope at rates above the stick-slip rates and temperatures below the stick-slip range. The tearing results reviewed thus far have been for the tearing of elastomeric sheets with a tensile state of stress at the crack tip. Tensile tearing tests exhibit the return of steady tearing as the tearing rate is increased or equivalently the test temperature is lowered. However, in tearing, with the same material, that approached a state of pure shear at the crack tip [58] the stick-slip behavior did not vanish at the higher tear rates or lower temperatures. Qualitatively this result is in excellent agreement with the friction-velocity curves that have been determined in this research where the slope is zero or even positive. Additionally, the stick-slip amplitude does not vanish with increasing velocity.

## CONCLUSIONS

The following conclusions were determined from this research:

The "viscoelastic" peak or negative slope of the friction-velocity curve as noted in Grosch's [8,18] work is not evident in this work at the onset of stick-slip. The lack of a peak in the friction-velocity curve is similar to the results obtained by Barquins and Roberts in Fig. 10.

Unlike the results of previous researchers [8,18,25,59,24,60,29,32] stick-slip did not require either a static greater than a kinetic coefficient of friction or a negative slope of the friction-velocity curve as generated in the historical manner. There was no experimental evidence in this research that the static coefficient of friction was larger than kinetic coefficient of friction.

This research also showed that a minimum level of friction was required to cause frictional oscillations. When the friction-velocity curves for chromium oxide and epoxy counterfaces are compared, the general shapes of the maximum kinetic friction curves are virtually identical. Noise occurs only for the counterface with the higher coefficient of friction (e.g. chromium oxide). Excluding Schallamach waves, this value is related to the minimum level required to cause cohesive failure of the elastomer prior to adhesive failure.

Frictional oscillations occur when cohesive failure leads to a deposited transfer film of elastomeric material.

Qualitatively, the dry stick-slip friction resembles tearing of elastomeric sheets

and the viscoelastic peeling of pressure sensitive tape. Mechanistically, the friction process is closer to tearing where it has been observed for shear that the unsteady tearing does not disappear with increasing tear rates.

There are 3 possible modes of noise generation in sliding elastomeric systems; stick-slip, harmonic oscillations, and Schallamach waves.

Noise generation is not dependent solely on viscoelastic material properties. Geometric stiffness also determines when noise is generated.

There is a load-velocity interaction. At high loads the onset of noise occurs at much lower velocities. For some of the natural rubber elastomers it was impossible to generate noise at low loads (8.9 N). The critical velocity curve was exponential in nature.

In dry oscillatory behavior it has been shown that sliding that starts out with stick-slip motion can lock onto the tangential vibrational frequency of the elastomer. Additionally, harmonic oscillations (at the elastomer tangential natural frequency) can build up to and result in stick-slip motion. This motion is not true stick-slip since the relative velocity is never zero.

There was an attempt to correlate surface roughness and energy to the observed coefficient of friction and hence the propensity to generate noise. Theoretical considerations lead one to believe that surface energy and roughness should correlate with observed friction. Counterfaces with high surface energy did not correspond to surfaces with high coefficients of friction. There are obviously additional factors to consider that are not accounted for in the previous surface properties.

For wet sliding, the elastomer goes from slip to "more" or greater slip reminiscent of true stick-slip. Wet sliding also evidences a peak in friction at the velocity corresponding to the onset of noise. Even though there is a peak in the friction-velocity curve, there does not appear to be an appreciable negative slope at the higher velocities where noise is also generated. The maximum friction force for stick-slip under wet conditions is a factor of 2 less than the maximum force for dry conditions, yet stick-slip still occurs.

The dry tests are not an indicator of noise generation potential in the wet environment as evidenced by the wet natural rubber/epoxy counterface results. This is expected since dry sliding or boundary lubricated sliding requires transfer to generate noise. In wet conditions noise occurs without transfer to the opposing surface and without evidence of elastomer/counterface contact.

The wet natural rubber results show no dependence of the critical velocity on viscoelastic or elastic properties.

## RECOMMENDATIONS

The classical results of Grosch [8,18] and others [25,59,15,24,60,29,32] indicate a drop off in friction at higher velocities when the data is transformed by the WLF equation. The purported viscoelastic nature of adhesion is considered to be the reason for this result. The recent results of Barquins and Roberts [16] and those presented here indicate that the maximum coefficient of friction does not drop off with increasing velocity, but remains constant or experiences a slight increase with increasing speed. However, if the mean values of the coefficient of friction are considered the friction-velocity curves would yield a negative slope after the onset of frictional oscillations.

It appears that the simple model of friction proposed by Ludema and Tabor [15] is more appropriate than the molecular-kinetic theories. When employing the WLF transformation to shift experimental friction data, the bulk temperature of the elastomer is changed, resulting in changes in both the storage and loss moduli. Obviously, changes in the storage modulus results in changes in the area of contact. Since there are results [16] that indicate that the coefficient of friction is proportional to the contact area, it is not surprising that we obtain a reduced friction force, due to the dramatic increase in modulus, as the test (i.e. environment ) temperature approaches $T_g$.

Essentially the friction force can be described as a function doubly dependent on the WLF transformation. If the simple theory of rubber friction is used both the area and shear strength are dependent on temperature and/or rate. Therefore $F(T,v) = A(T,v) \cdot S(T,v)$. If the system is area invariant to rate (i.e. elastomer on hard flat counterface)

changing the environment temperature artificially changes the area with respect to rate.

For testing configurations such as an elastomeric hemisphere on a hard, flat counterface there should be no change in area with changes in velocity. Therefore, changing the area by changing the test temperature artificially changes the coefficient of friction beyond the temperature effect on shear properties. Transformation of the coefficient of friction by the WLF equation for the test procedures mentioned in the literature is not surprising, since both the change in area and the shear strength of the elastomer are transformable with the WLF equation.

Additionally, since most of the previous work has been with very low speed sliding (i.e. $10^{-2} < v < 10^{0}$ mm/s) verification of the friction-velocity relationship determined by changing the environment temperature is necessary. Excluding rolling friction (i.e. tires etc., where the forward velocity deforms the elastomer cyclicly due to the normal load deformation), verification is more important for the onset of stick-slip than the coefficient of friction since in elastomeric sliding absolute velocities are rarely very high ($v > 100$ mm/s). The friction information obtained at reduced velocities via the WLF transformation is certainly important, because even though absolute velocities are not very high, the combined effect of low operating temperatures and velocity may be encountered. In this situation the friction values generated by the reduced variable method is certainly applicable. It appears that the onset of stick-slip is greatly affected by the method of testing or even the test apparatus. Comparison of Barquins and Roberts [16] results to Grosch [8,18] shows that with the same materials the onset of stick-slip changes by 3-4 decades of velocity.

The recommendation is that a test apparatus similar to the one used in this study be used to vary the sliding rate over a much larger range of velocities ($10^{-2} < v < 10^{3}$). Additionally varying the counterface temperature for a series of tests and then varying the environment temperature for a series of tests would yield more insight into the reduced variable method of determining the friction-velocity relationship. The main reason for this last proposal is to determine if the negative slope arises solely due to area changes.

A stiffer measuring system would be beneficial to measure the true friction-time relationship during slip. Normal load and the true relative velocity should be measured to obtain a better picture of what is actually happening during the slip event.

Possible solutions to the Ford problem are to provide low friction counterfaces for the elastomer to slide against. Even though the results of this study point to the epoxy coatings as potential low friction surfaces, the wet tests show the fallacy in just performing dry tests. Ford has unsuccessfully attempted to mold in teflon fabric to the elastomer. A possible alternative to the molding is to provide this low friction surface as a counterface.

Possible copolymers with PDMS would be good replacement candidates for the natural rubber bushings. The PDMS elastomer in a block copolymer would provide a low shear strength constituent as well as providing a low shear strength transfer film. It was noted in the butyl tests that a transfer of PDMS would eliminate Schallamach waves. Fluorocarbon elastomers can also be made with tetrafluoroethylene ($C_2F_4$). Even though the addition is typically done to increase the solvent resistance of the elastomer

[64], $C_2F_4$ is the monomer repeat unit for Teflon and therefore has the potential to act as an in-situ lubricant. Elastomers are often compounded with other internal lubricants such as graphite or Molydenum disulfide to decrease the coefficient of friction.

The tearing of elastomeric sheets may provide a method of screening potential elastomers that would not yield stick-slip in dry sliding conditions. The qualitative agreement between the frictional stick-slip and tearing stick-slip suggests that elastomers such as PDMS would not evidence stick-slip tearing. Validation of this possible correspondence between the two events would add additional insight to the frictional stick-slip mechanism. This screening method is based upon the cohesive transfer mechanism shown here for dry sliding.

The wet tests show the need for testing sliding elastomer systems in whatever potential liquids or other contaminants that may possibly exist in the interface. This can be related to the theoretical requirements for relaxation oscillations to occur. Since the friction-velocity relationship cannot be determined a priori, the material combinations and lubricants/contaminants, if any, must be tested to determine if the friction-velocity relationship will induce oscillations.

## REFERENCES


1. Bowden, F. P., and Tabor, D., "The Friction and Lubrication of Solids", Oxford University Press, 1986

2. Rowson, D. M., "An Analysis of Stick-slip Motion", Wear, Vol. 31, 1975, pp. 213-218.

3. Antoniou, S. S., Cameron, A. and Gentle, C. R., "The Friction-Speed Relation from Stick-slip Data", Wear, Vol. 36, 1976, pp. 235-254.

4. Bo, L. C., and Pavelescu, D., "The Friction-Speed Relation and Its Influence on the Critical Velocity of Stick-slip Motion", Wear, Vol. 82, 1982, pp. 277-289.

5. Gao, C. and Kuhlmann-Wilsdorf, D., "On Stick-slip and the Velocity Dependence of Friction at low Speeds", Transactions of the ASME, Vol. 112, April 1990, pp. 354-366.

6. Ko, P. L., and Brockley, C. A., "The Measurement of Friction and Friction-Induced Vibration", Journal of Lubrication Technology, October 1970, pp. 543-549.

7. Brockley, C. A., and Ko, P. O., "Quasi-Harmonic Friction Induced Vibration", Transactions of ASME, October 1970, pp. 550-556.

8. Grosch, K. A., "The Relation between the Friction Visco-elastic Properies of Rubber", Proceeding of Royal Society (London), A 274, 1963, pp. 21-39.

9. Moore, D. F., The Friction and Lubrication of Elastomers, Pergamon Press, Oxford, 1972.

10. Bhushan, B., "Stick-slip Induced Noise Generation in Water Compliant Rubber Bearings", Journal of Lubrication Technology, April 1980, Vol. 102, pp. 201-212.

11. Kiryu, K., Yanai, T., Matsumoto, S., and Koga, T., "An Analysis of "Ringing" Phenomena on a Water Pump Mechanical Seal", ASLE Transactions, Vol. 28, No. 2, 1985, pp. 261-267.

12. Kiryu, K., Yanai, T., Matsumoto, S., and Koga, T., "An Analysis of "Ringing" Phenomena on a Water Pump Mechanical Seal(Part II)", ASLE Transactions, Vol. 29, No. 1, 1986, pp. 25-34.

13. Kiryu, K., Yanai, T., Matsumoto, S., and Koga, T., "An Analysis of "Ringing" Phenomena on a Water Pump Mechanical Seal(Part III)", ASLE Transactions, Vol. 31, No. 2, 1988, pp. 269-275.

14. Antoniou, S. S., Cameron, A. and Gentle, C. R., "The Friction-Speed Relation from Stick-slip Data", Wear, Vol. 36, 1976, pp. 235-254.

15. Ludema, K. C. and Tabor, D., "The Friction and Visco-elastic Properties of Polymeric Solids", Wear, Vol. 9, 1966, pp. 329-348.

16. Barquins, M. and Roberts, A. D., "Rubber Friction Variation with Rate and Temperature: Some New Observations", Journal Applied Physics, Vol. 19, 1986, pp. 547-563.

17. Cockerham, G. and Cole, M., "Stick-slip Stability by Analogue Simulation", Wear, Vol. 36, 1976, pp. 189-198.

18. Grosch, K. A., "Relation Between the Friction and Visco-Elastic Properties of Rubber", Nature, Vol. 197, March 2, 1963, pp. 858-859.

19. Williams, M. L., Landel, R. F., and Ferry, J. D., Journal of American Chemical Society, Vol. 77, 1955, p. 3701.

20. Roberts, A. D., "Theories of Dry Rubber Friction", Tribology International, Vol. 9, No. 2, April 1976, pp. 75-82.

21. Moore, D. F., and Geyer, W., "The Review of Adhesion Theories for Elastomers", Wear, Vol. 22, 1972, pp. 113-141.

22. Chernyak, Y. B., and Leonov, A. I., " On the Theory of the Adhesive Friction of Elastomers", Wear, Vol. 108, 1986, pp. 105-138.

23. Bartenev, G. M. and El'kin, A. L., "Friction Properties of High Elastics Materials", Wear, Vol. 8, 1965, pp. 8-21.

24. Schallamach, A., "A Theory of Dynamic Rubber Friction", Wear, Vol. 6, 1963, pp. 375-382.

25. Savkoor, A. R., "Mechanics of Sliding Friction of Elastomers", Wear, Vol. 113, 1986, pp. 37-60.

26. Schallamach, A., "How does rubber slide?", Wear, Vol. 17, 1971, pp. 301-312.

27. Biot, M. A., "Incremental Elastic Coefficients of an Isotropic Medium in Finite Strain", Applied Scientific Research, Vol. 12, 1963, pp. 151-167.

28. Barquins, M., and Courtel, R., "Rubber Friction and the Rheology of Viscoelastic Contact", Wear, vol. 32, 1975, pp. 133-150.

29. Roberts, A. D., and Thomas, A. G., "The Adhesion and Friction of Smooth Rubber Surfaces", Wear, Vol. 33, 1975, pp. 45-64.

30. Cherry, B. W., Polymer surfaces, Cambridge University Press, Cambridge, 1981.

31. Johnson, K. L., Kendall, K. and Roberts, A. D., "Surface Energy and the Contact of Elastic Solids", Proceedings of the Royal Society (London), A 324, 1971, pp. 301-313.

32. Savakoor, A. R., "Adhesion and Deformation Friction of Polymers on Hard Solid", Advances in Polymer Friction and Wear, Volume 1,Lee, L. H., editor, Plenum Press, N.Y., pp. 69-122.

33. Minorsky, N.,Introduction to Non-linear Mechanics, J. W. Edwards, Ann Arbor, Michigan, 1947.

34. Minorsky, N., Non-linear Oscillations, D. Van Nostrand Co., Inc., New Jersey, 1962.

35. Nayfeh, A. H., and Mook, D. T., Nonlinear Oscillations, John Wiley & Sons, New York, 1979.

36. Thomson, W. T., Theory of Vibrations with Applications, Prentice Hall, New Jersey, 1988, 3rd edition.

37. Leinard, A., Etude des Oscillations Entretenues, Rev. Gen. d Elect, Vol. 23, No. 118, pp.901-946.

38. Rabinowicz, E., Friction and Wear of Materials, John Wiley and Sons, Inc., New York, 1965, pp. 62-65.

39. Simons, W. W., The Stadler Handbook of Infrared Spectra, Philadelphia, Pennsylvania, Stadler Research Laboratories, 1978.

40. Barquins, M., "Energy Dissipation in Schallamach Waves", Wear, Vol. 91, 1983, pp. 103-110.

41. Briggs, G. A. D., and Briscoe, B. J., "How Rubber Grips and Slips, Schallamach Waves and the Friction of Elastomers", Philosophical Magazine A, Vol. 38, 1978, No. 4, pp. 387-399.

42. Briscoe, B. J., "The Role of Adhesion in the Friction, Wear and Lubrication of Polymers", Adhesion, Vol. 5, 1981, pp. 49-80.

43. Maugis, D. and Barquins, M., "Stick-slip Peeling of Adhesive Tapes", Adhesion, Vol. 12, 1987, pp. 205-222.

44. Smith, T. L., "Strength of Elastomers. A Perspective", Rubber and Chemistry Technology, Vol. 51, No. 2, 1978, pp. 225-252.

45. Ferry, J. D., Viscoelastic Properties of Polymers, John Wiley & Sons, New York, 3rd ed., 1980

46. De Togni, R., The Role of System Dynamics on the Behavior of Elastomeric Friction, Masters Thesis, V.P.I. & S.U., 1991 (To be Published)

47. Briggs, G. A. D., and Briscoe, B. J., "The Dissipation of Energy in the Friction of Rubber", Wear, Vol. 35, 1975, pp. 357-364.

48. Briggs, G. A. D., and Briscoe, B. J., "How Rubber Grips and Slips, Schallamach Waves and the Friction of Elastomers", Philosophical Magazine A, Vol. 38, 1978, No. 4, pp. 387-399.

49. Biot, M. A., "Surface Instability of Rubber in Compression", Applied Scientific Research, Vol. 12, 1963, pp. 168-198.

50. Hamilton, G. M., and Goodman, L. E., "The Stress Field Created by a Circular Sliding Contact", Journal of Applied Mechanics, Vol. 33, June 1966, pp. 371-376.

51. Johnson, K. L., Contact Mechanics, Cambridge University Press, Cambridge, 1985.

52. Elder, J. A. and Eiss, N. S., Jr., "A Study of the effect of Normal Stiffness on Kinetic Friction Forces between Two Bodies in Sliding Contact", ASLE Transactions, Vol. 12, n. 4, 1969, pp. 234-241.

53. Sakamato, T., "Normal Displacement of the Sliding Body in a Stick-slip Friction Process", Proceedings of the JSLE International Tribology Conference, July 8-10, 1985, pp. 141-146.

55. Thomas, A. G.,"Rupture of Rubber. VI. Further Experiments on the Tear Criterion", Journal of Applied Polymer Science, Vol. III, n. 8, 1960, pp. 168-174.

56. Greensmith, H. W., "Rupture of Rubber. VIII. Comparisons of Tear and Tensile Rupture Measurements", Journal of Applied Polymer Science, Vol. III, n. 8, 1960, pp. 183-193.

57. Williams, J. G., Fracture Mechanics of Polymers, John Wiley & Sons, New York, 1984, pp. 175-189.

58. Greensmith, H. W. and Thomas, A. G., "Rupture of Rubber. III. Determination of Tear Properties", Journal of Polymer Science, Vol. XVIII, 1955, pp. 189-200.

59. McLaren, K. G. and Tabor D., "Visco-elastic Properties and the Friction of Solids", Nature, Vol. 197, March 2, 1963, pp. 856-858.

60. Roberts, A. D., and Jackson, S. A., " Sliding Friction of Rubber", Nature, Vol. 257, September 11, 1975, pp. 118-120.

# APPENDICES

# APPENDIX A

# LIST OF EQUIPMENT

1. Force Transducer

| | |
|---|---|
| Manufacturer: | PCB Piezotronics, Inc. |
| Model No.: | 208 A02 |
| Serial No.: | 7000 |

2. Force Transducer Power Supply

| | |
|---|---|
| Manufacturer: | PCB Piezotronics, Inc. |
| Model No.: | 484B |
| Serial No.: | 2121 |

3. Data Acquisition Board

| | |
|---|---|
| Manufacturer: | Data Translation |
| Model No.: | DT-2821 |

4. Motor Controller

| | |
|---|---|
| Manufacturer: | Copley |
| Model No.: | 201 |

5. Ellipsometer

| | |
|---|---|
| Manufacturer: | Gaertner Scientific Corp. |
| Model No.: | L116A Dual Mode Automatic Ellipsometer |

4. Profilometer

| | |
|---|---|
| Manufacturer: | Rank Precision Industries LTD. |
| Model No.: | 112 |
| Serial No.: | 1000-F-3113 |

# APPENDIX B

# FORCE TRANSDUCER CALIBRATION

Figure B-1 shows the calibration curve for static load input to the force transducer.

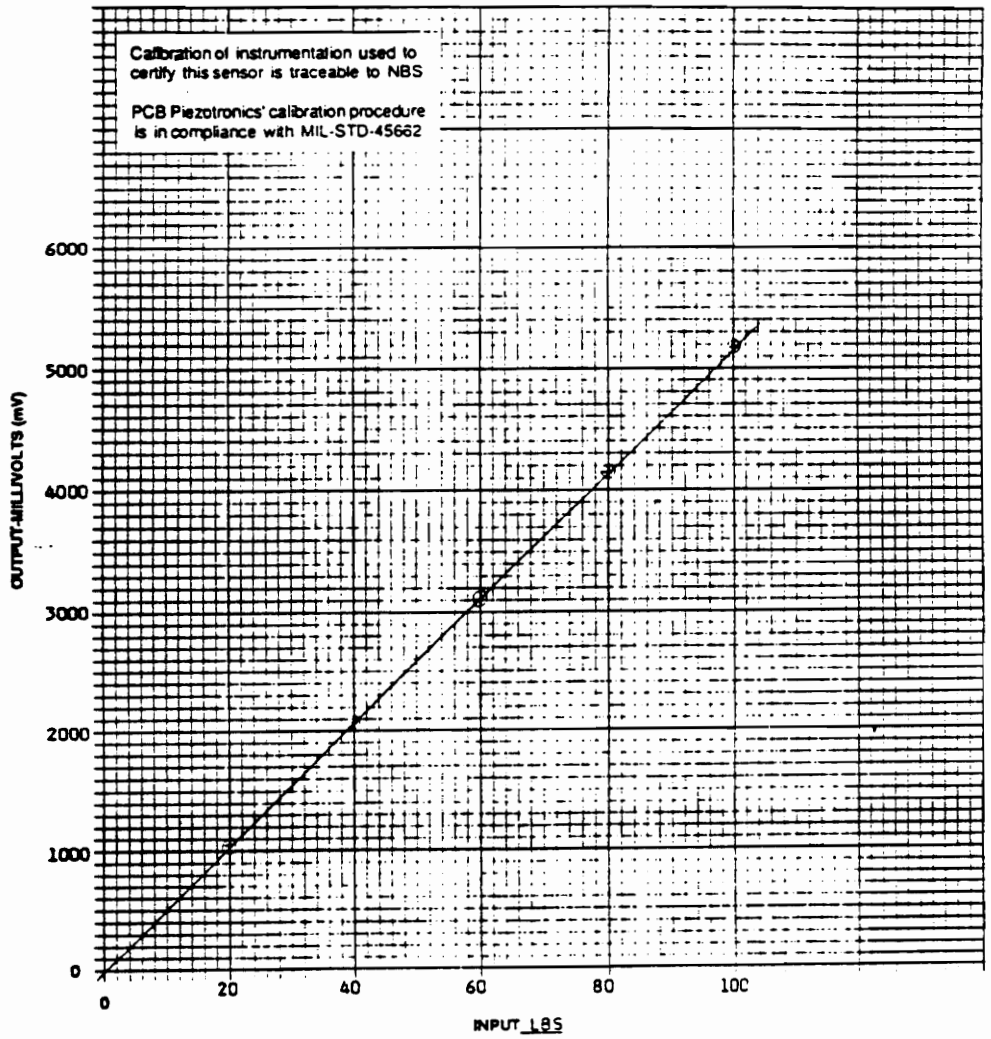


Figure B-1. Calibration of Curve of Force Transducer to Static Input.

# APPENDIX C

# MATERIAL RECIPES

The following "recipes" are the material formulation for the elastomers used in this study. The convention for presenting the amount of the various components is to compare the weight amount relative to a 100 units of the rubber. For example, an elastomer with 100 kg of natural rubber and 5 kg of carbon black would be represented as 5 phr (parts per hundred rubber) carbon black.

The following Tables C-1 thru C-4 contain the material recipes for the four elastomers used in this study. The recipe for the natural rubber elastomers is shown in Table C-1.

| Ingredient | Quantity (phr) |
|---|---|
| cis-1,4 polyisoprene (94%) | 100.00 |
| Carbon Black | 0, 5, 10, 20, or 50 |
| Zinc Oxide | 5.00 |
| Octadecanoic Acid | 2.00 |
| Sytrenated Diphenylamine | 1.50 |
| 2-mercapto-4(5)-methylbenzimidazole | 1.50 |
| Thiocarbamyl sulfenamide | 1.80 |
| N-oxydiethlene benzothiazole-2-sulfenamide | .83 |
| Sulfur | .60 |

Table C-1. Recipe for Natural Rubber Elastomer.

The recipe for the PDMS elastomer is shown in Table C-2. The hemispheres were molded at 160 °C for 30 minutes and then post-cured for 24 hours at 200 °C.

| Ingredient | Quantity (phr) |
|---|---|
| PDMS | 100.00 |
| 1,4 di- (2-tert-butylperoxyisopropyl) benzene | 1.00 |
| Synthetic, amorphous silica powder | 10.00 |

Table C-2. Recipe for PDMS Elastomer.

The recipe for the fluorocarbon elastomer is shown in Table C-3. The hemispheres were molded at 160 °C for 30 minutes.

| Ingredient | Quantity (phr) |
|---|---|
| Fluorel FT-2481 | 100.00 |
| MgO | 3.00 |
| CaOH | 6.00 |
| Carbon Black N990 | 30.00 |
| Blend of 33% organophosphonium salt and 67% of a fluoroelastomer. | 3.00 |
| Blend of 50% of a dihydroxy aromatic compound and 50% of a fluorocarbon | 4.00 |

Table C-3. Recipe for Fluorocarbon Elastomer.

The butyl rubber recipe is shown in Table C-4. The hemispheres were molded at 160 °C for 45 minutes.

| Ingredient | Quantity (phr) |
|---|---|
| Polysar Butyl 100 | 100.00 |
| Zinc Oxide | 3.00 |
| Stearic Acid | .75 |
| Sulfur | 1.50 |
| Tetramethylthiuram disulfide | 1.00 |
| 2-Mercaptobenzothiazole, oil modified | .50 |

Table C-4. Recipe for Butyl Elastomer.

# APPENDIX D

# TIME CONSTANT FOR FORCE TRANSDUCER

Figure D-1 shows the voltage dissipation of the force transducer after being loaded with a static 8.896 N load. The tranducer usually dropped approximately 1% in 20 s. Since the maximum test time reported was on the order of 20 s, this dissipation rate was well within acceptable limits.

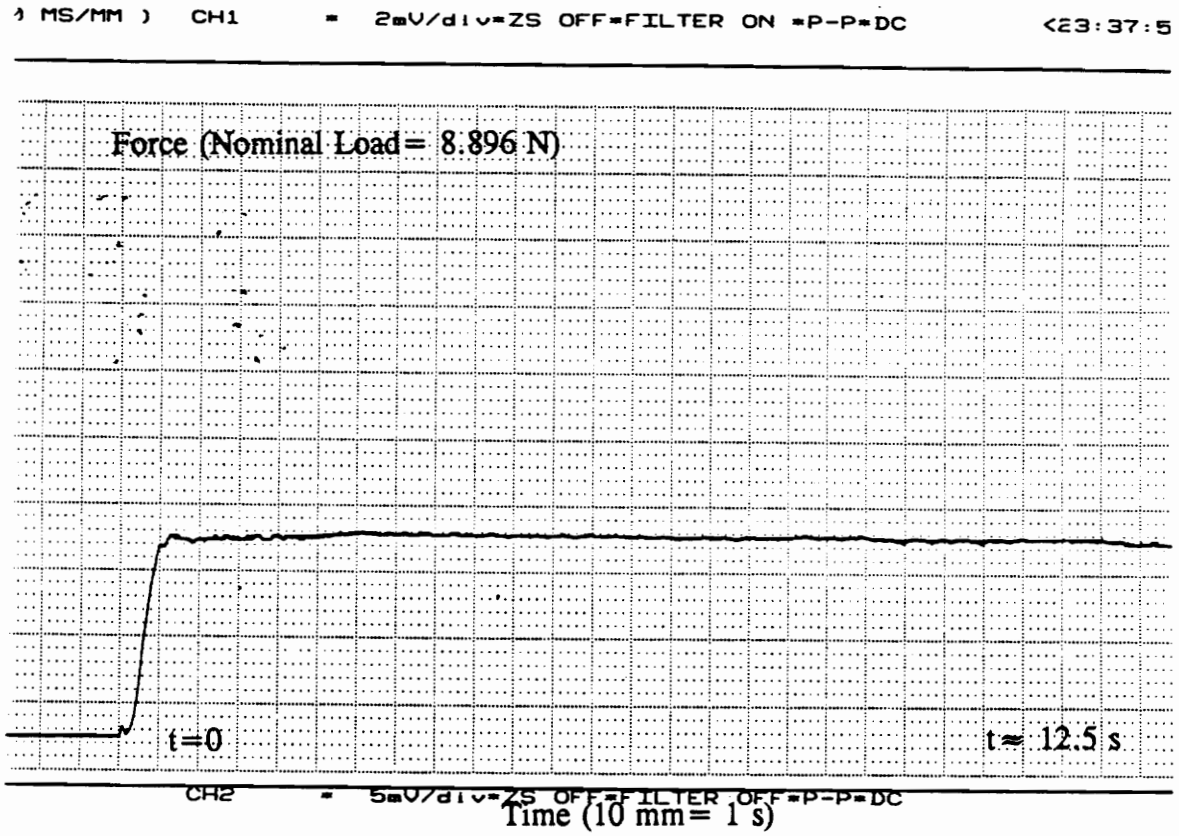


Figure D-1. Voltage Dissipation of Force Transducer.

## VITA

Ronald Alvin Lee Rorrer, the author, was born on March 29, 1962, in Heidelberg, West Germany. In 1980, he graduated from George Washington Carver High School in Fieldale, Virginia. In June of 1984, he graduated from Virginia Polytechnic Institute & State University with a Bachelor of Science degree in Mechanical Engineering. In December of 1985, he graduated with his Master of Science degree in Mechanical Engineering. After graduating with his masters degree he was employed by Martin Marietta in Orlando, Florida as a precision mechanical design engineer. He started the Doctoral Program in September of 1987. The author will begin work at The Gates Rubber Company in Denver, Colorado on January 6, 1992 in the Adhesives/Lubricant group as a Project Leader.

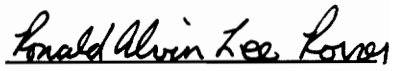

Ronald Alvin Lee Rorrer